RAC 2612
20 October 1964

ZA-3 AIR CUSHION

VEHICLE TEST PROGRAM

FINAL REPORT

Prepared for the

Office of Naval Research
Department of the Navy
Washington, D.C.

Under

Contract Nonr 4500(00)

NOTICE

Address inquiries to:

Director, Advanced Aircraft Systems
REPUBLIC AVIATION CORPORATION
Farmingdale, L.I., N.Y.

PAGES _____

ARE

MISSING

IN

ORIGINAL

DOCUMENT

CONTENTS

CONTENTS (Cont'd)

ILLUSTRATIONS

ILLUSTRATIONS (Cont'd)

ILLUSTRATIONS (Cont'd)

ILLUSTRATIONS (Cont'd)

ILLUSTRATIONS (Cont'd)

ILLUSTRATIONS (Cont'd)

ILLUSTRATIONS (Cont'd)

TABLES

SECTION I

INTRODUCTION

The United States Marine Corps has for some time been interested in evaluating the technical and operational feasibility of the air cushion vehicle (or ground effect machine) in the amphibious support mission of an amphibious assault. Important experimental data, however, has been lacking on the capabilities of GEMs in rough water, in surf, and over rough ground. In a comprehensive study of the Marine Corps' requirements, appearing in ONR Report ACR/NAR-26, it was recommended that "Experiments, including design study aspects, should be supported on certain soundly engineered vehicles to provide data for establishing the feasibility of a 5-ton GEM."

Under certain agreements concluded between Vickers-Armstrongs Limited and Republic Aviation Corporation, the VA-3, an air cushion vehicle in the 5-ton-payload class and developed by Vickers-Armstrongs, was leased for experimental operation by Republic at its Montauk, Long Island, base.

Accordingly, the Marine Corps implemented the study recommendations by requesting ONR to award a contract to Republic to perform certain tests with the VA-3. The primary purpose of these tests has been to measure performance, establish operating techniques, and observe characteristics of the VA-3 in sea states 0 through 3, in heavy breaking surf and over land. All tests have been satisfactorily concluded and are reported upon here.

SECTION II

SUMMARY

The test program performed under the ONR contract and documented in this report has produced significant results that, in the opinion of Republic Aviation Corporation, should favorably influence the Navy Department's assessment of GEMs for amphibious landing as well as for other military uses.

This demonstration of successful continuous operations in heavy seas and surf is possibly the most significant result achieved. Landings and departures were performed through surf with breaking waves as high as 7 to 8 feet, and a capability for higher breakers is indicated. Repeated operations in sea state 3 were performed for data acquisition. On several occasions, with high-level Navy observers on board, the craft was able to maintain headway without sustaining structural damage in 8- to 12-foot short-crested waves.

Vehicle stability and ride characteristics are considered superior to those of hydrofoils and planing hull craft; no seasickness or discomfort was reported by passengers or crew. The maximum normal bow accelerations, recorded in the aforementioned 8- to 12-foot waves, were 1.5g. In sea state 3,

approximately 80 percent of all normal bow accelerations fell below 0.6g. Amidships, all accelerations were significantly lower. The moderate acceleration levels can be attributed to the damping effect of the air cushion.

Experience gained in training two separate drivers in this program indicates that no more than 5 to 6 hours will be required for trained coxswains to achieve proficiency in GEMs. No hazards are presented by the cushion exhaust; support personnel can stand adjacent to the skirts during operation.

Although the flexible skirt design was adequate for this program, it cannot be considered sufficiently developed for operational usage. Maintenance and repair hours were far in excess of acceptable values. A high degree of mission reliability with major skirt damage, however, was demonstrated on more than one occasion. Small arms fire damage, therefore, may be considered insignificant.

The theoretical techniques for estimating performance of air cushion vehicles have produced reasonably accurate results. Further refinement of measurement methods and techniques, as discussed in the body of the report, are necessary. The structural criteria established for the VA-3 design have proved adequate except for bow impact loads.

SECTION III

OUTLINE OF PROGRAM

A. INTRODUCTION

The four phases of the program were overwater sea trials, surf tests, long-crested wave runs, and overland runs. During the testing, motion pictures were taken to identify the water-shedding, spray-making, and other surface-disturbance characteristics of the craft. The operational log made during the testing is presented as Table 3-1. The detailed test results are presented in Section VI.

B. PHASE A: OVERWATER SEA TRIALS (TABLES 3-2 AND 3-3)

The overwater sea trials were conducted in sea conditions up to sea state 3. The craft was tested in three center-of-gravity conditions and at two weights. With all possible combinations of these conditions, the craft executed two maneuver patterns at two lift powers. The maneuver patterns consisted of four runs at maximum power at 0, 90, 180, and 270 degrees to the

prevailing seas, respectively; each run lasted approximately 30 seconds after constant speed was attained. (Maximum power is defined as the maximum thrust the driver would use and does not necessarily define a specific operating point).

In addition, reduced thrust power runs were conducted to obtain data for curves of drag versus forward speed. These runs encompassed the following: sea conditions up to sea state 3 in shallow and deep water, two lift-power settings, various forward speeds, one center of gravity, and one weight. The runs were conducted either upwind or downwind.

Static hovering tests overland were conducted to ascertain the relationship of propeller pitch to thrust, as well as pitch and roll responses with and without the propulsion engines operating, at three lift powers.

Measurements of damping in roll were conducted at three forward speeds and two lift-power settings at one weight and one center of gravity. This test was accomplished by forcing a roll with the spoiler system while traveling over a calm sea.

To obtain drag data at power settings below maximum, partial power runs were performed in sea states 0, 1, 2 and 3. Runs were made upwind and downwind in water about 12 feet

deep and in water about 60 feet deep. During a run, a constant heading was maintained, and power was increased in increments to yield speeds from just above hump speed to maximum. During each power increase, the speed was allowed to stabilize before the next power setting was made.

C. PHASE B: SURF TESTS (TABLE 3-4)

In surf tests, the craft negotiated surf heights up to 7 feet. The tests were conducted in two center-of-gravity conditions. The craft approached the beach at reduced speed, transitioned through the surf, stopped, turned, and reentered the surf. The speed of approach and reentry were varied to ascertain the effect of velocity on the ability of the craft to negotiate the transition. The angle of travel to the surf line was also investigated.

D. PHASE C: LONG CRESTED WAVE RUNS

The long crested wave runs were conducted on a day when the waves in the test area were 3 to 4 feet high and the crest length was 125 to 150 feet. The craft was tested at one weight and one center-of-gravity condition; it executed two maneuver patterns with runs at 0, 45, 90, 135, 180, 225, 270,

and 315 degrees to the prevailing sea. Each run lasted approximately 30 seconds after constant speed was attained. The lift and thrust power conditions employed during this phase were as follows:

1) Maximum lift and maximum thrust

2) Maximum lift and reduced thrust

3) Minimum lift and maximum thrust

4) Idle lift and maximum thrust

With the craft in a displacement mode, measurements were made to determine the metacenter heights about the roll and pitch axes. This was done by moving ballast weight along the transverse and longitudinal axes and measuring the resultant roll and pitch angles.

E. PHASE D: OVERLAND RUNS

The overland performance of the VA-3 was demonstrated over obstacles, negotiable gradients, rocky areas and marshland. The turning radius of the craft overland was determined at 5, 10, 15, and 20 knots. Several runs were made, in both directions, over a 5-foot high embankment.

TABLE 3-1. VA-3 MONTAUK OPERATIONAL LOG

Trial	Date (month-day)	Duration (hours: minutes)	Number of Passengers					Engine Time (hours: minutes)			
			Total	Republic	Vickers	Govt	Military	Lift Engines		Propulsion Engines	
								Forward	Aft	Port	Stbd
								(S/N 5024)	(S/N 5014)	(S/N 276)	(S/N 277)
			Accumulated prior time					8:21	0:00	24:53	24:44
A	3-17	0:08	4	2	2			0:23	0:29	0:46	0:55
1	3-28	1:38	17	15	2			2:12	2:02	1:48	1:48
	Subtotal	1:46						10:56	2:31	27:27	27:27
2	4-6	1:39	7	5	2			2:11	2:30	1:53	1:48
3	4-6	1:19	8	5	2	1		1:32	1:32	1:32	1:32
4	4-13	1:38	6	4	2			2:12	2:12	2:10	2:05
5	4-13	1:14	6	4	2			1:32	1:37	1:27	1:27
6	4-14	0:30	16	8	3	5		1:00	1:00	0:48	0:43
7	4-16	1:36	6	4	1	1		2:08	2:08	1:52	1:52
8	4-17	1:54	6	4	2			2:10	2:10	2:15	2:00
9	4-17	1:27	6	4	2			1:42	1:42	1:35	1:35

TABLE 3-1. VA-3 MONTAUK OPERATIONAL LOG (cont'd)

Trial	Date (month-day)	Duration (hours: minutes)	Number of Passengers					Engine Time (hours: minutes)			
			Total	Republic	Vickers	Govt	Military	Lift Engines		Propulsion Engines	
								Forward	Aft	Port	Stbd
10	4-21	1:15	6	4	2			1:52	1:52	1:37	1:37
11	4-23	0:56	16	6	2	8		2:02	2:27	1:37	1:37
12	4-24	0:22	11	8	2	1		0:42	0:42	0:42	0:42
13	4-24	1:26	8	6	2			1:53	1:53	1:36	1:36
	Subtotal	17:02						31:50	24:16	46:21	45:51
14	5-8	1:51	8	6	1	1		2:21	2:16	2:19	2:41
15	5-12	0:55	10	9	1			1:25	1:35	1:30	1:08
16	5-12	1:45	6	5	1			2:10	2:10	2:05	2:05
	5-13	Replaced S/N 277 with S/N 107, with accumulated prior time of 1:55								(S/N 277) 51:45 (S/N 107) 1:55	
17	5-18	1:33	12	7	2	3		2:15	2:15	2:17	2:17
	5-19	Replaced S/N 276 with S/N 296, with accum. time of 2.05						(S/N 276)		54:32 2:05 (S/N 296)	
18	5-20	1:38	6	4	2			2:02	2:02	2:25	2:02

TABLE 3-1. VA-3 MONTAUK OPERATIONAL LOG (cont'd)

Trial	Date (month-day)	Duration (hours: minutes)	Number of Passengers					Engine Time (hours: minutes)			
			Total	Republic	Vickers	Govt	Military	Lift Engines		Propulsion Engines	
								Forward	Aft	Port	Stbd
19	5-21	1:14	15	6	1	8		1:25	1:25	1:25	1:25
20	5-25	1:15	10	8	1		1	1:53	1:53	1:38	2:38
21	5-26	1:07	6	5	1			1:45	1:40	1:40	1:52
22	5-28	0:58	5	3	2			1:15	1:15	1:15	1:15
	Subtotal	29:16						48:21	40:47	10:28	13:24
23	6-1	1:02	5	3	2			1:22	1:22	1:22	1:22
24	6-1	0:13	5	3	2			0:20	o:20	0:20	0:20
25	6-1	1:11	5	4	1			1:23	1:23	1:23	1:23
26	6-2	0:51	5	4	1			1:08	1:08	1:08	1:08
27	6-2	1:09	5	4	1			1:30	1:30	1:30	1:30
28	6-2	0:50	6	5	1			1:00	1:00	1:00	1:00
29	6-3	1:23	8	5	1	2		2:22	2:22	2:05	2:05
30	6-3	1:17	9	8	1			2:05	2:05	1:55	1:55

TABLE 3-1. VA-3 MONTAUK OPERATIONAL LOG (cont'd)

Trial	Date (month-day)	Duration (hours: minutes)	Number of Passengers					Engine Time (hours: minutes)			
			Total	Republic	Vickers	Govt	Military	Lift Engines		Propulsion Engines	
								Forward	Aft	Port	Stbd
B	6-4	0:05	3	2	1			0:20	0:20	0:15	0:15
31	6-23	0:45	13	8	2	2	1	1:42	1:42	1:27	1:15
32	6-24	0:55	10	9			1	1:17	1:17	1:17	1:17
33	6-25	1:00	3	3				1:20	1:20	1:20	1:20
34	6-25	0:39	12	8		4		0:55	0:55	0:55	0:55
35	6-26	0:48	3	3				1:30	1:30	1:30	1:30
36	6-26	1:00	8	5		3		1:15	1:15	1:15	1:15
37	6-26	0:50	10	10				1:25	1:25	1:25	1:25
38	6-29	1:05	10	3	2		5	1:20	1:20	1:20	1:20
	Subtotal	44:21						70:35	63:01	31:55	34:39
39	7-6	1:20	3	2	1			1:50	2:05	1:50	1:50
40	7-7	1:11	3	2	1			1:38	1:38	1:38	1:38
41	7-7	1:15	12	8	1	3		1:30	1:30	1:30	1:35

TABLE 3-1. VA-3 MONTAUK OPERATIONAL LOG (cont'd)

Trial	Date (month-day)	Duration (hours: minutes)	Number of Passengers					Engine Time (hours: minutes)			
			Total	Republic	Vickers	Govt	Military	Lift Engines		Propulsion Engines	
								Forward	Aft	Port	Stbd
42	7-8	1:05	7	3	1	3		1:55	1:55	1:50	1:50
43	7-8	1:00	10	4	2	4		1:45	1:45	1:45	1:45
44	7-10	1:15	5	4	1			1:25	1:25	1:23	1:23
45	7-10	0:35	5	4	1			0:35	0:35	0:00	0:00
46	7-15	1:40	4	3	1			2:07	2:07	2:22	2:07
47	7-15	1:05	7	4	1	2		1:33	1:33	1:33	1:33
48	7-16	1:35	4	3	1			1:54	1:54	1:54	1:54
49	7-17	1:05	4	3	1			1:27	1:15	1:17	1:17
50	7-17	1:25	5	3	2			1:40	1:40	1:40	1:40
51	7-17	0:30	6	3	1	2		0:40	0:40	0:40	0:40
52	7-20	1:00	4	3	1			1:17	1:17	1:17	1:17
	7-20	Replaced S/N 296 with S/N 409, with accumulated prior time of 2:25							(S/N 296) (S/N 409)	52:34 2:25	

TABLE 3-1. VA-3 MONTAUK OPERATIONAL LOG (cont'd)

Trial	Date (month-day)	Duration (hours: minutes)	Number of Passengers					Engine Time (hours: minutes)			
			Total	Republic	Vickers	Govt	Military	Lift Engines		Propulsion Engines	
								Forward	Aft	Port	Stbd
53	7-21	1:44	6	4	2			2:00	2:00	2:00	2:00
54	7-22	1:15	13	5	1	7		1:47	1:37	2:27	1:37
55	7-23	0:20	4	3	1			0:20	0:20	0:20	0:20
56	7-23	1:10	6	4	2			1:38	1:38	2:05	1:58
57	7-23	1:20	10	4	1	5		1:33	1:33	1:28	1:43
	7-23	Replaced S/N 5024 with S/N 5018, with accumulated prior time of 5:44						99:09 (S/N 5024) 5:44 (S/N 5018)			
58	7-29	1:02	4	2	2			1:35	1:20	1:10	1:10
59	7-30	0:25	23	4	1	18		0:30	0:30	0:30	0:30
60	7-30	0:30	14	4	1	9		0:38	0:38	0:38	0:38
61	7-30	1:04	9,20	5,3	2,2	2,14		1:28	1:28	1:28	1:28
	Subtotal	69:13						9:55	95:24	14:31	66:32
62	8-3	0:30	10	8	2			0:45	0:45	0:45	0:55

TABLE 3-1. VA-3 MONTAUK OPERATIONAL LOG (cont'd)

Trial	Date (month-day)	Duration (hours: minutes)	Number of Passengers					Engine Time (hours: minutes)			
			Total	Republic	Vickers	Govt	Military	Lift Engines		Propulsion Engines	
								Forward	Aft	Port	Stbd
63	8-4	1:45	10	8	2			2:00	2:00	2:00	2:00
64	8-4	0:50	7	5	1	1		1:02	1:07	1:02	1:02
65	8-5	1:24	10	7	2	1		1:48	1:48	1:48	1:48
66	8-5	1:30	10	8	1	1		1:45	1:45	1:45	1:45
67	8-5	1:48	13	3		10		2:00	2:00	2:00	2:00
68	8-11	1:23	3	3				1:49	1:49	1:35	1:44
69	8-11	1:01	10	8		1	1	1:32	1:37	1:22	1:22
	8-11	Replaced S/N 5014 with S/N 5022, with no prior time						(S/N 5014) 108:15 (S/N 5022) 0:00			
70	8-17	0:24	9	5		4		1:42	1:52	0:54	0:54
71	8-18	1:00	10	3		7		1:17	1:17	1:17	1:17
72	8-18	1:38	3	3				1:48	1:48	1:48	1:48
73	8-19	1:00	5	5				1:27	1:32	1:10	1:10

TABLE 3-1. VA-3 MONTAUK OPERATIONAL LOG (cont'd)

Trial	Date (month-day)	Duration (hours: minutes)	Number of Passengers					Engine Time (hours: minutes)			
			Total	Republic	Vickers	Govt	Military	Lift Engines		Propulsion Engines	
								Forward	Aft	Port	Stbd
74	8-19	1:28	8	3	1	4		1:55	1:55	2:00	1:55
75	8-27	1:07	9	3		6		3:12	3:27	3:30	3:35
76	8-28	1:05	3	3				1:32	1:39	1:39	1:39
77	8:28	1:02	4	3		1		1:15	1:15	1:10	1:10
	Subtotal	88:08						36:44	14:45	40:16	92:36
78	9-1	1:03	3	3				1:38	1:33	1:23	1:23
79	9-2	0:54	3	3				1:11	1:11	1:11	1:11
80	9-2	1:13	5	4		1		1:22	1:27	1:22	1:22
81	9-2	1:04	5	3		2		1:18	1:24	1:18	1:18
82	9-4	0:29	3	3				1:21	1:21	0:51	0:51
83	9-8	0:42	3	3				1:03	1:03	1:03	1:03
84	9-8	2:03	2	2				2:25	2:25	2:25	2:25
85	9-10	1:26	15	9	1		6	1:55	1:55	2:17	2:17

TABLE 3-1. VA-3 MONTAUK OPERATIONAL LOG (cont'd)

Trial	Date (month-day)	Duration (hours: minutes)	Number of Passengers					Engine Time (hours: minutes)			
			Total	Republic	Vickers	Govt	Military	Lift Engines		Propulsion Engines	
								Forward	Aft	Port	Stbd
86	9-15	0:39	5	4		1		1:10	1:10	1:00	1:00
87	9-17	2:06	3	3				2:17	2:17	2:17	2:17
	9-17	Replaced S/N 409 with S/N 230, with accumulated prior time of 2:15							(S/N 409) (S/N 230)	55:23 0:00	
88	9-21	1:51	9	6		1	2	2:11	2:11	2:46	2:31
89	9-29	1:15	9	6		3		1:35	1:41	1:35	1:35
90	9-29	1:00	4	4				1:15	1:15	1:15	1:15
91	9-30	0:40	6	4		2		0:52	0:52	0:47	0:47
TOTAL		104:33	709	443	96	154	17	58:17	36:30	8:38	113:51

TABLE 3-2. ONR PHASE A RUN INDEX

Date		4-16	4-17	4-21	4-24	5-8	5-12	5-18	5-20	5-25
Weight, pounds	29,800	X X X X	X X X X	X X			X X			
	32,000				X X	X X X X	X X	X X	X X	X X
c.g., inches aft	+0.3									
	+5.6	X X X X	X X X X	X X	X X	X X X X	X X X X			
	+11.7							X X	X X	X X
Power	Max Lift	X	X	X	X	X X	X X	X	X	X
	Max Thrust									
	Min Lift	X	X	X	X	X X	X X	X	X	X
	Max Thrust									
	Max Lift	X	X							
	Const Speed									
	Min Lift	X	X							
	Const Speed									
Sea State	0					X X	X X X X			
	1		X X X X		X X	X X		X X		
	2	X X X X							X X	
	3			X X						X X
Heading to Prevailing Sea, degrees	0	3 7 11 15	20 24 27 32	35 39	43 47	51 55 43 47	51 55 59 63	67 71	75 79	83 86
	90	2 6 10 14	17 21 25 29	33 37	41 46	49 54 41 46	49 54 58 62	66 70	74 78	82 87
	180	4 8 12 16	19 23 28 31	36 40	44 48	52 56 44 48	52 56 60 64	68 72	76 80	81 88
	270	1 5 9 13	18 22 26 30	34 38	42 45	50 53 42 45	50 53 57 61	65 59	73 77	84 85
Repeated		X X	X X	X X	X X		X X		X X	X
			X X							
			X X							

* Numbers identify a specific run. A consecutive numbering system was used in data logs for each phase.

TABLE 3-2. ONR PHASE A RUN INDEX (cont'd)

Date		5-26	5-28	6-1	6-2	6-25	6-26	7-7	8-4	8-5	8-11
Weight, pounds	29,800		X X	X X	X X	X X		X X			X X
	32,000	X X			X X	X X	X X		X X	X X X X	
c.g. inches aft	+0.3 or +1.4		X X	X X	X X	X X	X X			X X	
	+5.6								X X	X X	
	+11.7 or +9.4	X X			X X	X X		X X			X X
Power	Max Lift	X	X	X	X X	X X	X	X	X	X X	X
	Max Thrust										
	Min Lift	X	X	X	X X	X X	X	X	X	X X	X
	Max Thrust										
	Max Lift										
	Const Speed										
	Min Lift										
	Const Speed										
Sea State	0				X X X X		X X	X X			
	1	X X		X X		X X X X					
	2		X X						X X		X X
	3									X X X X	
*Heading to Pre-vailing Sea, degrees	0	65 69	91 95	99 103	108 112 115 119	123 127 129 133	138 142	148 152	155 159	163 168 171 175	179 183
	90	68 72	90 94	97 102	106 110 114 118	122 126 131 134	140 144	146 149	154 158	161 165 169 173	177 181
	180	66 70	92 96	100 104	107 111 116 120	124 128 132 136	139 143	147 151	156 160	164 167 172 176	180 184
	270	67 71	89 93	98 101	105 109 113 117	121 125 130 135	137 141	145 150	153 157	162 166 170 174	178 182
Repeated			X X	X X	X X X X	X X X X		X X	X X	X X X X	X X
								X X			

TABLE 3-2. ONR PHASE A RUN INDEX (cont'd)

Date		9-2	9-17
Weight pounds	29,800		X X
	32,000	X X	X X
	+0.3 or	X X	
	+1.4		
	+5.6		
	+11.7 or		X X
	+ 9.4		
	Max Lift		
	Max Thrust	X	X
	Min Lift		
	Max Thrust	X	X
Sea State	0		
	1		
	2	X X	
	3		X X
*Heading to Prevailing Sea, degrees	0	185 192	195 199
	90	186 189	193 197
	180	188 191	196 200
	270	187 190	194 198
Repeated		X X	X X

TABLE 3-3. ONR ACCELERATION RUN INDEX

Date		6-25	6-26	7-7	7-15	8-4	9-2	9-17
Weight, pounds	29,800	X X	X X X X	X X	X X X X X X			X X X X
	32,000					X X X X	X X X	
cg, inches aft	+9.4	X X	X X X X	X X	X X X X X X			X X X X
	0					X X X X	X X X	
Sea State	0		X X X X	X X				
	1	X X			X X X X X X			
	2					X X X X	X X X	
	3							X X X X
Water	Shallow			X X	X X X X		X X X	
	Deep	X X	X X X X		X X	X X X X		X X X X
Wind	Up	X	X X	X	X X X	X X	X	X X
	Down	X	X X	X	X X X	X X	X X	X X
Power	Max Lift	X X	X X	X	X X	X X	X	X X
	Min Lift		X X	X	X X X X	X X	X X	X X
Runs at various thrust power increments from minimum to maximum		1 7 2 8 3 9 4 10 5 11 6	12 16 20 24 13 17 21 25 14 18 22 26 15 19 23 27	28 34 29 35 30 36 31 37 32 38 33 39	40 45 50 55 61 66 41 46 51 56 62 67 42 47 52 57 63 68 43 48 53 58 64 69 44 49 54 59 65 60	71 75 79 84 72 76 80 85 73 77 81 86 74 78 82 87 83	88 93 98 89 94 99 90 95 100 91 96 101 92 97 102	103 106 109 113 104 107 110 114 105 108 111 115 112 116

* Numbers identify a specific run. A consecutive numbering system was used on data logs for each phase.

TABLE 3-4. ONR PHASE B RUN INDEX

Date		6-3	9-8	9-10	9-21
Weight, pounds	29,800	X X X X X X	X X	X	X
cg, inches aft	+ 12.1	X X X	X X		
	+ 5.2	X X X		X	X
Power	Max Lift	X X X X	X		
	Min Lift	X X	X	X	X
Sea State	0	X[1] X[1] X[1]			
	1	X[2] X[2] X[2]		X[4]	
	2		X[3] X[3]		X[5]
	3				
Runs* See Figures 6-57 for speed identification		1 4 7 10 13 16 2 5 8 11 14 3 6 9 12 15	17 20 18 21 19 22 23	24 25 26	27 28

1. Surf, calm to 1 foot breakers
2. 6 inch to 2 foot breakers
3. Surf, 5 to 7 foot breakers approximately 50 feet apart
4. Surf, 4 to 5 foot breakers approximately 35 feet apart
5. Surf, 6 to 7 foot breakers approximately 50 feet apart

SECTION IV

VEHICLE DESCRIPTION

The VA-3 (Figure 4-1) is 55 feet long, 27 feet wide, and 18 feet high, and design gross weight is about 15 tons. A weight breakdown of the craft is as follows:

	(pounds)
Hull and structure	13,500
Power plant	2,000
Fans, propellors, transmissions, and driveshafts	3,200
Equipment and systems	2,700
Basic Operational Weight	21,400
Fuel	3,000
Payload and crew	4,600
Design gross weight (92-mile range)	29,000

The light weight for a craft of this size was achieved by building the VA-3 of aircraft-type structures. The main structure is a load-carrying platform, constructed between two, braced-together, full-length longerons. Bow wave impacts are

passed back into this platform; the cabin and engines are mounted to it; and the air ducts and main buoyancy tanks are built into it.

The main buoyancy tank extends over the full platform area and serves as the hull of the VA-3 when it is operating as a boat. Because the tank sits low in the structure, this tank provides good stability in rough water, maintaining that stability even when adjacent compartments have flooded. The buoyancy of the main tank is sufficient to support twice the weight of the loaded craft; additional buoyancy is provided by sealed compartments around the force and aft transverse ducts and in the side walls (Figure 4-2).

The buoyancy compartments provide one surface of the ducts from the lift fan to the cushion area. The highly positioned air intakes for the two lift fans provide relatively spray-free air to centrifugal fans. The fans drive the air into a ducting system that carries most of the air to nozzles at the periphery of the hull. The air cushion that supports the craft is contained within a flexible 36-inch skirt (Figures 4-3 and 4-4). The air from the nozzles inflates the skirts and develops a cushion within

FRAMES

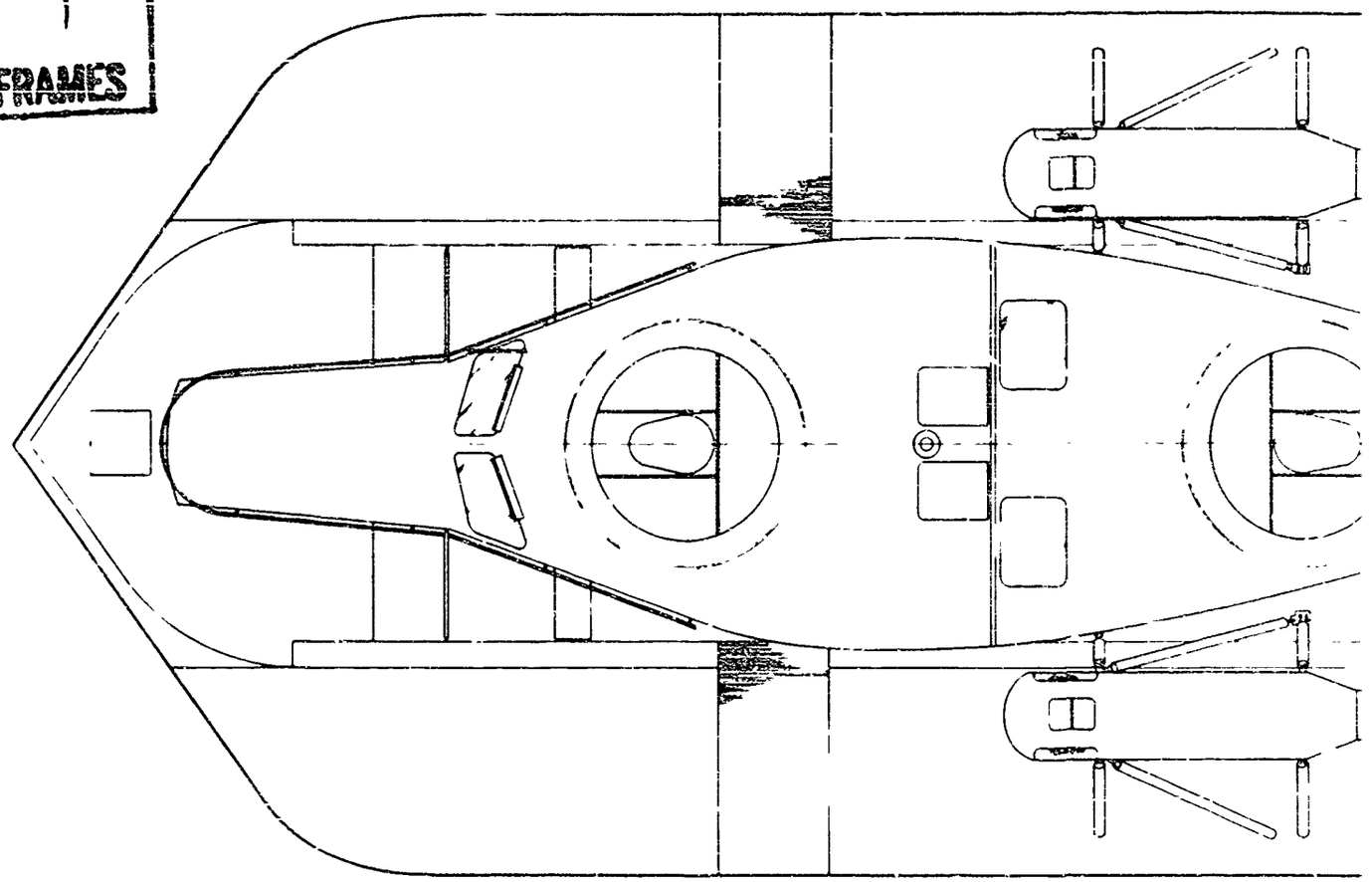

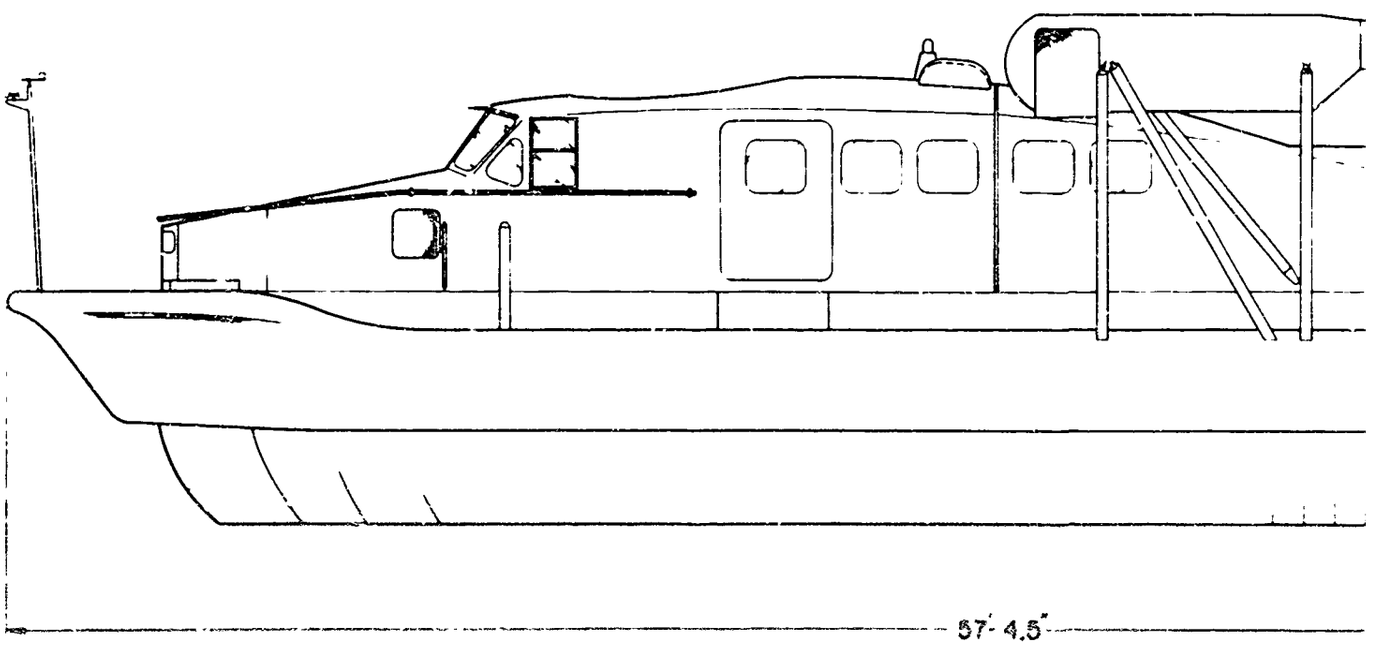

57' 4.5"

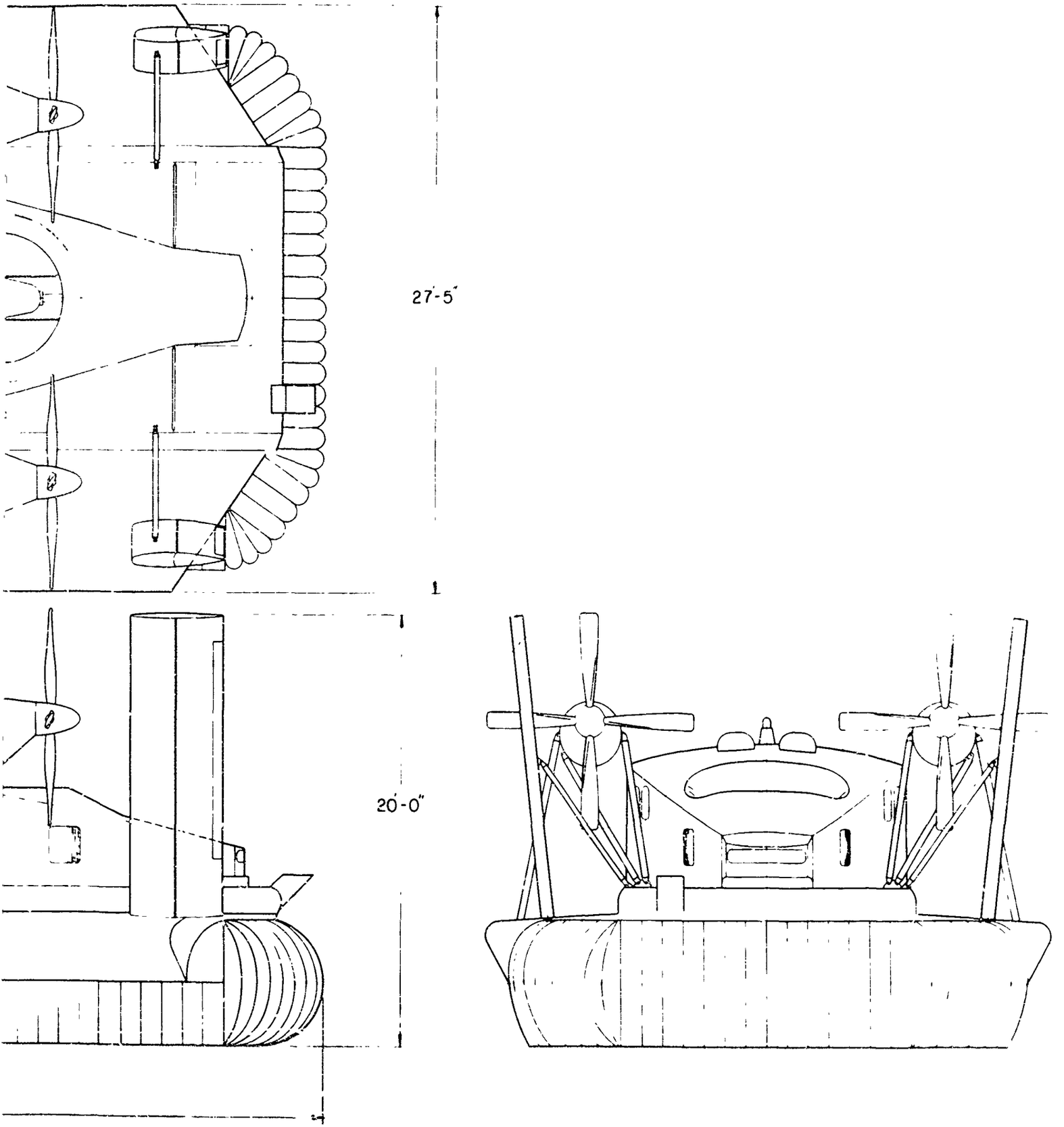

Figure 4-1. 3-View of VA-3

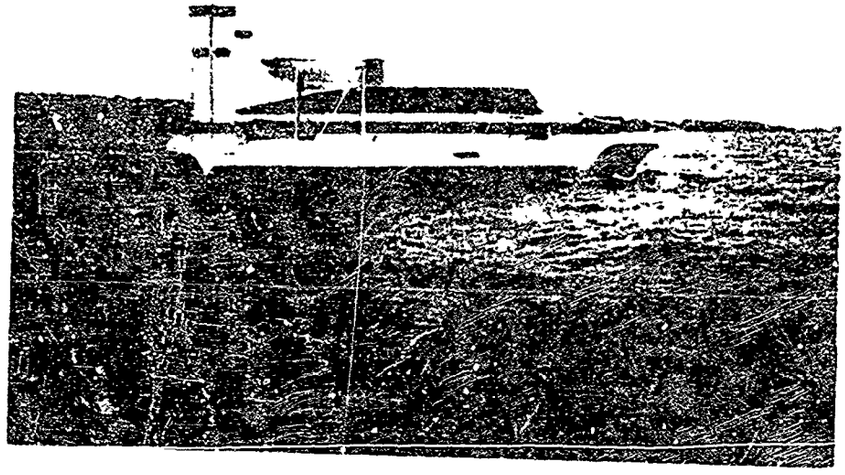

Figure 4-2. The VA-3 as a Displacement Vessel

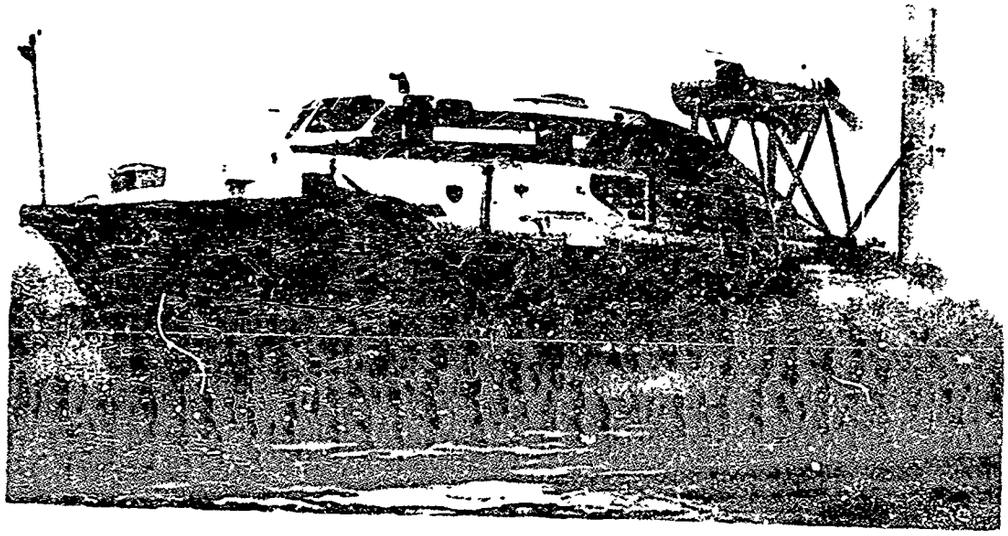

Figure 4-3. Skirt Configuration over Water

the skirts and between the bottom of the hull and the water (or ground) surface. Roll stability is controlled by spoilers within the ducting.

Two internal Bristol-Siddeley Turmo 603 engines drive the two lift fans, which are mounted with transmissions and drive shafts in the lift air intakes; two Artouste IIC engines propel the VA-3 by powering two reversible-pitch, four-bladed, 10-foot-diameter propellers. The Turmo is a free-turbine engine producing 380 shaft horsepower, while the Artouste is a fixed-turbine engine producing 380 shaft horsepower. For over-water operation, each engine air intake is protected by efficient water separators.

Four 1-kilowatt engine-driven generators produce power for the VA-3 28-volt dc system. Three generators are sufficient for emergency operation of the craft. Two batteries of 25-ampere-hour capacity provide power for engine starting and for emergencies. Separately fused supplies are provided for engine starting, operating engine instruments, detecting and extinguishing fires, pumping fuel, cabin lighting, and for operation of the radio, navigation lights, fog horn, and windshield wipers.

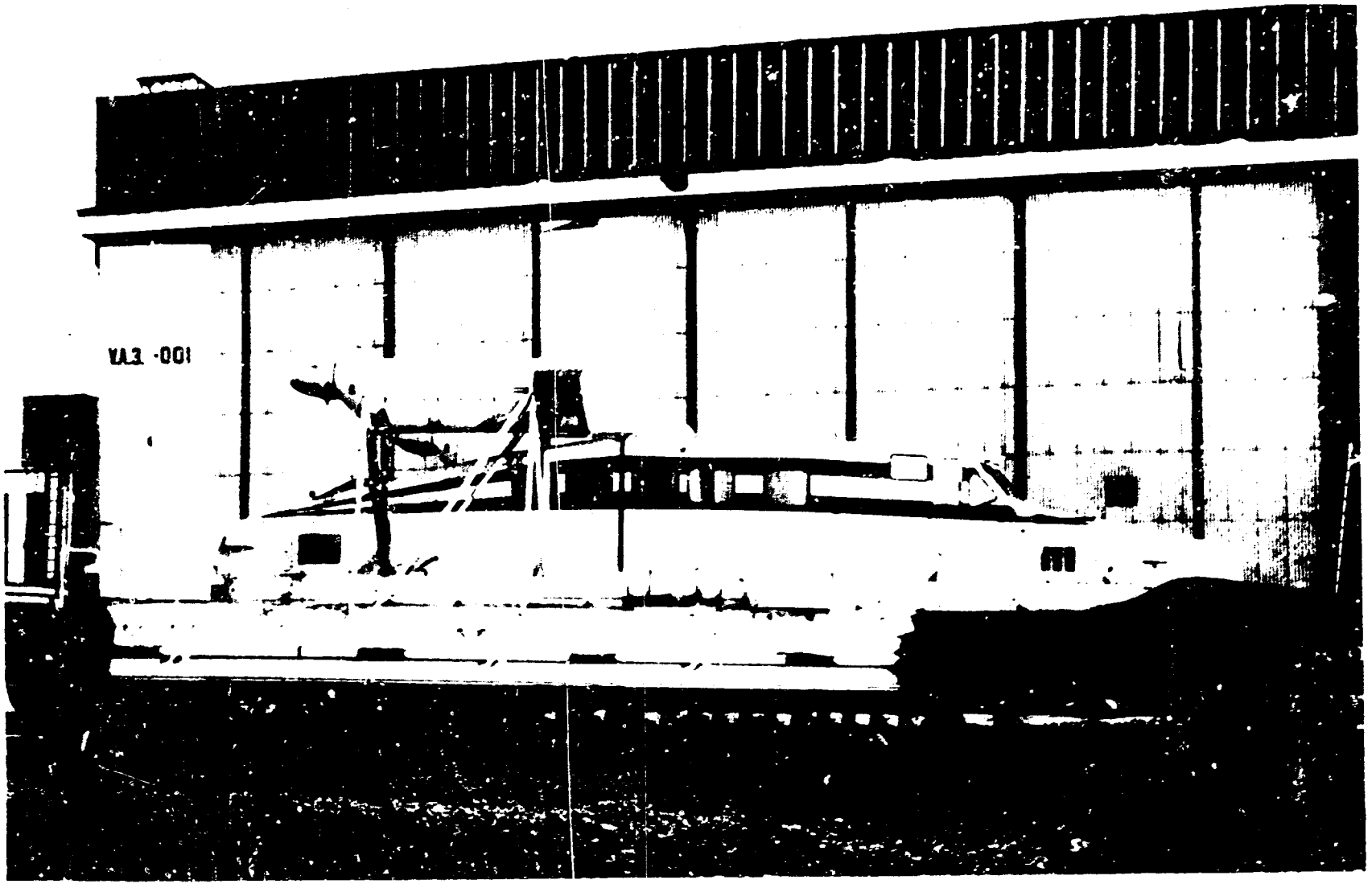

Figure 4-4. Skirt Configuration during Land Hovering

JP-4 fuel for the engines is supplied from a single fuel tank integral with the main cross bulkhead. This tank is divided by an internal baffle into two compartments so that, if a compartment is damaged, the baffle will retain up to 40 percent of the tank capacity in the other compartment. An electrically driven submerged fuel pump is located in each compartment. Each of these pumps can handle maximum fuel demands alone; and, if one pump fails, the fuel tank compartments can be connected by a cross-feed system. A fuel filter and water separator is incorporated in this system.

Gravity refueling is used. The fuel tank compartments vent to the atmosphere away from areas where spray can enter or there is risk of fire. Drain plugs are provided in the tank.

For civil operations, the VA-3 accommodates 24 passengers plus 2 crewmen. The passenger cabin has two large external waterproof doors for easy access, double-glazed windows, and sound-proofed walls and roof. A door links this cabin with the crew cabins. The crew cabin is equipped for the driver with space for a crewman. Large windows surround three sides of this cabin.

For operational evaluation communications, the driver has a Motorola vhf f-m transceiver. Also available to him is a conventional 50-watt Bendix marine transceiver (installed for emergency use). The driver instruments consist of an airspeed indicator, waterspeed indicator, fuel gages, tachometers, engine oil temperature and pressure gages, tailpipe temperature gages, a magnetic compass, and pitch and roll indicators. Driver controls for the VA-3 include a wheel, rudder pedals, propeller pitch controls, and engine throttles. Directional control is effected by combined use of propeller pitch and rudder. Pitch control is generally accomplished by varying lift fan rpm as required by varying throttle settings. Roll control is a function of wheel movement, which activates spoilers in air ducts.

Because it is not in direct contact with the surface, the VA-3 can range over water, beach, tidal flats, sand bars, swamps, and unpaved surfaces, but it is considered primarily as a marine craft. The VA-3 is outfitted with 36-inch skirts fabricated from neoprene-nylon fabric, which enables the craft to transverse objects and rough seas without impacting its solid structure (Figures 4-5 through 4-7).

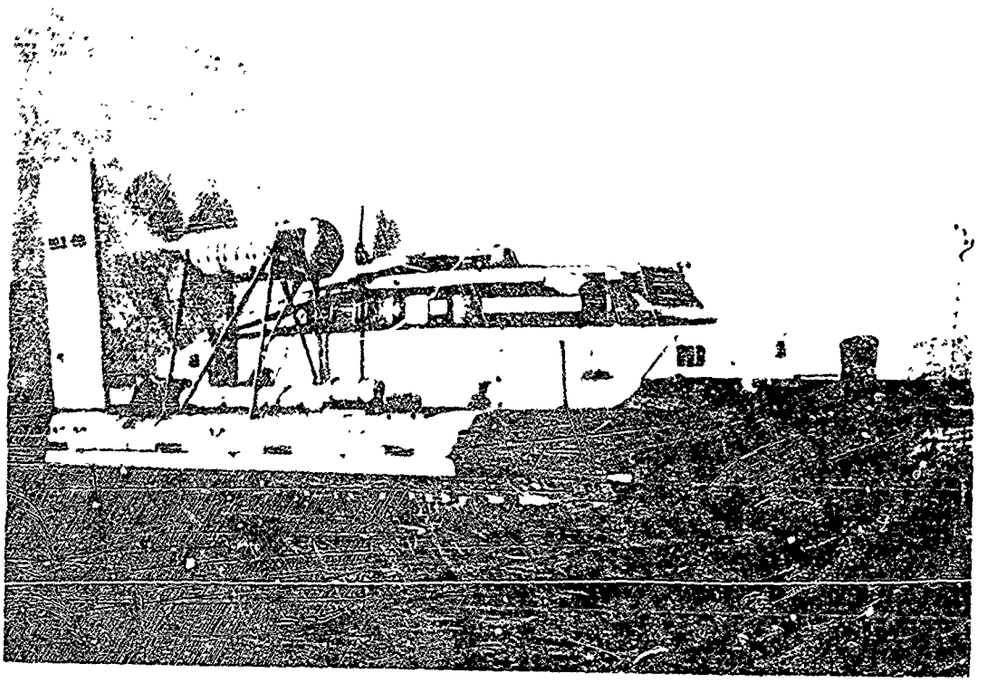

Figure 4-5. Skirt Configuration While Moving up Ramp

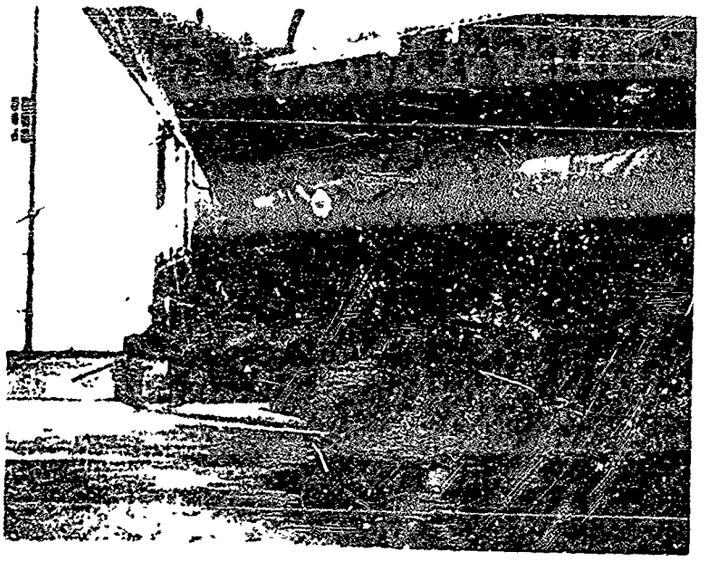

Figure 4-6. Bow Skirt Detail (VA-3 Resting on Hard Stands)

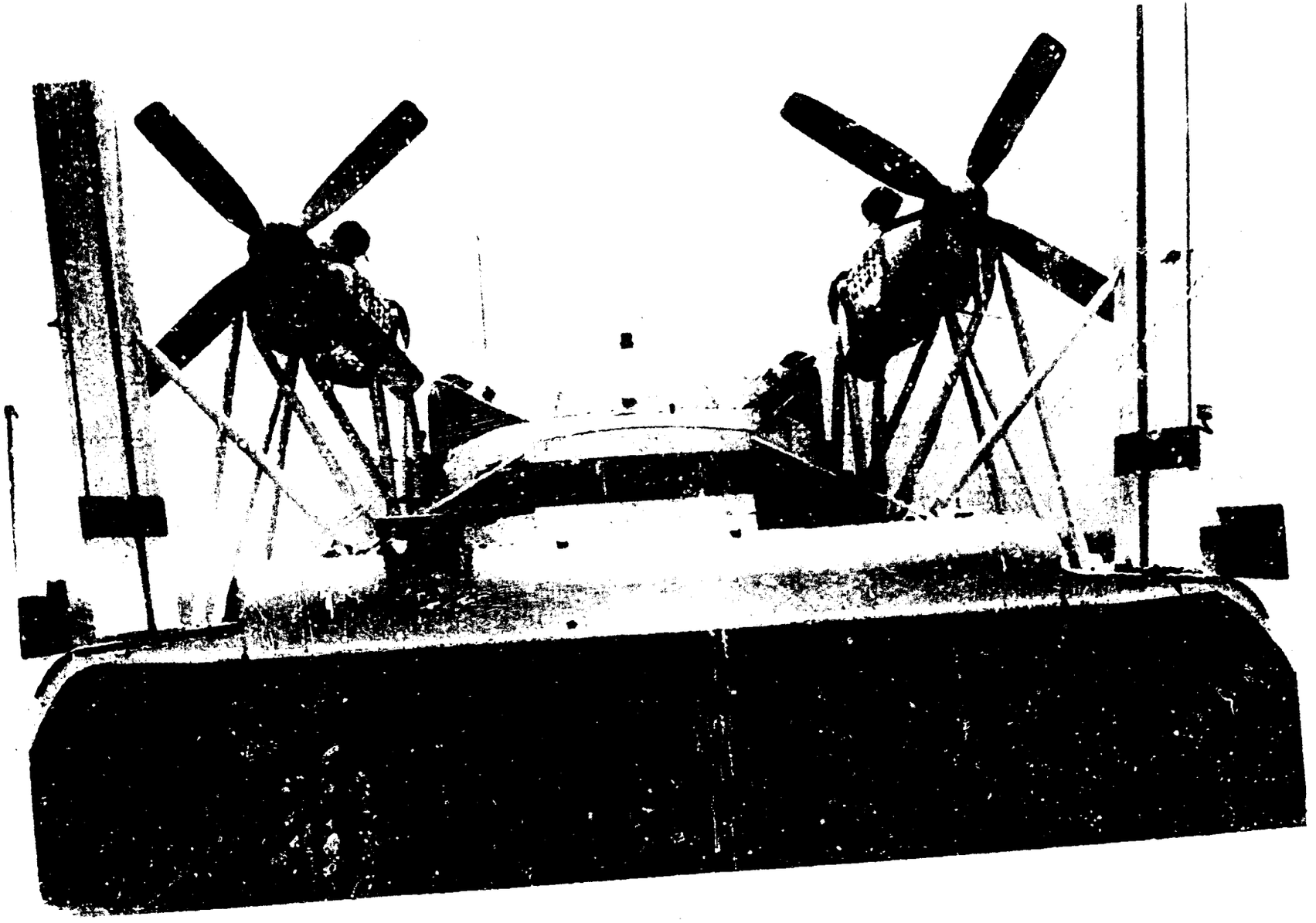

Figure 4-7. Aft Flexible Skirt (Resting on Ground)

SECTION V

INSTRUMENTATION

A. INTRODUCTION

Instrumentation was divided between the craft and an attending work boat. The VA-3 contained, in addition to its operational instruments, necessary transducers and recording equipment for collecting sea-keeping data. The work boat made sea-state measurements while the VA-3 was under test. The equipment used and its calibration is discussed in this section. Figure 5-1 illustrates the major elements and associated equipment requirements for the GEM tests. The GEM system contained pilot and copilot displays, an instrumentation console, and necessary transducers.

The pilot displays received, as their inputs, information required for craft operation and navigation. Portions of this data, coupled with the remaining transducer outputs, were presented to the instrumentation console for manual and automatic recording.

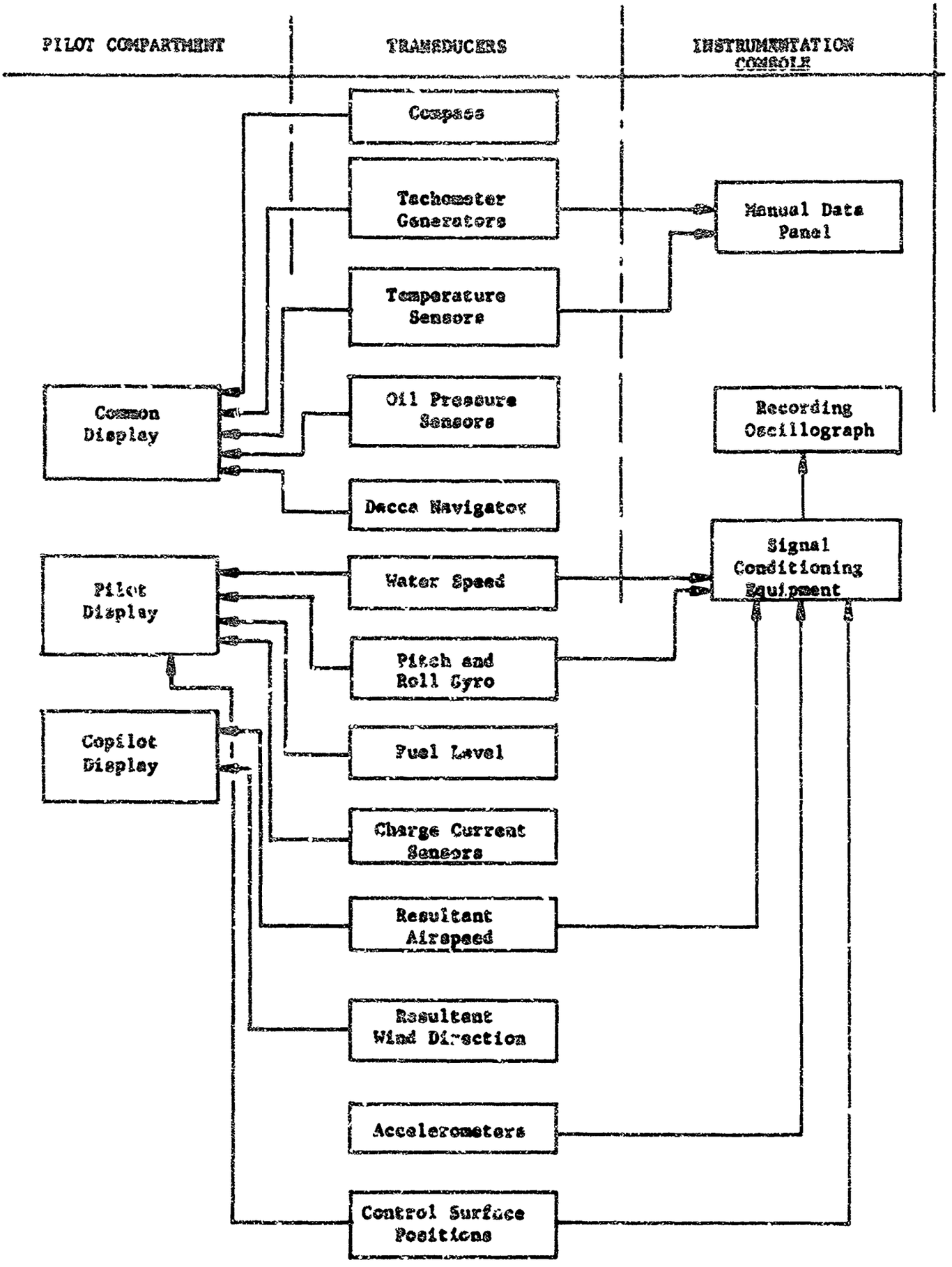

Figure 5-1. VA-3 Instrumentation

Table 5-1 lists the measured parameters and their displayed or recorded ranges.

B. INSTRUMENTATION INSTALLED IN THE VA-3

1. Data Recording Equipment

Most of the test data was recorded on a C.E.C. type 5-119-P 3-36 12-inch recording oscillograph. This data included accelerations, control surface positions, propulsion (blade) pitch angles, wind and water direction and speed, and craft attitude. Lift engine gas generator and free turbine speeds, propulsion engine speed, and all engine exhaust temperatures were recorded manually.

2. Doppler Speedmeter

The speedmeter was a continuous-wave radar that used the Doppler principal to produce a signal frequency proportional to vehicle speed.

Direct calibration of the speedmeter was accomplished by timed runs over a measured course. The results are discussed in Section VD. An internal calibration oscillator provided an audio frequency at the receiver input that corresponded to an

TABLE 5-1. INSTRUMENTATION SUMMARY

Measured Parameter	Scale	Pilot Display	Copilot Display	Manual Data Panel	Recording Oscillograph
Bow vertical acceleration	± 8g				X
Bow lateral acceleration	± 4g				X
Port vertical acceleration	± 8g				X
Aft vertical acceleration	± 4g				X
CG longitudinal acceleration	± 2g				X
CG vertical acceleration	± 4g				X
Pitch attitude	± 5°	X			X
Roll attitude	± 4°	X			X
Wind speed	0-100 knots		X		X
Wind direction	0-360°		X		X
Water speed	0-100 knots	X			X
Water direction	± 50°				X
Rudder position	± 30°				X

TABLE 5-1. INSTRUMENTATION SUMMARY (cont'd)

Measured Parameter	Scale	Pilot Display	Copilot Display	Manual Data Panel	Recording Oscillograph
Rudder trim tab position	$\pm$ 15°				X
Port spoiler position	70°				X
Starboard spoiler position	70°				X
Port propulsion blade angle					X
Starboard propulsion bland angle					X
Propulsion engines overtemperature		X			X
Propulsion engine rpm		X	X	X	
Lift engines gas generator rpm		X	X	X	
Lift engines free turbine rpm		X	X	X	
Engine exhaust temperature		X	X	X	
Engine oil temperature		X	X		
Gas generator oil pressure		X	X		

TABLE 5-1. INSTRUMENTATION SUMMARY (cont'd)

Measured Parameter	Scale	Pilot Display	Copilot Display	Manual Data Panel	Recording Oscillograph
Lift engine free turbine oil pressure		X	X		
Propeller gear box oil pressure		X	X		
Propeller gear box oil temperature		X	X		
Fuel level		X			
Generator charging current		X			

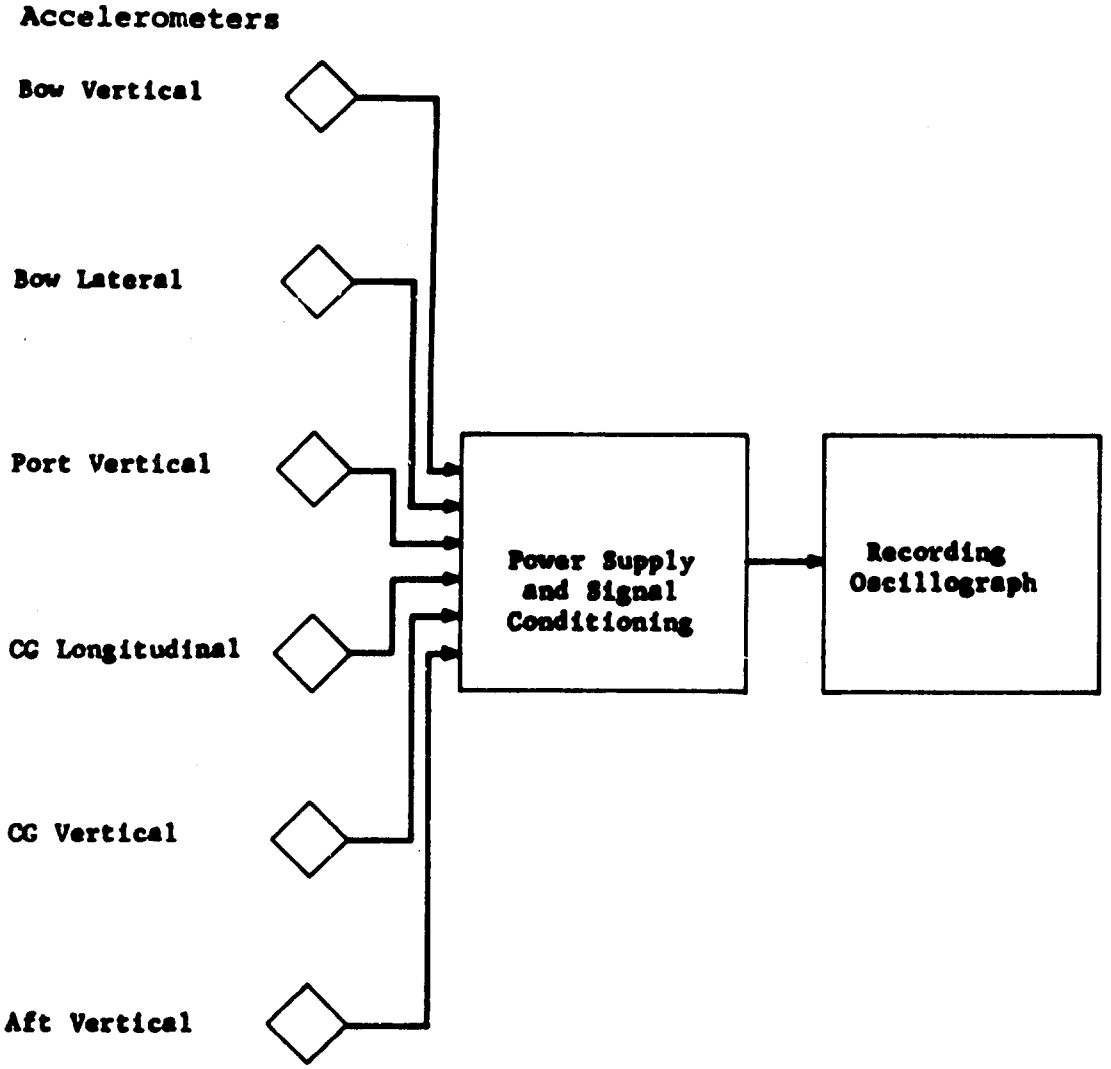

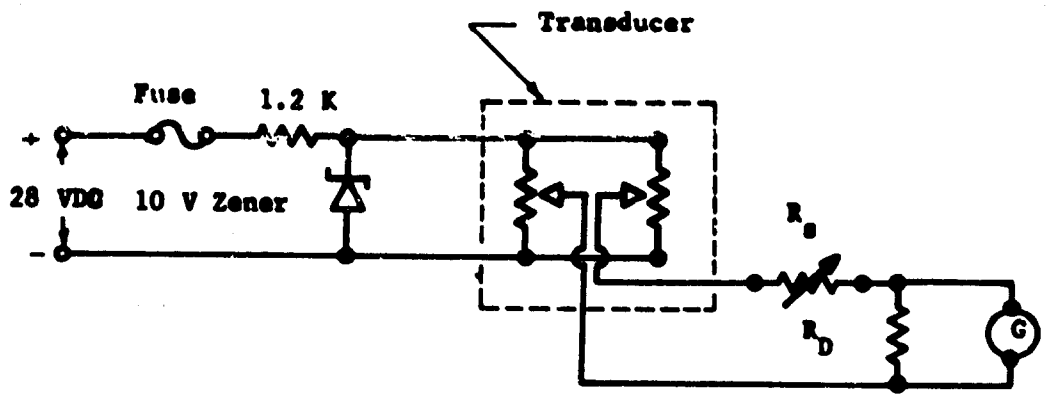

Figure 5-2. Accelerometer Connections

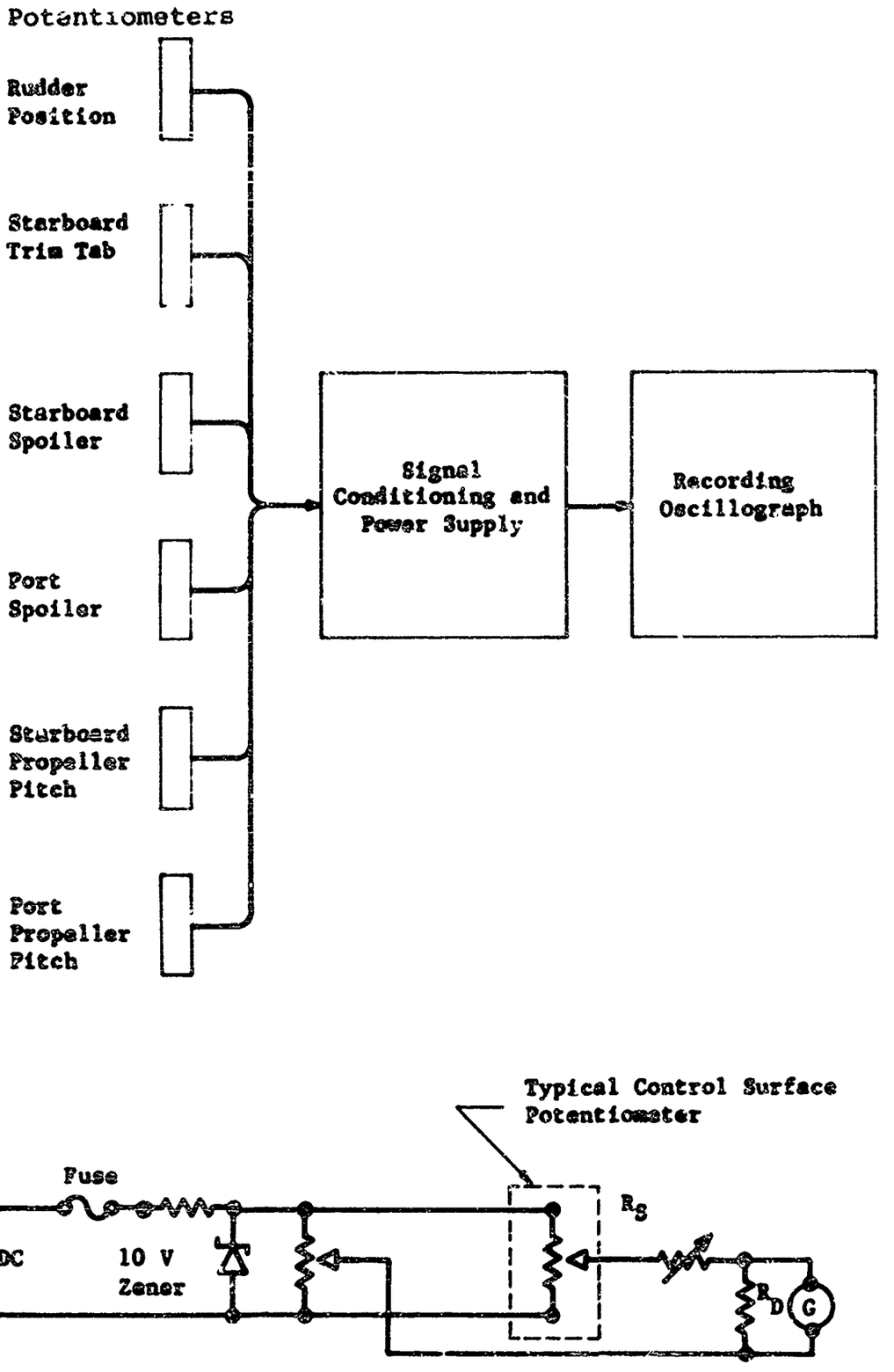

Figure 5-3. Control Surface Position Instrumentation

80-knot Doppler frequency. Thus a functional check of the system operation could be made at the pilot's discretion.

3. Accelerometers

Six potentiometer-type accelerometers were used to sense vehicle accelerations. Their locations, axes of sensitivity, and ranges are shown in Table 5-1. Figure 5-2 illustrates signal paths and typical electrical connections.

On-site static calibrations were performed periodically throughout the test program. Good calibration stability was achieved.

4. Surface Position Potentiometers

Control surface positions were measured by potentiometers mechanically linked to them. Table 5-1 summarizes the positions measured, and Figure 5-3 shows the typical circuits used.

5. Wind Speed and Direction Instrumentation

A cup-type anemometer that operated a switch contact as it rotated was used to measure resultant wind speed. The switch output was converted to a direct current proportional to anemometer speed. This current supplied the pilot display and provided an output for the oscillograph recorder.

The resultant wind direction transducer was like a conventional weather-vane connected to a potentiometer. The potentiometer output was processed in the same manner as the potentiometer outputs for control surface positions except that an additional output was provided for the pilot display.

Calibration for wind direction measurement was similar to that for the control surface positions. An angular scale was fastened to the vane base against which various positions were recorded. The anemometer was compared to a commercial velometer with an electric fan as a wind source. As a further check, data were added as various windspeeds were available.

Periodic recalibration showed good stability for both wind speed and wind direction indicators. Figure 5-4 shows circuit connections for the anemometer, and Figure 5-5 gives circuit details for the wind direction transducer.

6. Craft Attitude Instrumentation

A Sperry horizon gyro was used to measure pitch and yaw attitudes of the craft. The gyro had potentiometer outputs, the signals from which were recorded on the oscillograph and displayed to the pilot.

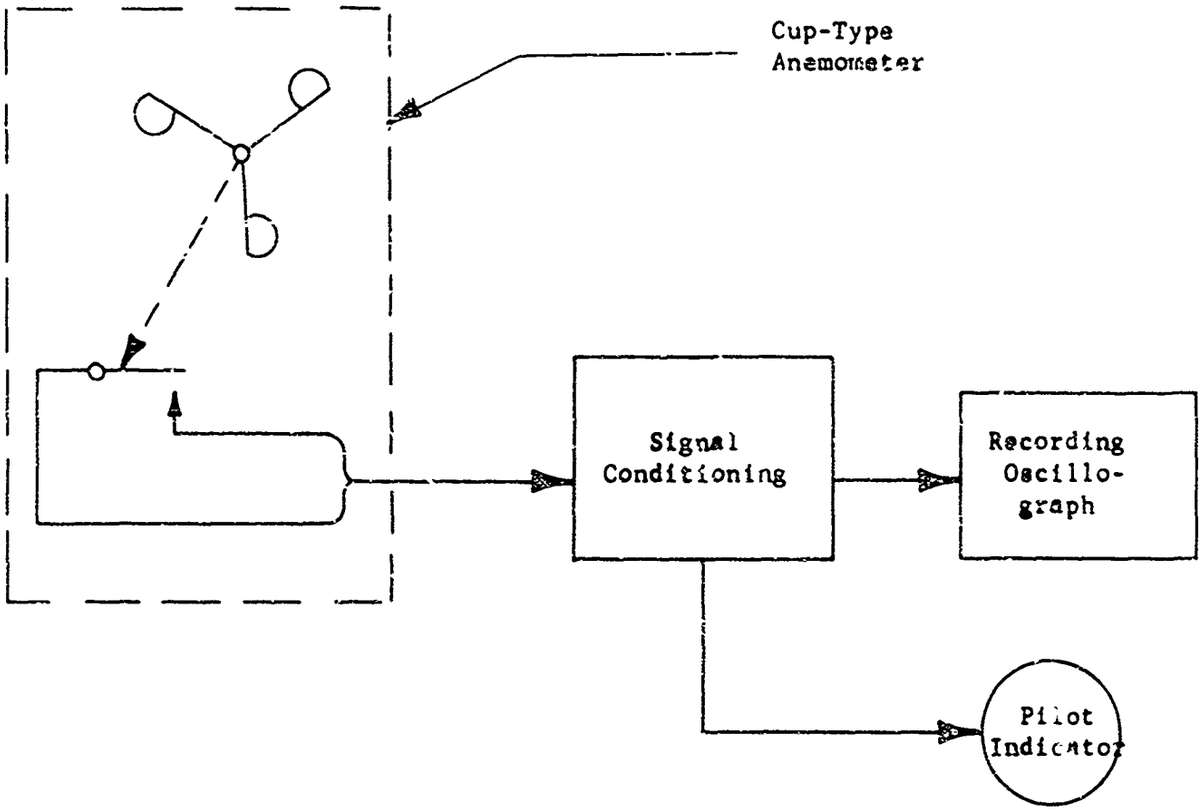

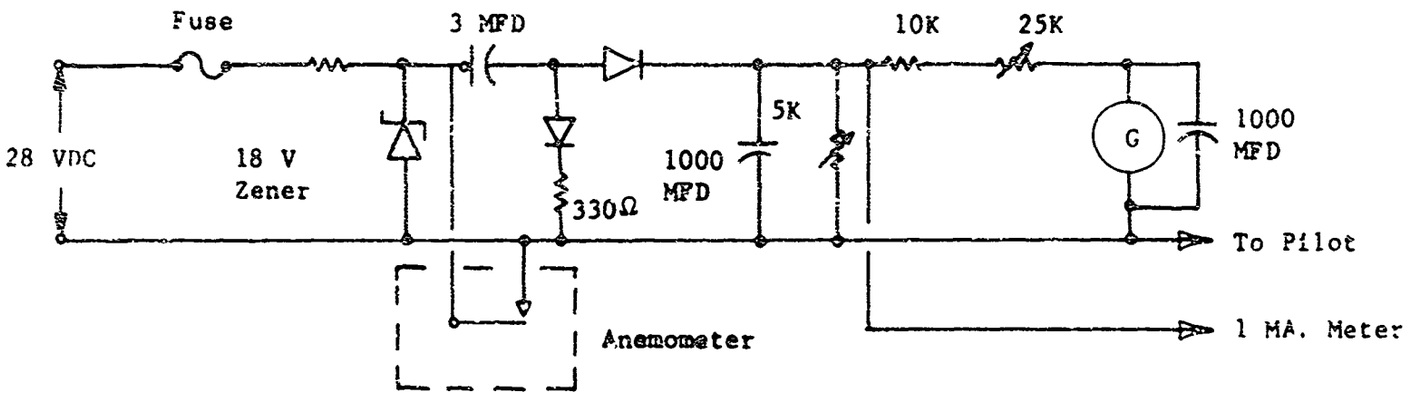

Figure 5-4. Anemometer Connections

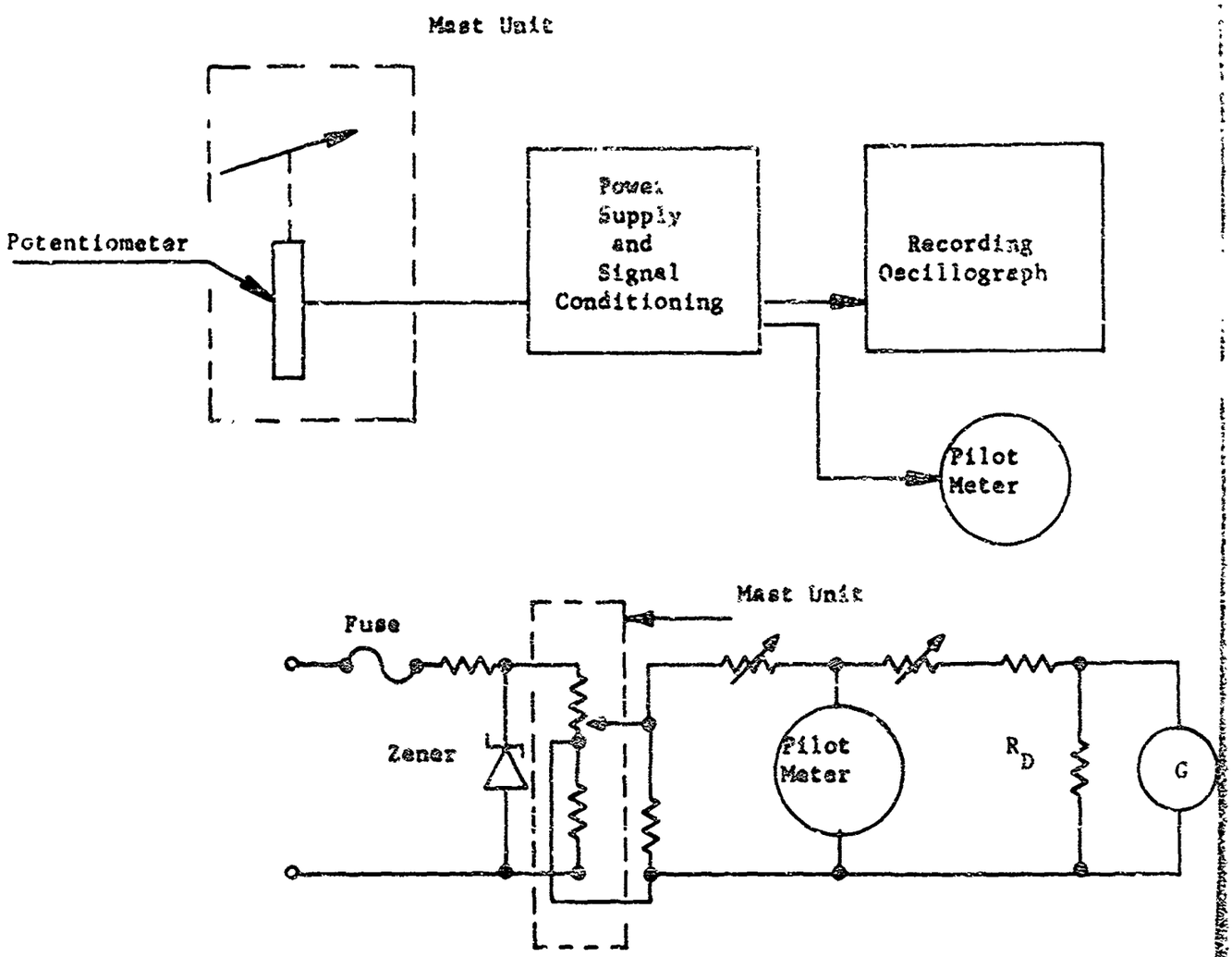

Figure 5-5. Resultant Wind Direction Indicator

For calibration purposes, the assembly was tipped to known angles, along appropriate axes; and the results were recorded.

7. Water Direction Indicator

A trailing wire connected to a potentiometer was used to indicate the relative direction of the craft to the water. Although simple in concept, some difficulty was encountered in properly damping the wire. Further, the method was not satisfactory for overland tests.

Calibration of the water direction indicator was accomplished by recording various known angles of the trailing arm.

C. INSTRUMENTATION INSTALLED IN THE WORKBOAT

1. Water Current Meter

A surface water current speed measurement device was required for the tests. The instrument contruction was similar to a conventional taff-rail log; the current velocity was recorded on a strip-chart recorder. Although a direct indication of water speed was desired, the method employed offered sufficiently greater calibration stability to justify a simple, manual data reduction.

The mechanism consisted of an impeller and a rotating magnet mounted on a common shaft. The shaft had pointed ends that form simple but low-friction bearings. As it rotated, the reed switch was operated by the rotating magnet. The unit was mounted on a finned boom that pointed it into the current. The entire assembly was supported below the surface by a float; a line (actually the signal-carrying wire) connected the float to the attending anchored boat with its associated instrumentation.

Several methods were considered for converting the output of the reed switches to useful recorded data. The reed switch employed had insufficient capacity to carry high instantaneous currents, because the simplest method for integrating required the switch to discharge a capacitor rapidly, some form of isolation was indicated. Further, conventional integration methods required table circuit components and power supplied, if long-term precision was desired. The method employed provided maximum calibration stability.

The reed switch operated a Schmitt trigger whose output drove a simple binary counter. A front panel switch selected a stage output compatible with the recorder bandwidth during the test period. The record was thus a precise total

count of impeller revolutions divided by a known power of 2, versus time. From this data, after initial calibration, average water current is easily computed.

Calibration of the Republic water current meter was accomplished by pulling the device through still water. Several distances and times were used for the calibration, the results of which are summarized in Figure 5-6.

2. Wave Buoy

Two wave-height measuring staffs were constructed and successfully operated in this program. Both employed a buoyant wave staff anchored to the sea floor. The first staff had its center of gravity above its center of buoyancy; the second unit, which was considered more successful, had a lower center of gravity than center of buoyancy and a much lower overall weight. This greatly facilitated installation in the water.

Two measurement techniques were employed: one incremental, the other continuous. Both methods were satisfactory, although the continuous system appeared preferable. Several methods were investigated for measurement of wave heights, including acceleration, acoustic, pressure, and direct-displacement measuring systems.

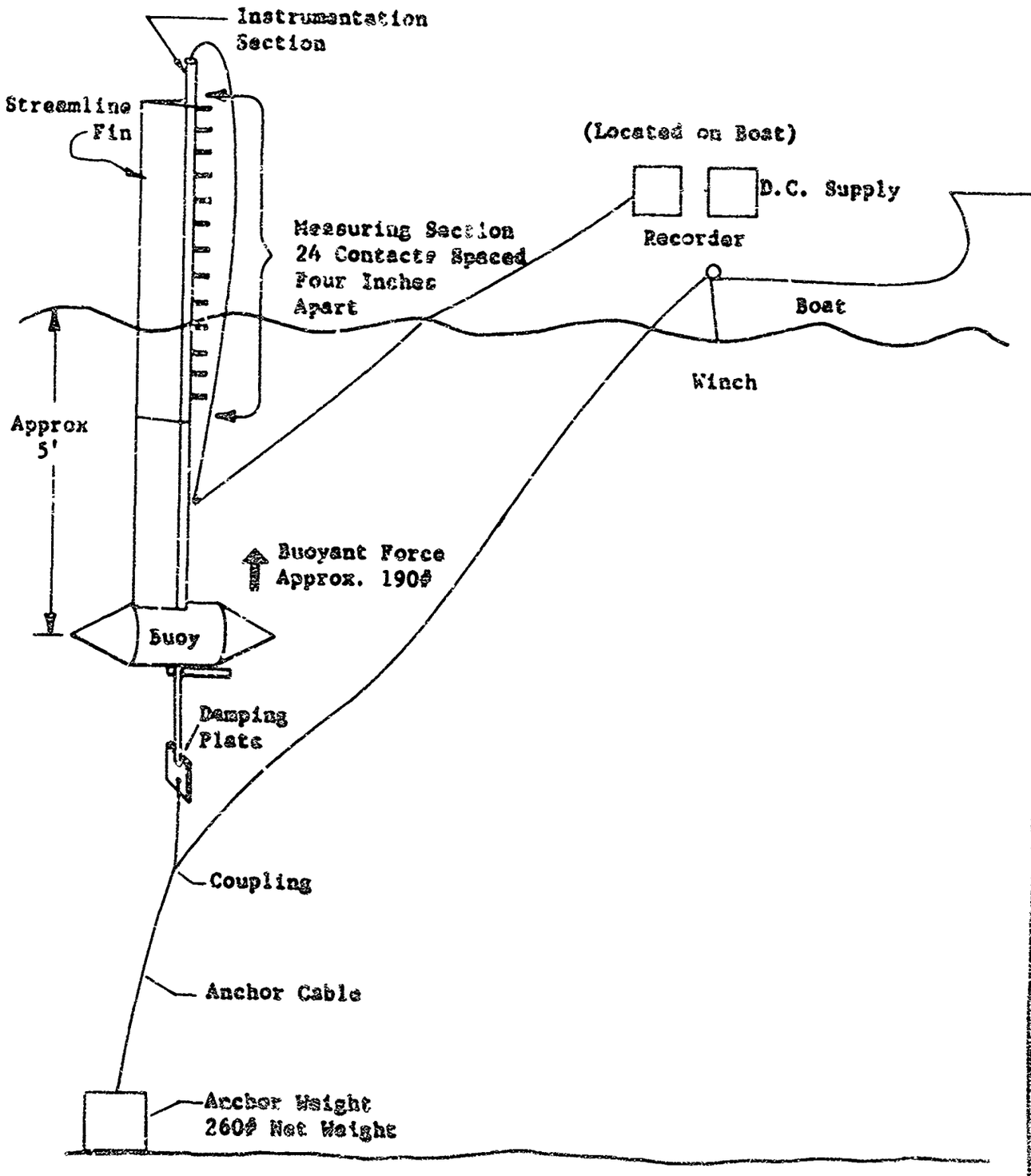

Figure 5-7. Wave Height Measuring System A

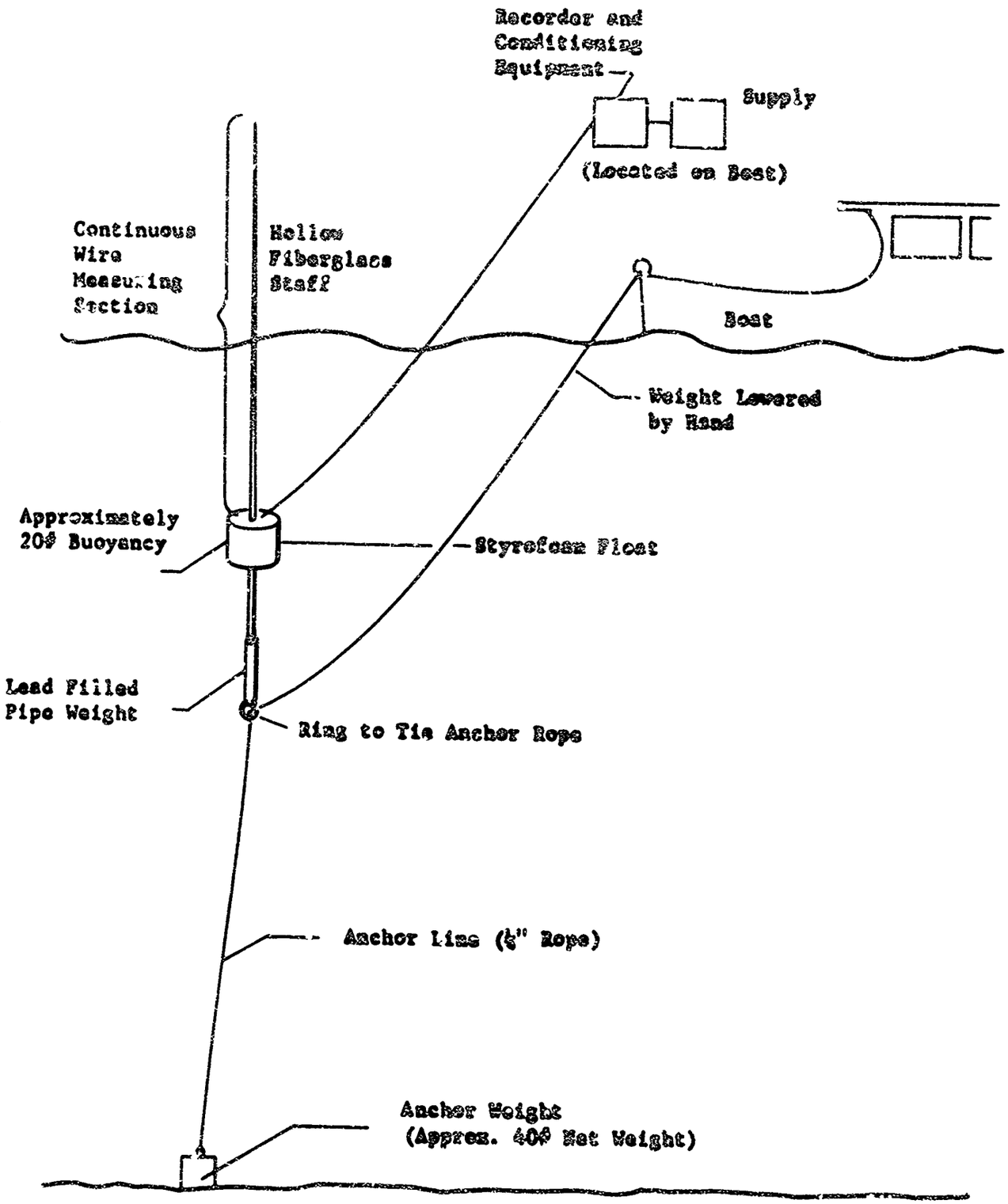

Figure 5-8. Wave Height Measuring System B

distance between the sea floor and the measuring section but also keeps the measuring section vertically. Thus, the result is a reasonably close approximation of a long pole driven into the sea floor. Water level changes on the measuring section are converted to electrical signals, which are then recorded on a strip-chart recorder.

Two methods of instrumenting the wave staff were employed. Figure 5-9 illustrates the method employed on the first buoy. Electrical contacts were spaced four inches apart on the measuring section. Each contact was connected to a transistor that was normally turned off. When the contact was covered by water its transistor was on; When the contact was out of the water, its transistor was off. The recorder simply measured the total collector current of the transistors. Because the record was incremental, it was possible to calibrate the system from the data directly.

The second system used (Figure 5-10) was easier to implement than the above but required more careful calibration. This method used a simple resistance wire, glued to the measuring section. This wire formed one arm of a Wheatstone bridge, the remainder of which was placed on the attending

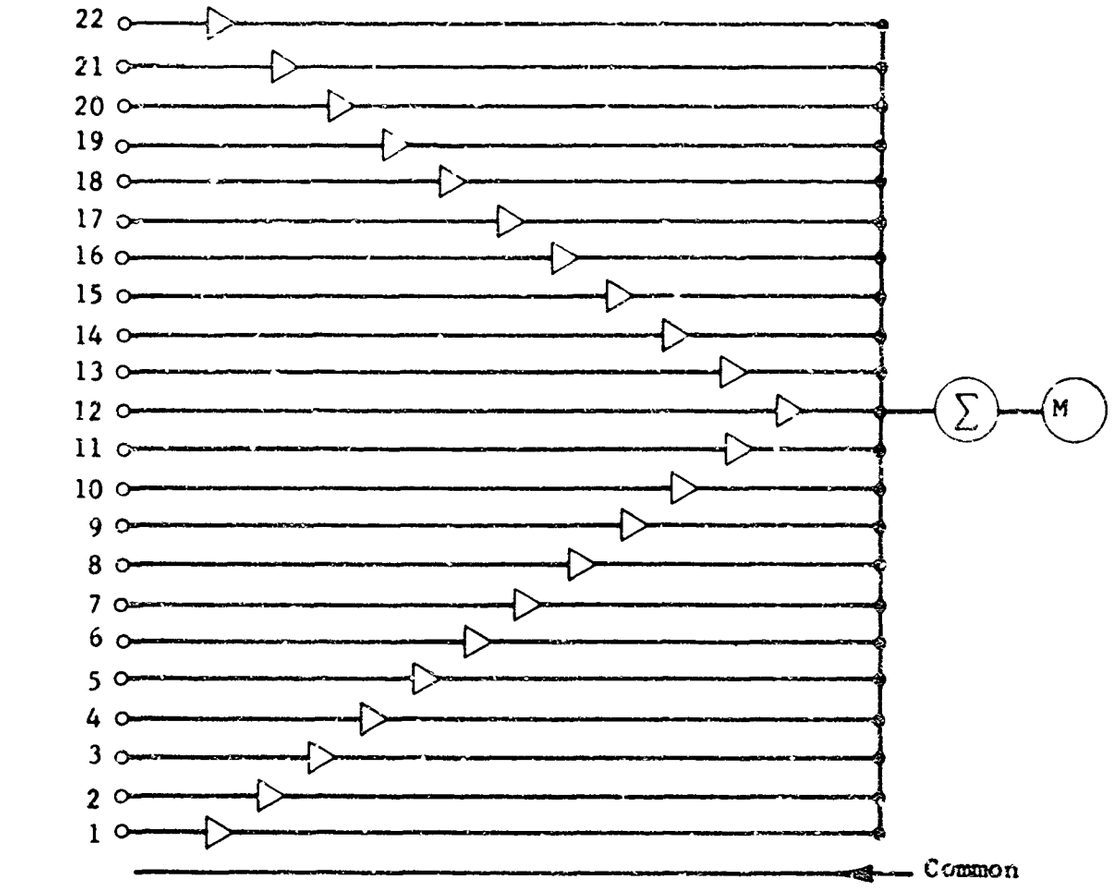

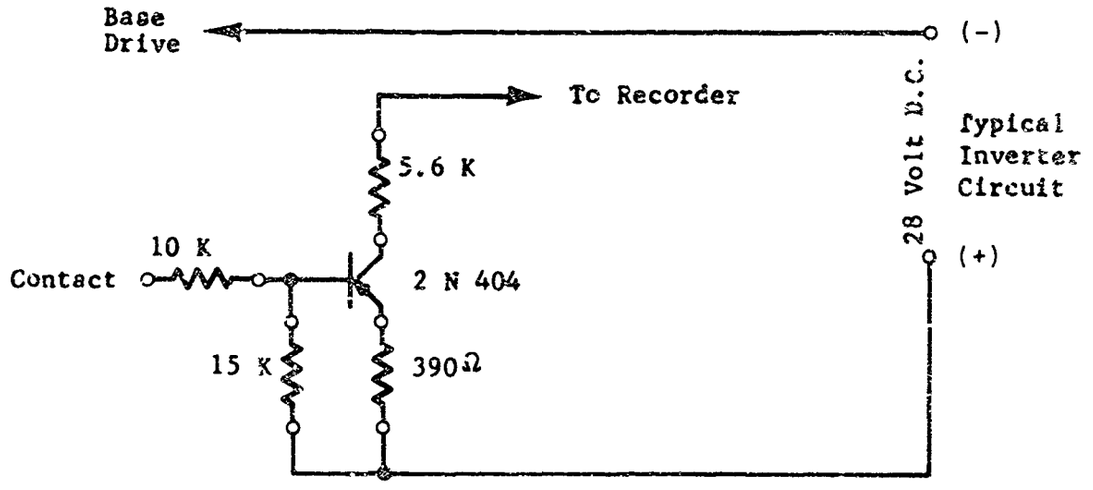

Figure 5-9. Wave Meter Circuits

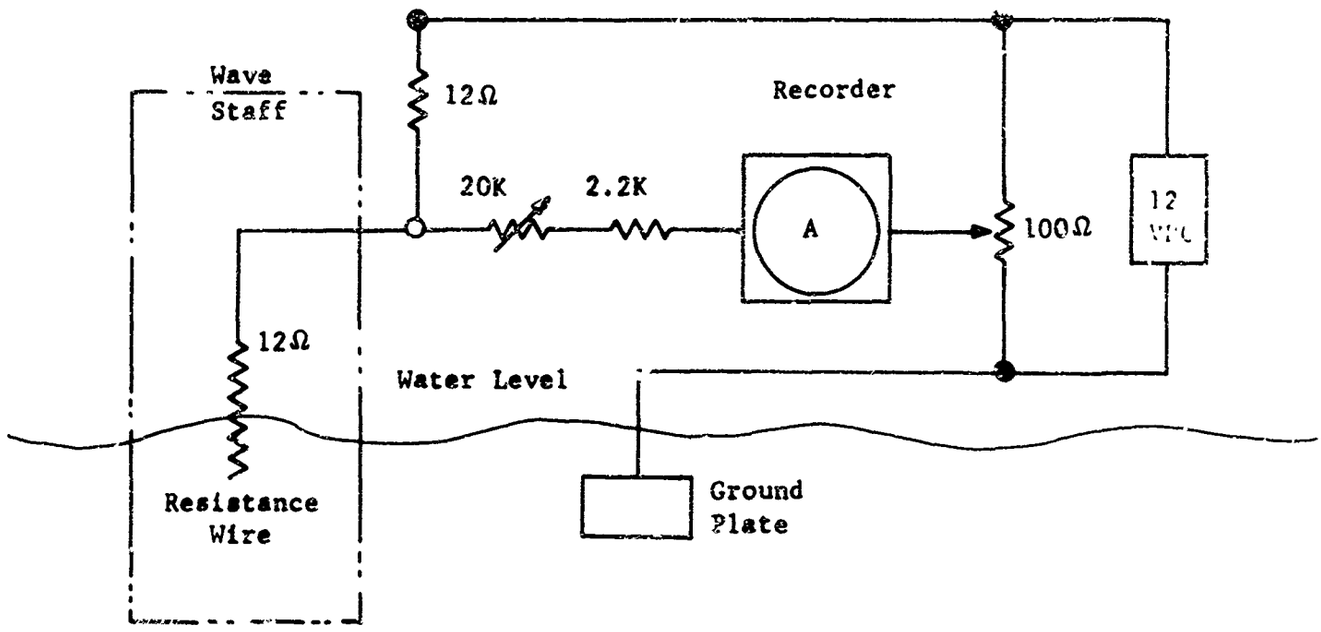

Figure 5-10. Wave Meter Circuit -- Continuous Measurement System

boat. As the water rose on the measuring section, the wire was, for practical purposes, shorted by it. This change of resistance was then recorded on a strip-chart recorder.

Calibration of both systems was accomplished by immersing the staffs in still water to a known depth and adjusting the recorded results. The contacts themselves were used as a scale on the incremental device; painted strips were used on the resistance wire unit. On the latter, a regulated supply in addition to fairly high detector impedance produced satisfactory system linearity. The recorder used had a sensitivity of 1 ma over a 50-division full-scale. Chart width was about 2½ inches. The measuring portion of the wave staff was 96 inches. The chart can be read to ½ a division. Therefore, it is possible to distinguish a difference in wave heights of 1 inch or greater.

The wave staffs operated by Republic functioned satisfactorily under various sea state conditions. Experience indicates that a high buoyant force and a low center of gravity are desirable; however, the high buoyant force must be offset by large anchor weights, which makes insertion more difficult.

In water bodies where appreciable water currents are present (over 5 knots), it is probable that this method would not be satisfactory. Excessive drag forces on the buoy tend to submerge it. This has not been a serious limitation in the GEM tests because fairly low currents have been measured in the test areas.

D. CALIBRATION OF DOPPLER SPEEDMETER

The doppler speedometer was calibrated over a measured course for craft speeds between 7 and 40 knots. Yaw angle, wind and water currents, and total elapsed time were used to correct the recorded data. Figure 5-11 shows the resultant oscillograph trace calibration as a function of true craft water speed.

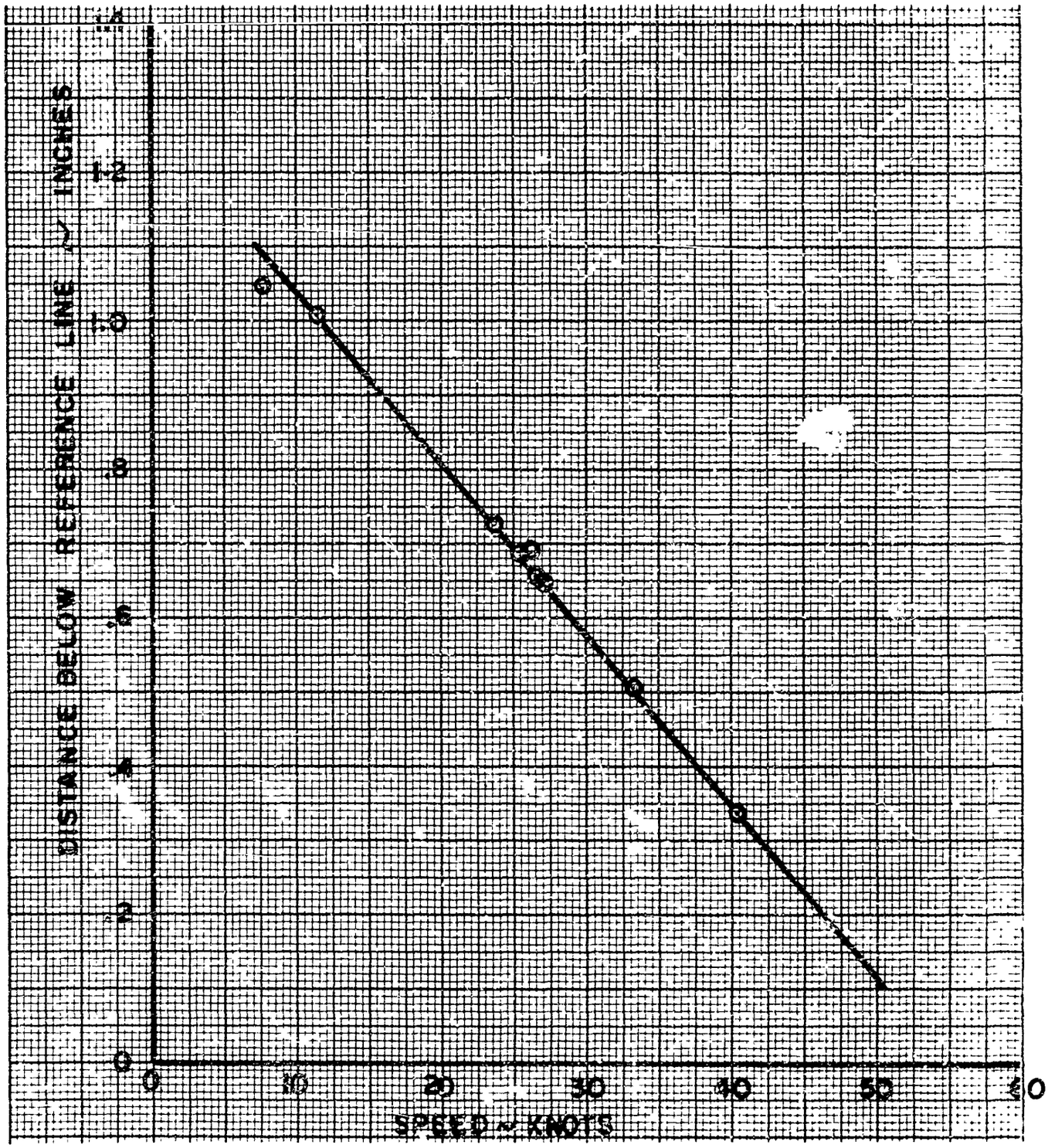

Figure 5-11. Doppler Speedmeter Calibration

TABLE 6-2. LIFT SYSTEM

Component	Required Data
Engines: Two Turmo 603 gas turbines, each rated at 380 hp	a) Jet pipe temperature b) Gas generator rpm c) Free turbine rpm
Fans: Two Dowty-Rotol 11-foot diameter fans	Velocity profiles upstream of fan inlet

It should be noted that operation of the propulsion engines is always at a power turbine speed of 34,000 rpm, thus providing a constant propeller speed, through the 28.5:1 gearbox ratio, of 1192 rpm. Power and thrust variation is accomplished by modulating the propeller blade angle.

The lift fan inlet instrumentation was not installed during normal test operation but was used to determine the lift system characteristics during static tests.

In addition to the operational characteristics of the lift and propulsion systems, which were derived with the above required data, the craft drag characteristics were obtained. Before discussing these results, it is appropriate

to examine the engine characteristics because the availability of power is fundamental to the operation of all systems.

2. Description of Engines

Table 6-3 summarizes the characteristics of the VA-3 power plants.

TABLE 6-3. POWER PLANT DATA

	Propulsion	Lift
Air mover	10-ft Dowty-Rotol propeller per engine	11-ft Dowty-Rotol fan per engine
Engine designation	Artouste IIC	Turmo 603
Manufacturer	Turbomeca (France)	Blackburn (England)
Type of power	fixed shaft turbine	free turbine
Engine length x diameter	57 x 24	60 x 24
Engine weight, pounds	317	
Maximum continuous rating, hp	465	380
SFC at maximum continuous power, (lb/hr)/bhp	1.15	1.10
Power turbine speed, rpm	34,000	22,300*
Turbine speed reduction, prop or fan	28.5	62

TABLE 6-3. POWER PLANT DATE (cont'd)

	Propulsion	Lift
Propeller or fan speed, rpm	1192	360
Propeller or fan tip speed, ft/sec	625	208
Maximum continuous power available to propeller or fan, horsepower	400	300
SFC at matched maximum power, (lb/hr)/bhp	0.95	1.11

* Lift engine operation corresponds to installed jet pipe temperature limit

Because the lift engines are equipped with free turbines, they can supply a range of power requirements at a constant output shaft speed. The propulsion engines are fixed-shaft turbine engines and can supply only one power at any shaft speed.

The engine performance characteristics are presented in Figures 6-1 and 6-2,which include the manufacturers' stipulations governing engine operating limits. The performance shown corresponds to the manufacturers' estimate of a new, "average" engine. This performance has been reduced somewhat

SHAFT HORSE POWER

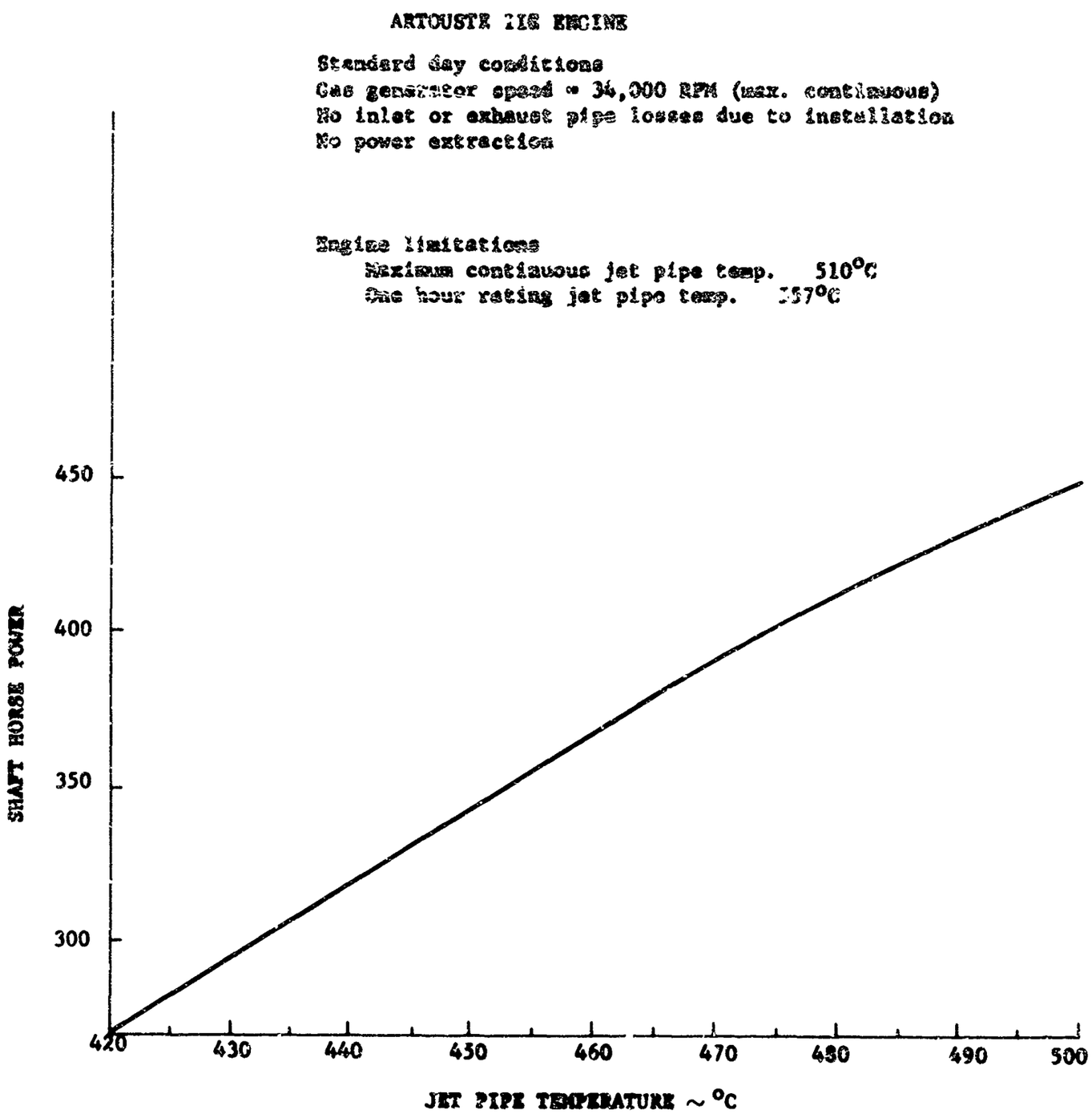

Figure 6-1. Propulsion Engine Performance

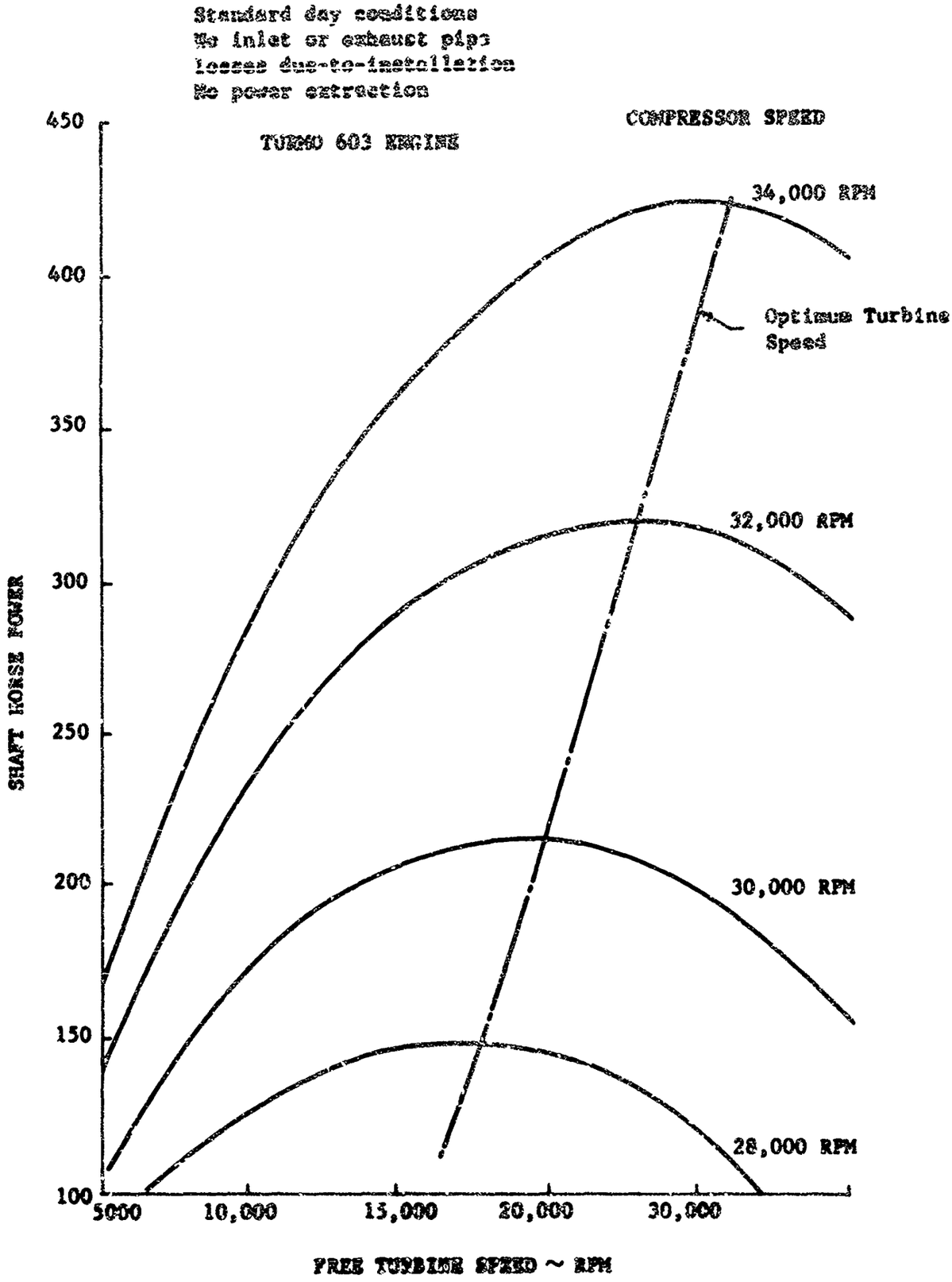

Figure 6-2. Lift Engine Performance

due to long periods of operation in a corrosive environment as well as due to the normal degradation resulting from continued use. There have been a total of six propulsion engines and four lift engines installed in the craft during the sea trial program. Tables 6-4 and 6-5 list the total operational time for these engines since their manufacture, in the order of their installation during the program.

TABLE 6-4. PROPULSION ENGINES

(Artouste IIC)

	Serial Number	Total Time (hours)
Port Engines	276	54.5
	296	52.5
	409	55.4
	230	8.5
Starboard Engines	277	51.75
	107	113.8

TABLE 6-5. LIFT ENGINES
(Turmo 603)

	Serial Number	Total Time (hours)
Forward Engines	5024	99.15
	5018	58.3
Aft Engines	5014	108.25
	5022	36.5

The tables indicate that the propulsion engines have been averaging on the order of 53.5 hours before removal, and the lift engines have been averaging twice as many hours. Apparent causes for this are as follows: The propulsion engines are located externally and are relatively susceptible to the effects of salt water spray, while the lift engines are located inside the craft structure, relatively remote from the salt water environment. In addition, stalling the propulsion engines under high loading conditions (sudden accelerations) and sporadic operation at high jet pipe temperatures (1240°F) have depreciated propulsion engine performance considerably. It has been documented* that operation at turbine inlet temperature above 1600°F induces

* G.L. Graves, "Gas Turbines for Unconventional Craft", SAE Paper 685A, April 1963

corrosion of engine parts, thus limiting engine life. Therefore, the results of operating in a marine environment with an engine that is not marinized causes performance degradation that in turn requires frequent operation at maximum power (high temperatures), thus accelerating the rate of degradation.

Two steps were taken to minimize these effects in the VA-3: washing the "hot sections" of both engines with fresh water, and limiting lift engine loadings to be consistent with a maximum jet pipe temperature of 1120°F or 1200°F, depending upon the particular engines in use.

In general, the adverse effects of operating gas turbine engines in a marine environment can be reduced or eliminated by employing any combination of the following steps:

1) Provide a marinized engine that has been proved to be capable of high performance during long service

2) Provide an over-sized engine so that the continuous operating power requirement corresponds to a sufficiently low turbine inlet temperature to preclude corrosion effects

3) Locate the engines as far from the marine environment (salt water spray) as possible, consistent with ease of accessibility

4) Require fresh water washing of the engine hot sections at suitable intervals

3. Propeller Characteristics

Although no testing of the propellers was performed during the program at Montauk, the results of propeller tests conducted by Vickers-Armstrong Limited were made available to Republic. Wind tunnel tests by the propeller manufacturer, Dowty-Rotol, have provided the thrust-speed characteristics corresponding to operation in an unobstructed free stream; these characteristics are presented in Figure 6-3 for a propeller rotary speed of 1192 rpm, which corresponds to the engine operating speed of 34,000 rpm. The thrust speed characteristics of the propellers operating on board the VA-3, obtained by mounting the nacelles upon strain gages, were determined by Vickers-Armstrong engineers prior to the craft's arrival in this country. These characteristics are shown on Figure 6-4 and include the effects of propeller airflow blockage by

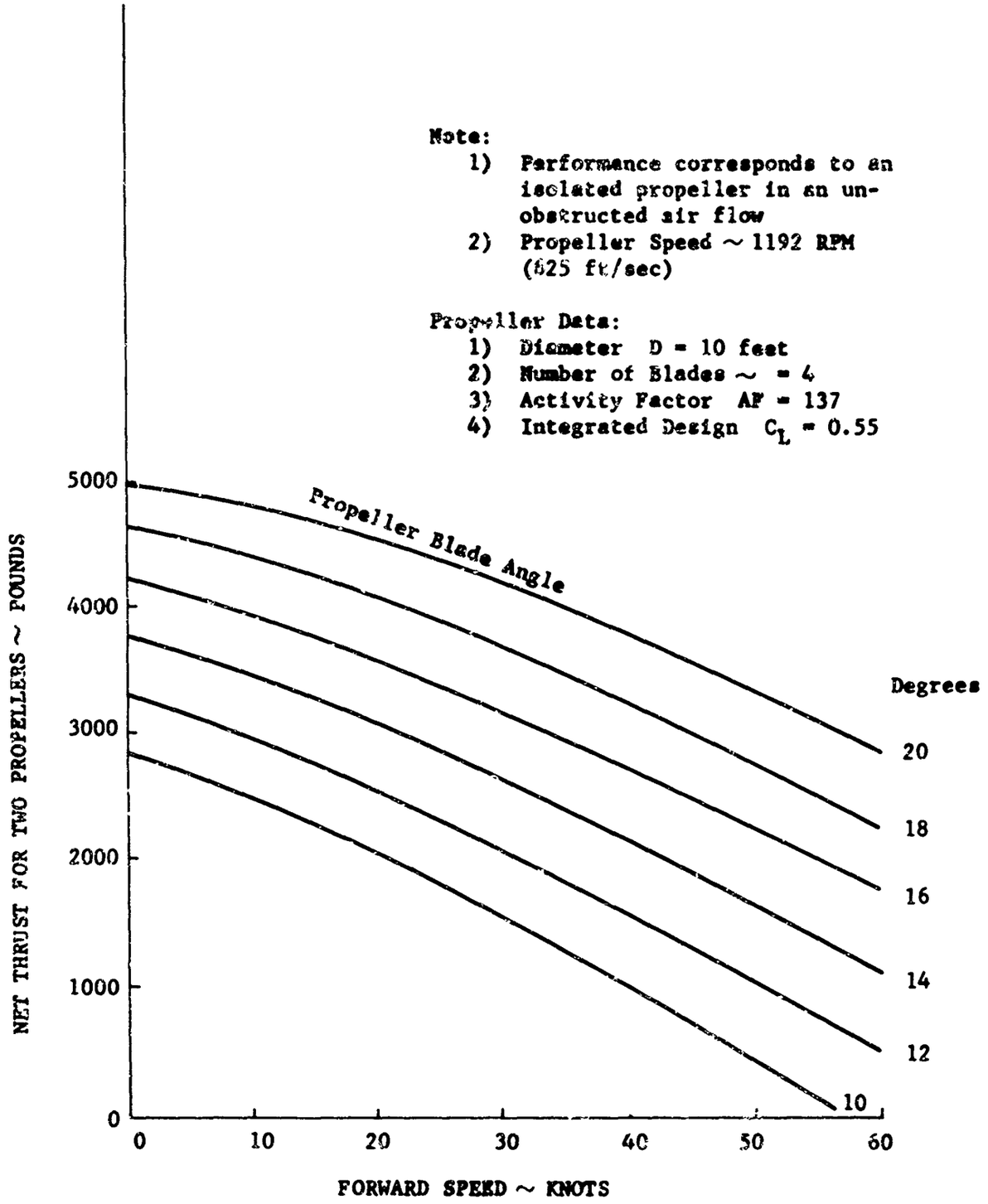

Figure 6-3. Propeller Performance — Manufacturer's Performance Estimates

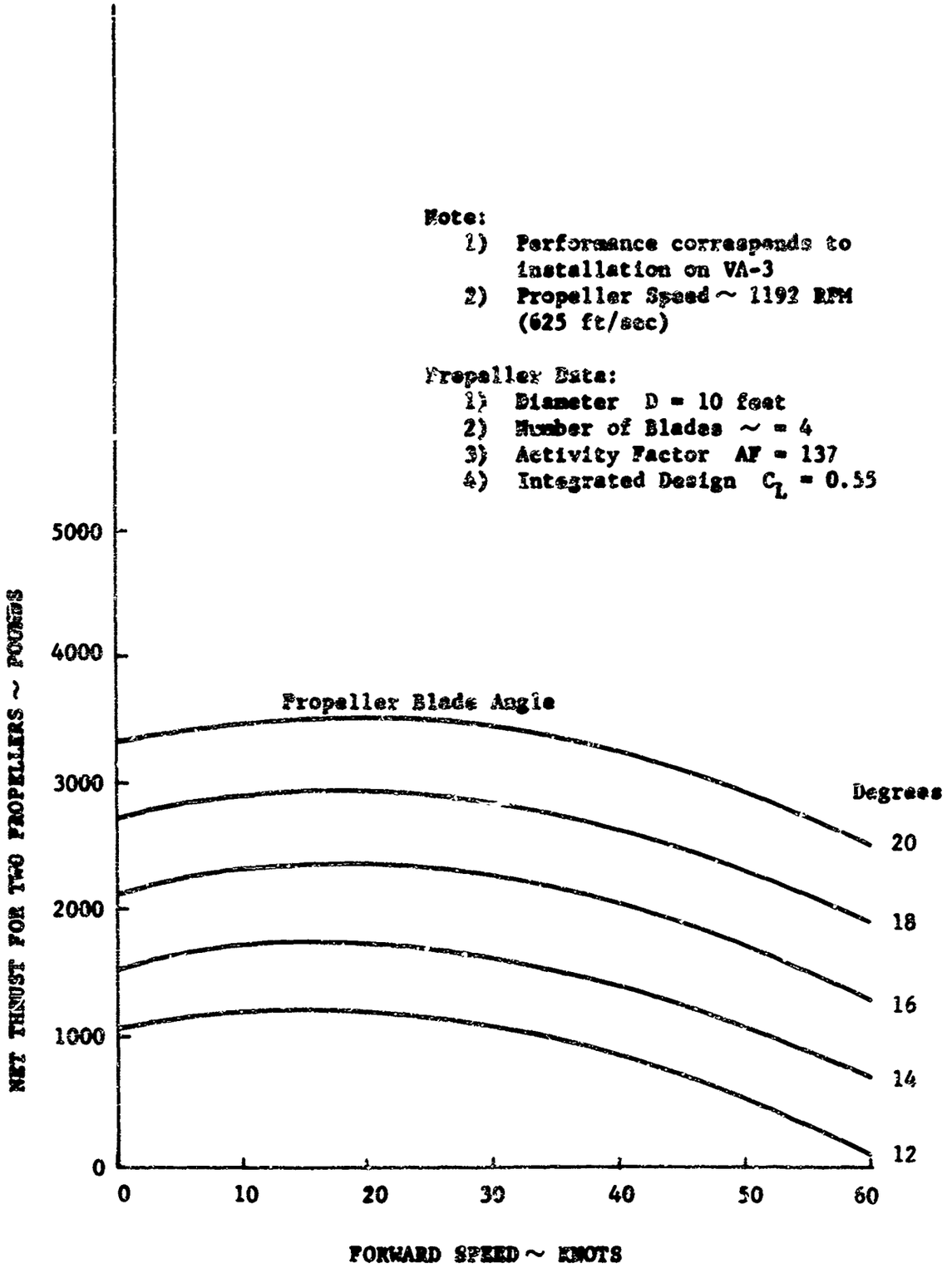

Figure 6-4. Propeller Performance — Results of Test Data

the superstructure and the fan airflow streams. It is important to note that even when the craft is operating straight into the wind, thus minimizing propeller blockage by the fan airflow streams, the superstructure and nacelle supports blank out 15 per cent of the propeller disk area.

A comparison of Figures 6-3 and 6-4 has been made to determine the effect upon thrust of the blockage caused by the propeller installation. Figure 6-5 shows the results of this comparison in terms of the fraction of the manufacturer's estimate of thrust that has not been realized on the VA-3 installation. It is seen that the greatest losses occur at the lower blade angles. This is reasonable in view of the fact that, because low blade angles dictate low total pressure rises across the propeller, a given total pressure deficit upstream of the propeller will induce a relatively large reduction of total pressure rise for low angle settings. This is directly responsible for a loss of thrust, because thrust equals propeller disk area times the pressure rise.

Adequate performance of the VA-3 is obtained even though the installation losses are relatively large. This is the result of good preliminary design and indicates that Vickers engineers were aware of the order of installation

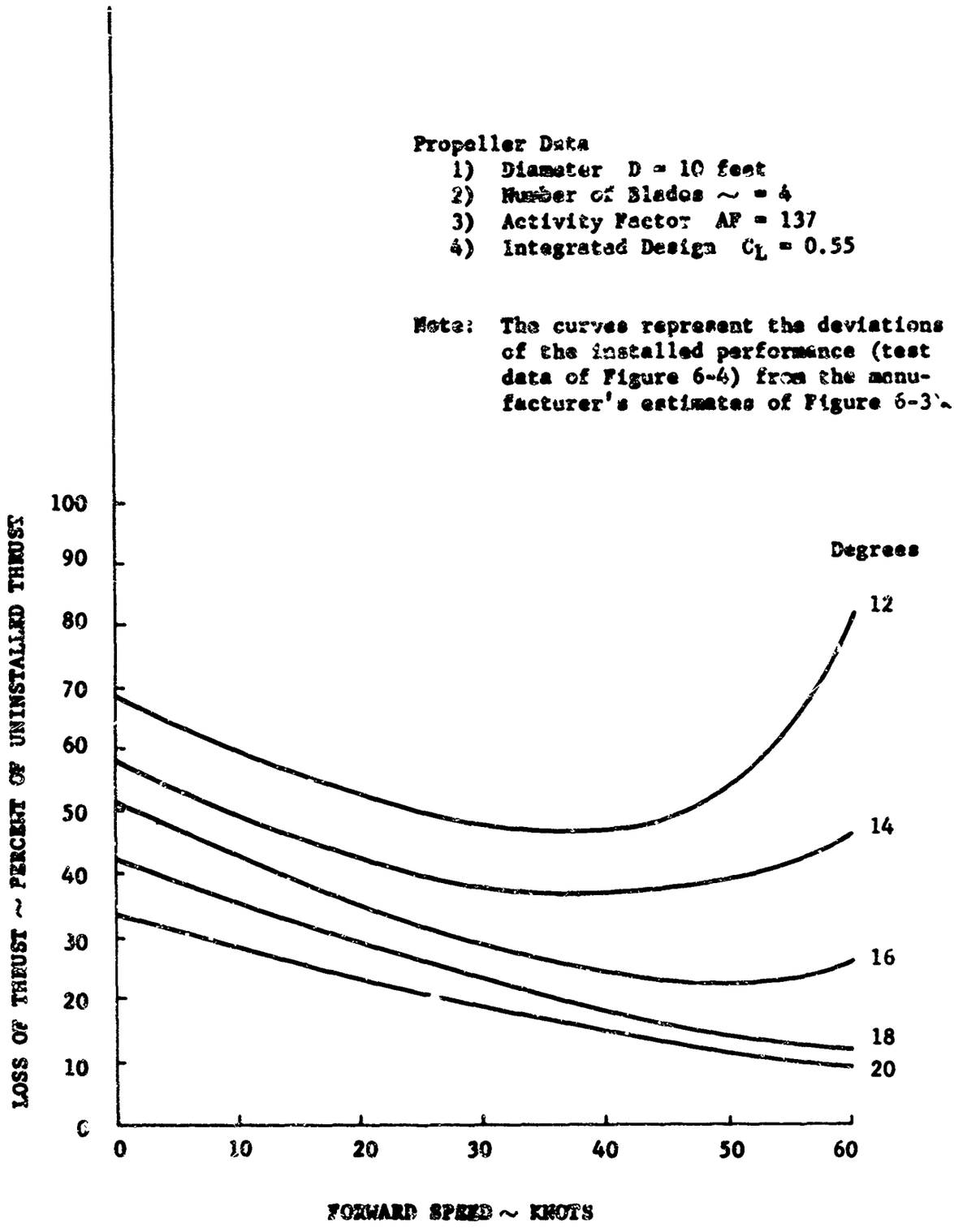

Figure 6-5. Propeller Performance -- Thrust Loss Due to Installation Effects on VA-3

losses that would be incurred in the preliminary stages of the VA-3 development.

The drag characteristics and other aspects of craft performance will be discussed in Section VIB of this report. A key element in the derivation of these characteristics is the propeller thrust-speed characteristics, which have been used in conjunction with the reported values of propeller blade angle and relative wind speed to determine total thrust delivered.

To establish the tolerances of error corresponding to calculated results,it is necessary to determine the individual errors of the factors used in any calculation. The accuracy with which the propeller blade angle is reported has been determined by comparing a direct measurement of angle, using a protractor, with a corresponding oscillograph reading. The resulting calibration provides a means for reducing oscillograph traces made during test runs to useful information,and it establishes the maximum possible error in blade angle. Figure 6-6 presents the blade angle calibration of the port propeller; the starboard propeller calibration is almost identical. The spread of data is considered to be representative

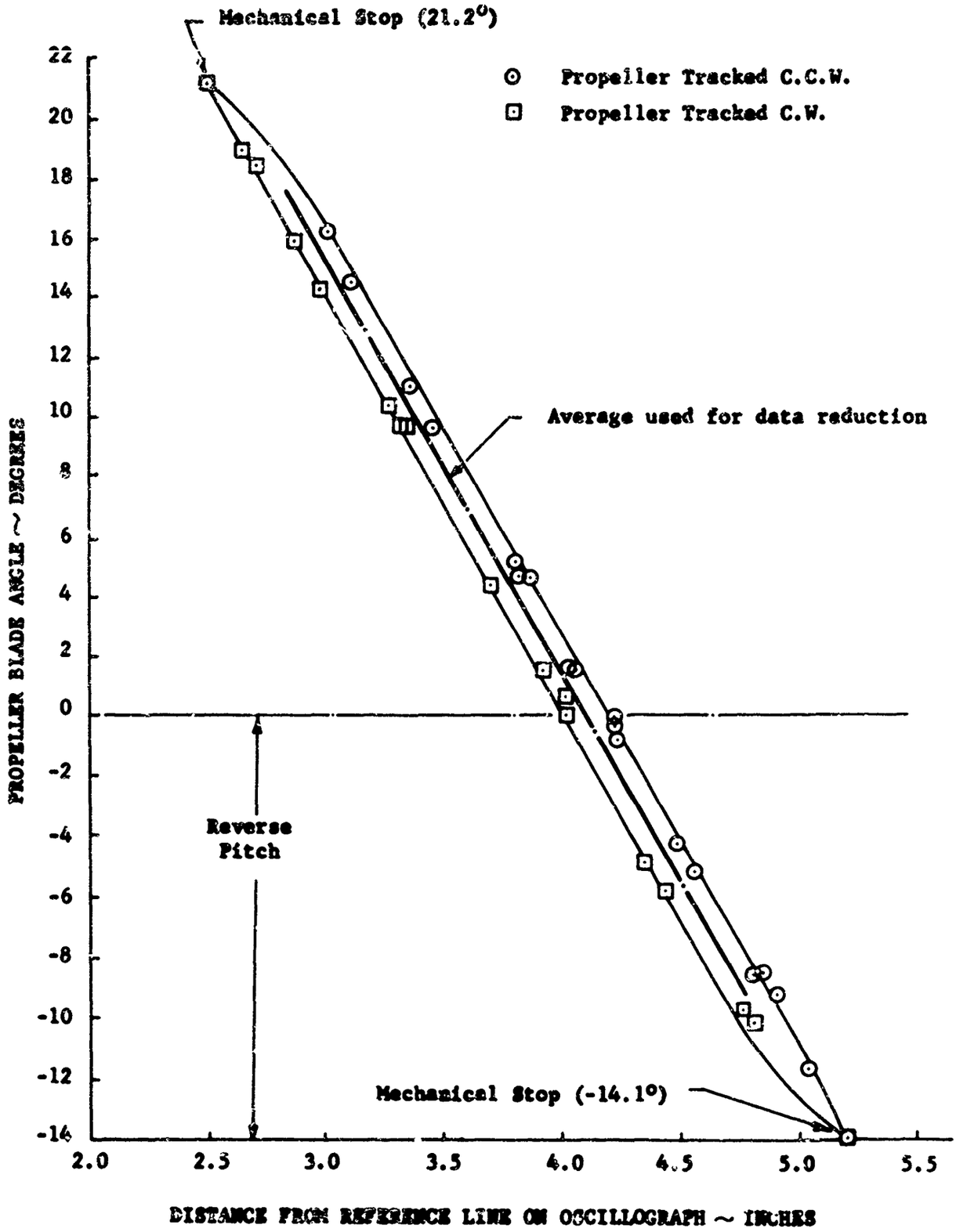

Figure 6-6. Port Propeller Blade Angle Calibration

of the maximum scatter of data due to such factors as hysteresis and oscillograph scale error. A maximum error of about 1 degree of blade angle is indicated, based upon using the centerline of the data spread. This corresponds to a maximum error of about 300 pounds of thrust for both propellers, based upon the characteristics of Figure 6-4. Therefore, based upon the craft drag characteristics in still-air conditions, the maximum possible error in drag calculated from test data is 22 per cent at 15 knots and 6 per cent at 50 knots, assuming that the relative wind speed measurements are exact.

4. Lift System Performance

The lift system of the VA-3 includes the following components:

1) An air induction system that captures air from the free stream, bends it 90 degrees into a vertical plane, and delivers it to the fan inlets

2) Two lift fans that increase the total energy of the inducted air flow to overcome system flow losses and to provide a cushion pressure that supports the vehicle

3) An annular jet nozzle, located around the periphery of the vehicle, that ensures an adequate distribution of the energized airflow and, consequently of the cushion pressure

4) Two engines that provide the power source for the lift fans

The net effect of the systems operation is to provide an air cushion under the vehicle, of sufficient thickness to separate the "hard structure" from the water surface by a significant distance. During its initial sea trials in England, the VA-3 had no flexible extensions below the "hard structure" and the greatest separation distance was on the order of 10 inches. The addition of a 36-inch flexible extension to the annular jet, just prior to the VA-3's arrival in this country, provided a maximum separation between the "hard structure" and the water surface (called rise height) of approximately 38 inches, thus significantly improving the vehicle's operational flexibility. This addition enabled operation in sea states up to and including 3, and in 7-foot surfs.

The curves of Figure 6-7 present the rise height characteristics of the present configuration based upon Vickers-Armstrongs test data. These curves show that the variation of rise height with gas generator rpm and gross weight is approximately linear.

It is common practice to present the performance characteristics of a fan-duct system on a supply-and-demand basis. The fan performance characteristics are considered the "supply", and the system flow characteristics represent the "demand". When curves that describe the "supply" and "demand" characteristics are superimposed, the intersections of these curves define the locus of "matched" operating points.

The operating characteristics of the VA-3 lift system are presented on Figure 6-8. The fan or "supply" curves are based upon the fan manufacturer's performance data, and the "demand" or system flow characteristics have been generated by obtaining velocity profiles in the fan inlet during the Montauk tests. Two important points should be noted:

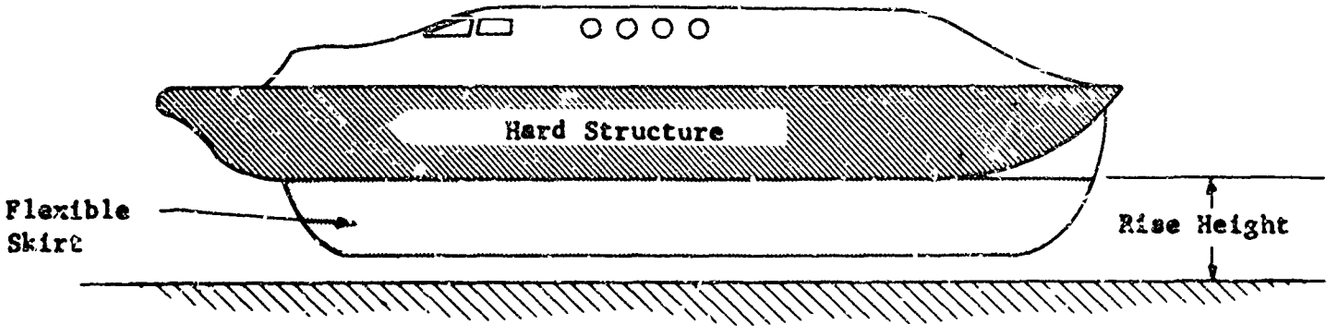

Note:
Data Corresponds to
Standard Day Operation

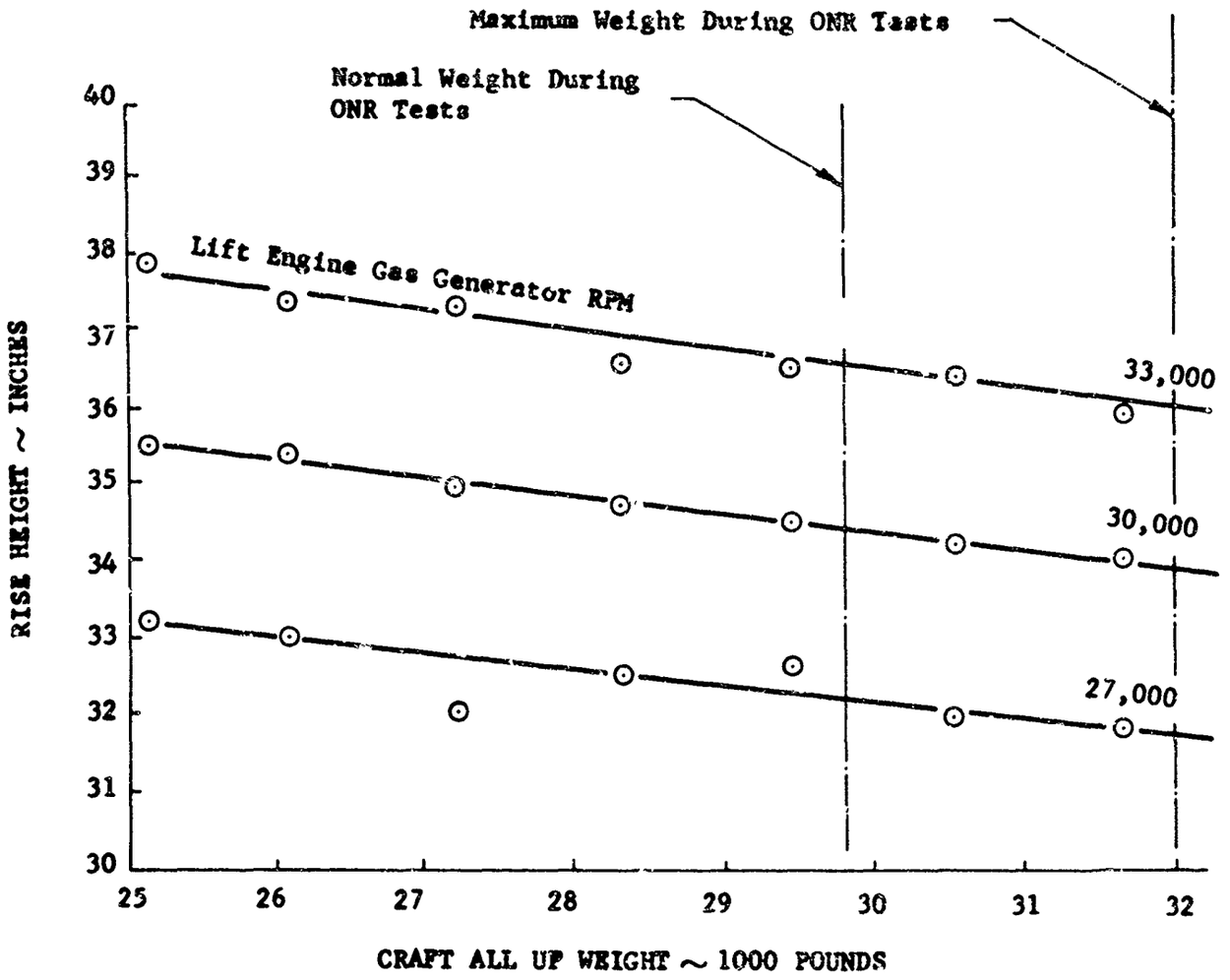

Figure 6-7. Rise Height Characteristics of the VA-3

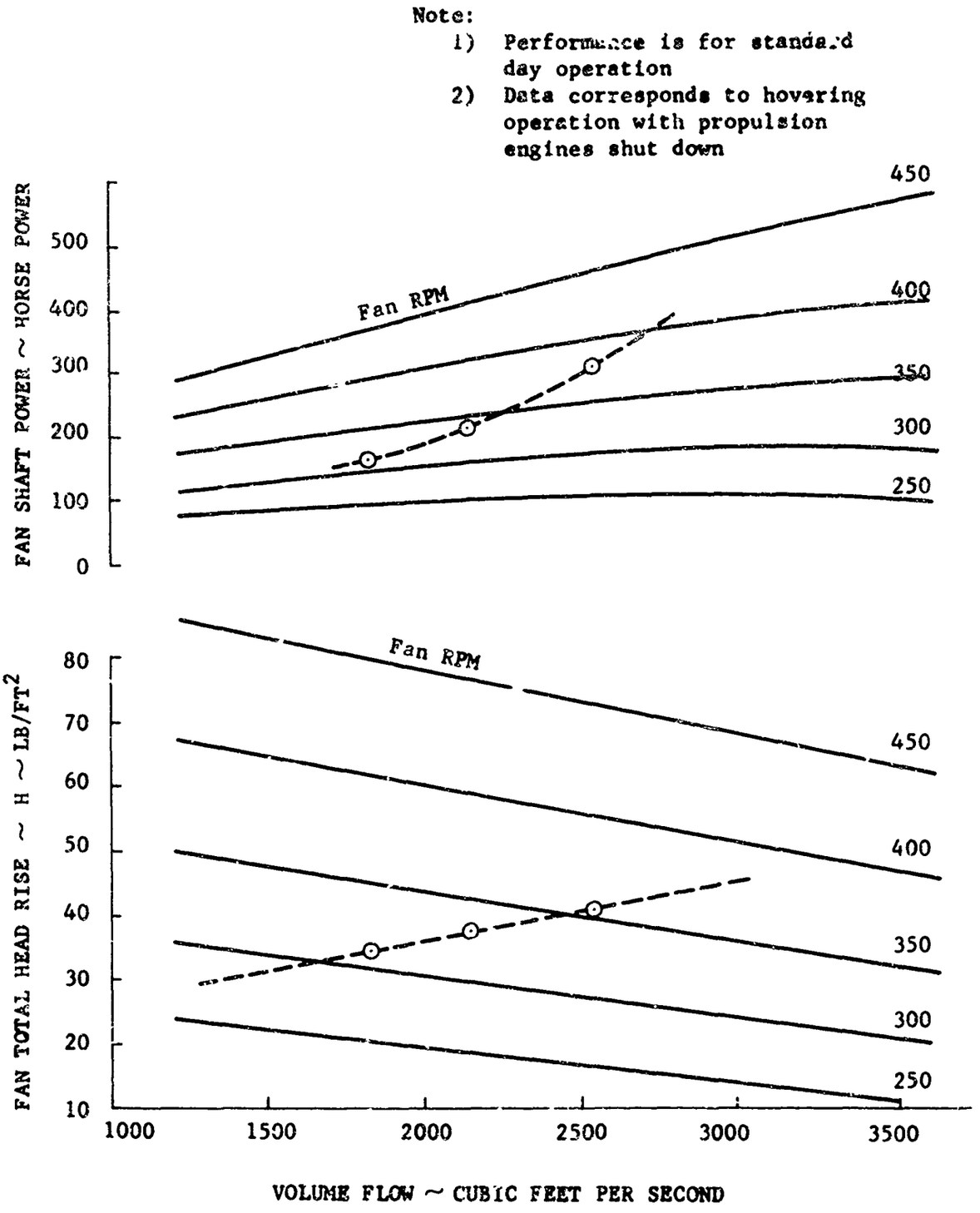

Figure 6-8. Lift System Performance Characteristics

1) The largest power delivered corresponds to operation at the limiting jet pipe temperature and is significantly lower than the maximum rating of 380 hoursepower

2) Because the data of Figure 6-8 corresponds to a gross weight of 28,500 pounds and the cushion area is 1,024 square feet, the cushion pressure is 27.8 psfg. Therefore, the data of Figures 6-8 shows that the system total pressure loss varies from 6 psf to 13 psf, within the range of airflows tested

The two most probable reasons for the decrement in engine power are deviations of individual engine performance from the "average" estimated performance of Figure 6-2 and the effects of the marine environment. Information received from Vickers-Armstrongs Limited indicates that shaft horsepower deviations of up to -15 per cent of the specification values are possible.

The system total pressure loss data indicates that the internal flow path is a relatively efficient one. The total pressure-loss characteristics of ducts containing

relatively low-speed flows are generally described by a nondimensional coefficient, which is the ratio of the total pressure loss, ΔP_T , to the incompressible dynamic head at any reference station, $\frac{1}{2} \rho V_{ref}^2 = q_{ref}$. When Reynolds number effects are relatively insignificant, this coefficient is approximately independent of the flow rate. The results of analyzing the data of Figure 6-8 indicates that the VA-3 lift system characteristic may be described by a coefficient of $\Delta P_T / q_{inlet} = 1.25$.

Hovering of the VA-3 with one lift unit shut down was conducted to determine the effect of an assymetrical airflow distribution upon hovering attitude. Measurements of hover height and craft inclination angle were not taken; the qualitative results are felt to be quite useful and inexpensive.

Initial tests did not include any attempts to seal the inlet of the shut-down unit. In this mode, when the operative unit was run at its maximum power, the VA-3 could not hover. The same result was noticed with either forward or aft lift engine shut down. When the forward fan was shut down and its inlet sealed, however, the vehicle hovered at a relatively level attitude corresponding to approximately the height

that was normally attained with both engines operating at half of maximum power. A nose up attitude was produced when the aft engine was shut down and the inlet sealed; however, this was expected since the test configuration had the center of gravity approximately 3 inches aft of the geometric centerline of the craft.

B. DRAG ANALYSIS

1. Theoretical Drag Estimates

a. General

Air cushion vehicle drag is comprised of aerodynamic and hydrodynamic components. The analysis performed by Vickers-Armstrongs Limited for the VA-3 follows.

b. Aerodynamic Drag

The aerodynamic drag component has two subcomponents, profile drag and momentum drag. Profile drag can be expressed in the form

$$D_{profile} = C_{D_p} \cdot \frac{1}{2} \rho V^2 S$$

where: C_{D_P} = 0.5, based on wind tunnel test results

ρ = air density (slugs/ft^3)

V = air velocity (ft/sec)

S = surface area, square feet

The initial estimates were based on taking the full momentum drag of the air mass flow required for lift. This results in:

$$D_{mom} = \dot{m} V$$

where $\dot{m}$ is the intake mass flow in slugs/sec, and V is the same air velocity in ft/sec used in the profile drag equation shown above. The air velocity, V, is the sum of the absolute wind velocity and the vehicle velocity relative to the ground or water. Therefore,

$$V = V_D + V_W \quad \text{upwind}$$

$$V = V_D - V_W \quad \text{downwind}$$

where: V_D = relative ground (water) velocity measured by Doppler, ft/sec

V_W = wind velocity, ft/sec

In comparing the data with theory, account must be taken of the wind conditions for each data point. The components given above are shown in Figure 6-9 as a function of V and were used to produce average estimated drag curves for comparison with the test points.

c. Hydrodynamic Drag

Hydrodynamic drag is comprised of wave drag, skirt drag, and spray drag. Visual observations of the VA-3 at speed show that spray is swept sideways along the craft without significant impacting. This factor together with the absence of other concrete information on spray drag for air cushion craft has caused this drag component to be neglected in the estimate for VA-3.

Wave drag depends upon the velocity of the craft relative to the water surface (V_D) and the water depth, and it can be expressed as a function of the craft Froude number, F_N .

$$F_N = \frac{V_D}{\sqrt{g\ell_L}}$$

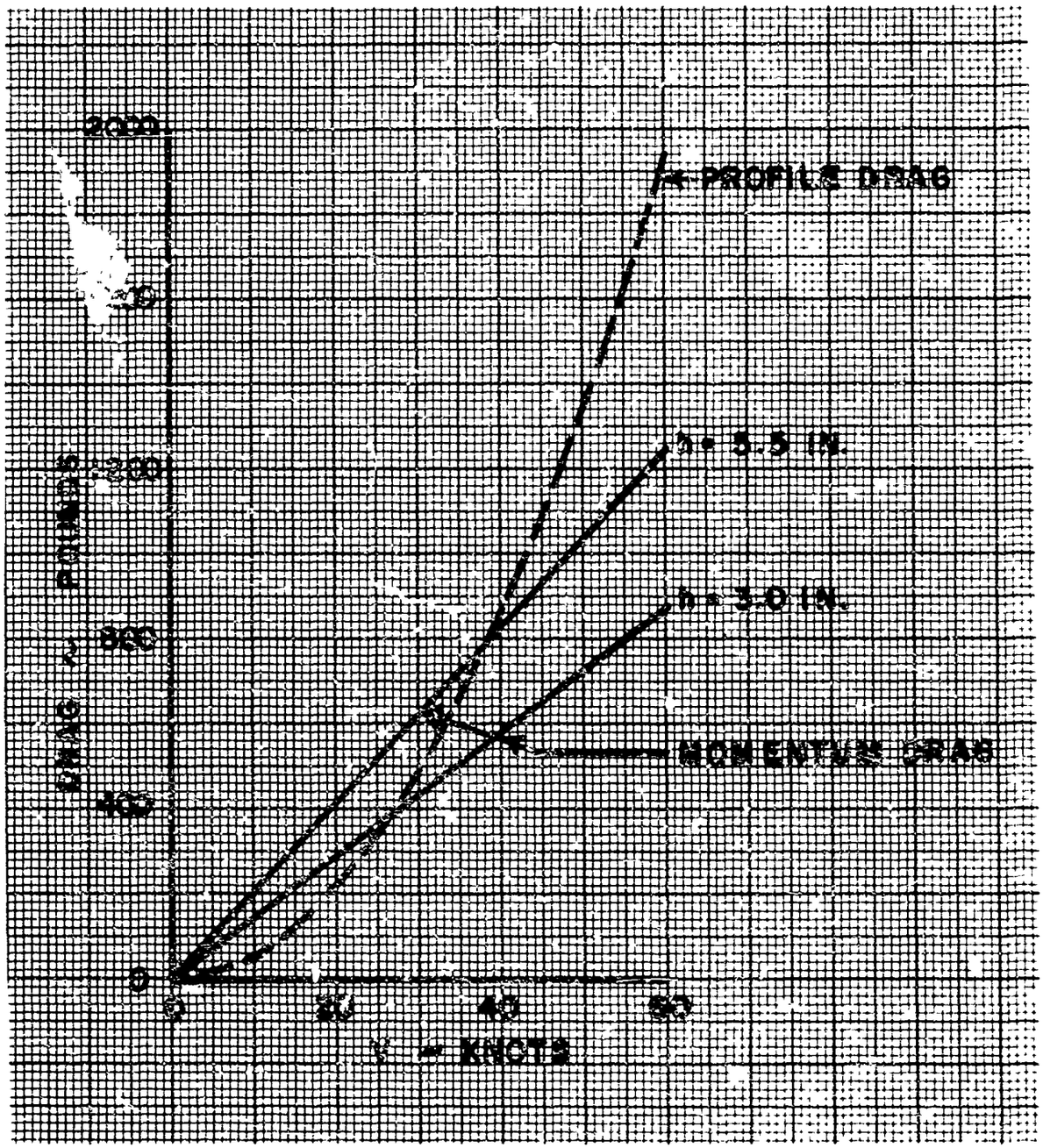

Figure 6-9. VA-3 Aerodynamic Drag Characteristics

where: g = gravitational acceleration, feet/sec^2

ℓ_L = average cushion length at the bottom of the skirt, feet

The tests were conducted over water, with a water depth greater than the craft length (the water was therefore considered deep when estimating the wave drag). The craft wave drag is computed from the analytically derived expression

$$D_W = 0.727 \frac{W_{P_C}}{V_D^2}$$

where: W = craft weight, pound

P_C = cushion pressure, lb/ft^2

Water tank tests of various models have shown that the wave drag is negligible below a Froude number of 0.2 and peaks at a K_N of 0.67, giving a drag value equal to 0.8 D_W. This component is shown in Figure 6-10 as a function of V_D.

An air cushion vehicle in overwater operation will spend a large proportion of its time in wave conditions such that there will be considerable contact between the water surface and the flexible skirts. Visual observations of the type of skirt used on the VA-3 has shown that the skirts

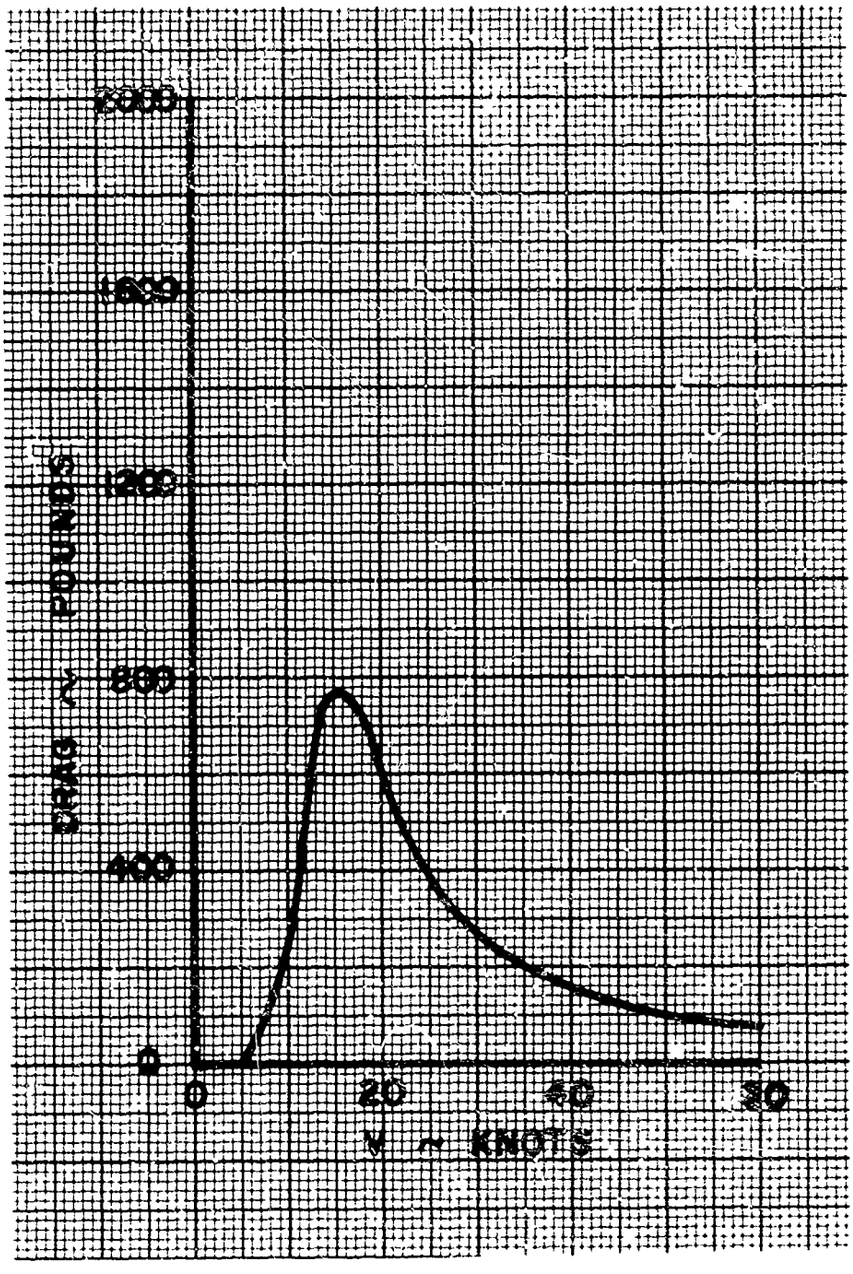

Figure 6-10. VA-3 Wave Drag Characteris' ics

"plane" on the water surface. Skirt drag is therefore a function of the craft velocity, skirt wetted area, and the ratio of wave height to air gap. Skirt drag has therefore been computed from the formula

$$D_{Skirt} = C_{D_F} \frac{1}{2} \rho' V_D^2 S_W$$

where: C_{D_K} = skin friction coefficient given in Hoerner's Fluid Dynamic Drag

S_W = skirt wetted area, based on trochoidal waves having a length-to-height ratio of 12:1

These components have been computed and are shown on Figure 6-11 for a 3-inch and a 5.5-inch hover height, as established experimentally on the VA-3 lift power settings used during the test period.

2. Data Accuracy

a. Measurement Errors

The data collected during the test is subject to error from craft instrumentation and from the accuracy with which the data could be read from the tracks. The reading accuracies are:

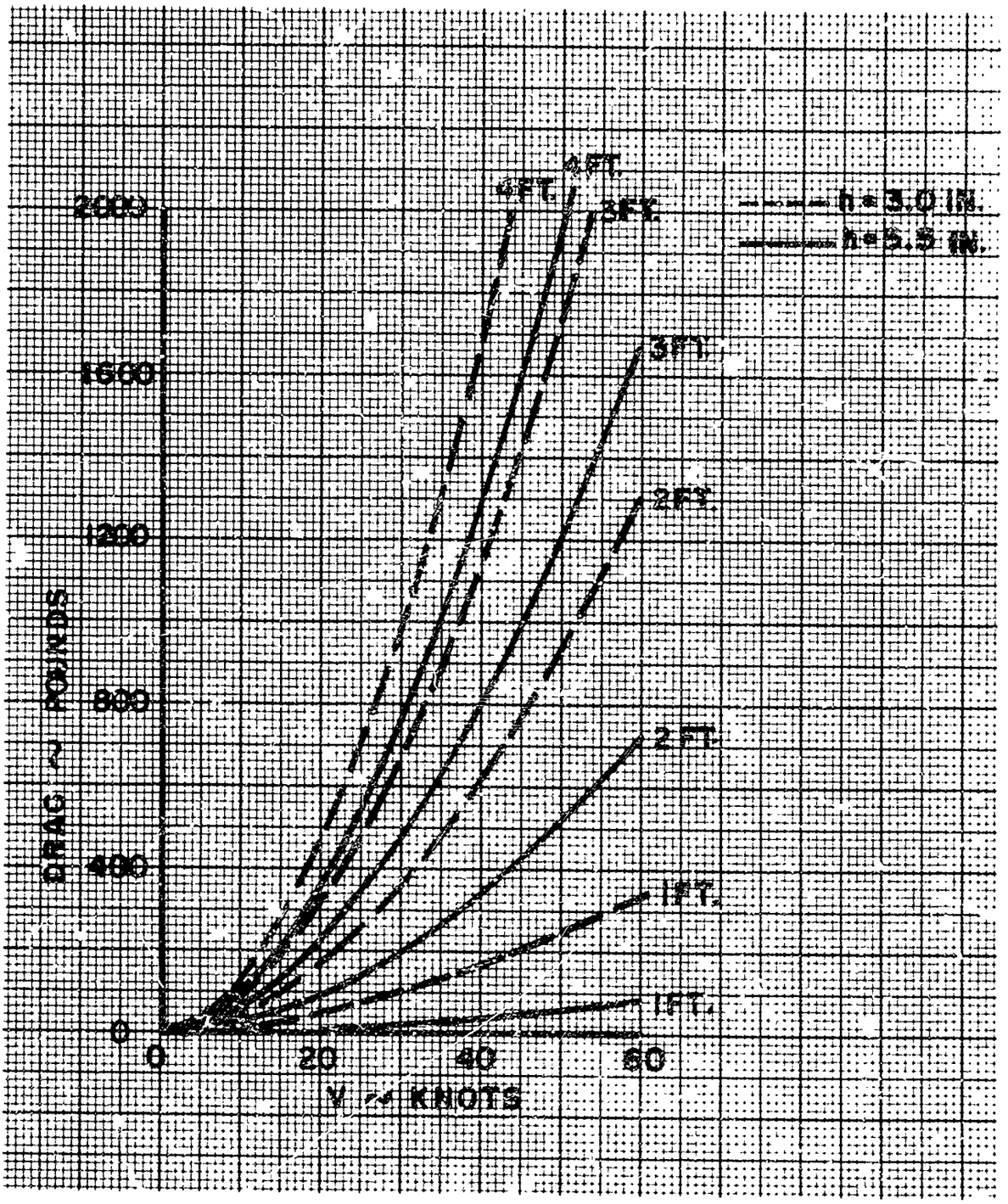

Figure 6-11. VA-3 Skirt Drag Characteristics

1) Propeller pitch: ± 1 degree

2) Relative wind: ± 1 knot

3) Velometer wind reading (taken on workboat): ± 0.5 knot

4) Doppler water speed: ± 1 knot

The basic instrument errors were taken out by calibration where possible. The larger random error introduced above is the ± 1 degree in propeller pitch angle, which corresponds to ± 300 pounds of drag. This error was due to hysteresis in the pitch control mechanism under load. The instrumentation pickup point was as close as possible to the propeller pitch change mechanism.

b. Errors Introduced by the Operational Environment

Any vehicle operating in close proximity to a surface interface is subject to measurement errors introduced by the interface. An air cushion craft is subjected to both wind and waves. To provide an accurate data correlation, instrumentation of a higher order than that used on this test should be provided. The wave-height variation actually experienced by the craft should be measured, and the craft response and phase lags established.

The water speed introduced by tidal and wind action in the test area is a correction that should be applied to the Doppler speed measurement, and therefore should be known over the test area.

For the present program, the test area could not be adequately covered by the work boat on which the current measuring instrument was mounted. It is estimated that the craft speed may therefore be in error by $\pm$ 2 knots.

The wind presents a far more difficult problem, in that surface wind gradients and gusts are presented that could have a serious effect on the propeller thrust estimates and on the profile drag and momentum drag components.

Tests run over level ground with accurate wind measurement and photographic coverage of the craft speed would establish the effect of wind speed, and also the interference effect of the craft flow field on the craft instrumentation. This was beyond the scope of the present tests, and therefore the relative wind was used for the craft airspeed rather than Doppler speed $\pm$ wind speed.

The results will therefore reflect errors due to variations in heading angle, wind speed, and direction. In fact, correlation between the Doppler speed, wind speed, and relative wind speed could not be established due to apparent errors in the wind-direction-measuring device. These errors would have been due to a combination of the dynamic response of the instrument and also to craft interference, showing that further studies in this area are required.

3. Drag Test Results

The data from the VA-3 test program has been reduced. The thrust available for a given propeller pitch angle and relative wind has been discussed in Section VIA, and has been used to establish the steady state drag under the following test conditions:

1) Wave heights, up to 54 inches

2) Wind speeds, up to 20 knots

3) Hover height, 3.0 inches and 5.5 inches average air gap between the flexible skirt and ground

4) Center of gravity, from 0.3 to 12.1 inches aft of the craft datum.

Drag is presented in Figures 6-12 through 6-19 as a function of water speed (Doppler) with sea state, wind direction, and hover height as parameters. Maximum speed variation with sea state is shown in Figure 6-20. For the purpose of data presentation, the sea state was assumed to depend on wave height only, in accordance with the definition given below:

Sea State	Wave Height
0	Less than 6 inches
1	6 to 12 inches
2	12 to 30 inches
3	30 to 54 inches

The normal weight variation fell between 29,800 and 32,100 pounds. Analysis indicated that any effect of weight variation was not distinguishable within the data scatter.

The effect of variation in pitch trim on drag, however, was evident in the data, as shown on Figures 6-12 and 6-13. A center-of-gravity movement of +10 inches forward corresponds to a decrease in drag of 500 pounds. There appears to be a pitch effect on drag, as indicated by the data in Figures 6-12 and 6-13 for sea state 0. A drag increment

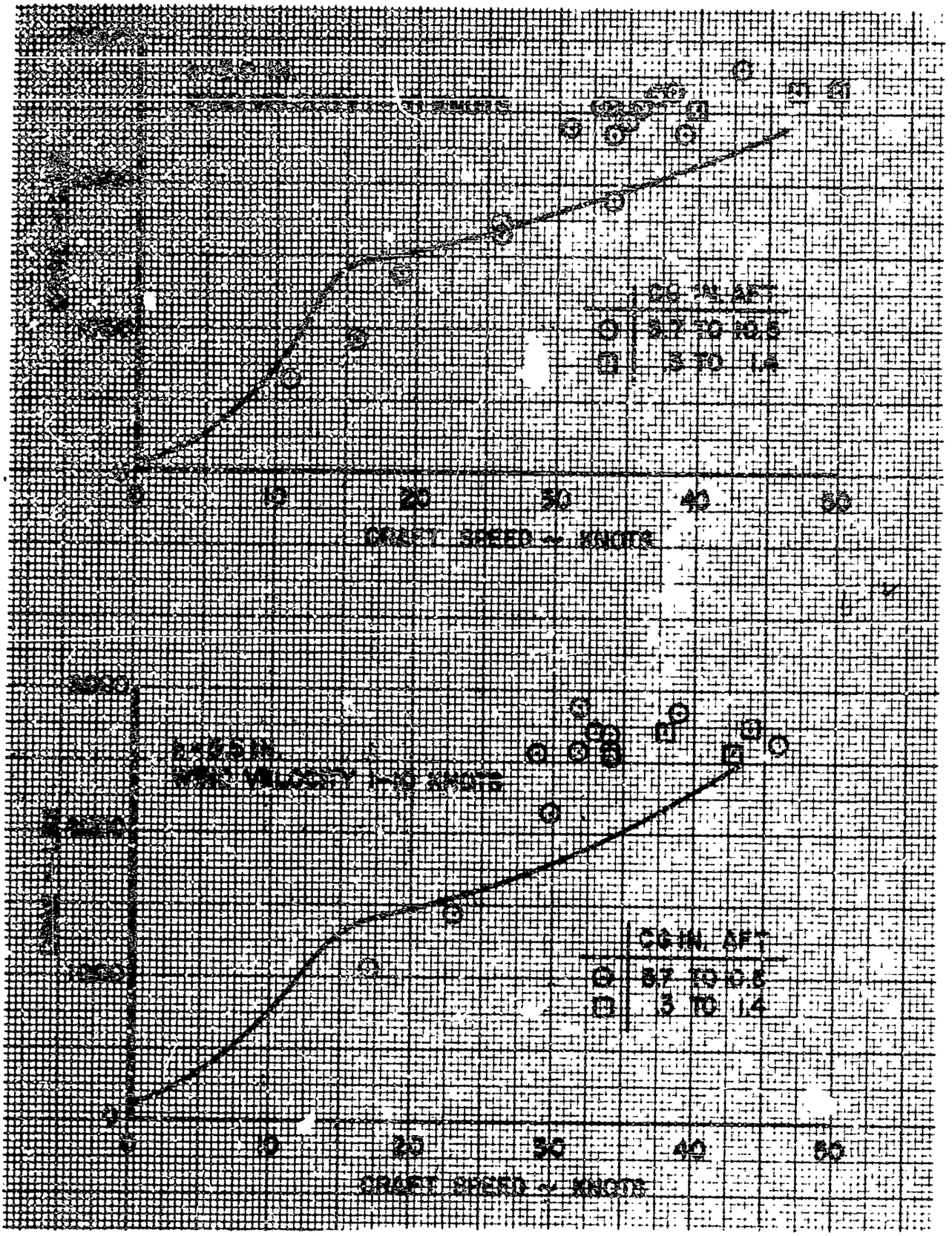

Figure 6-12. VA-3 Drag Data,Comparison of Test Data with Theory, Sea State 0, Headwind

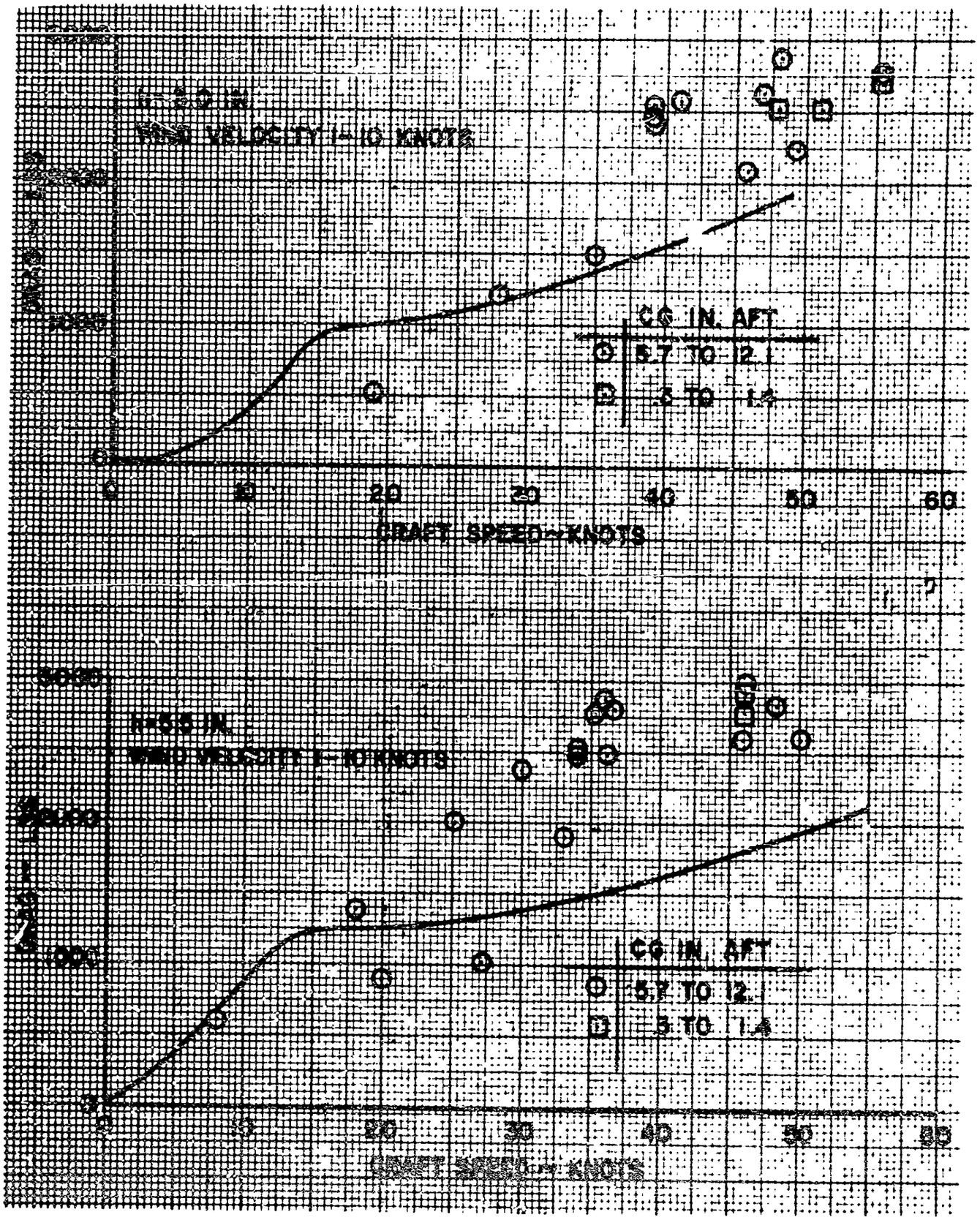

Figure 6-13. VA-3 Drag Data, Comparison of Test Data with Theory, Sea State 0, Tailwind

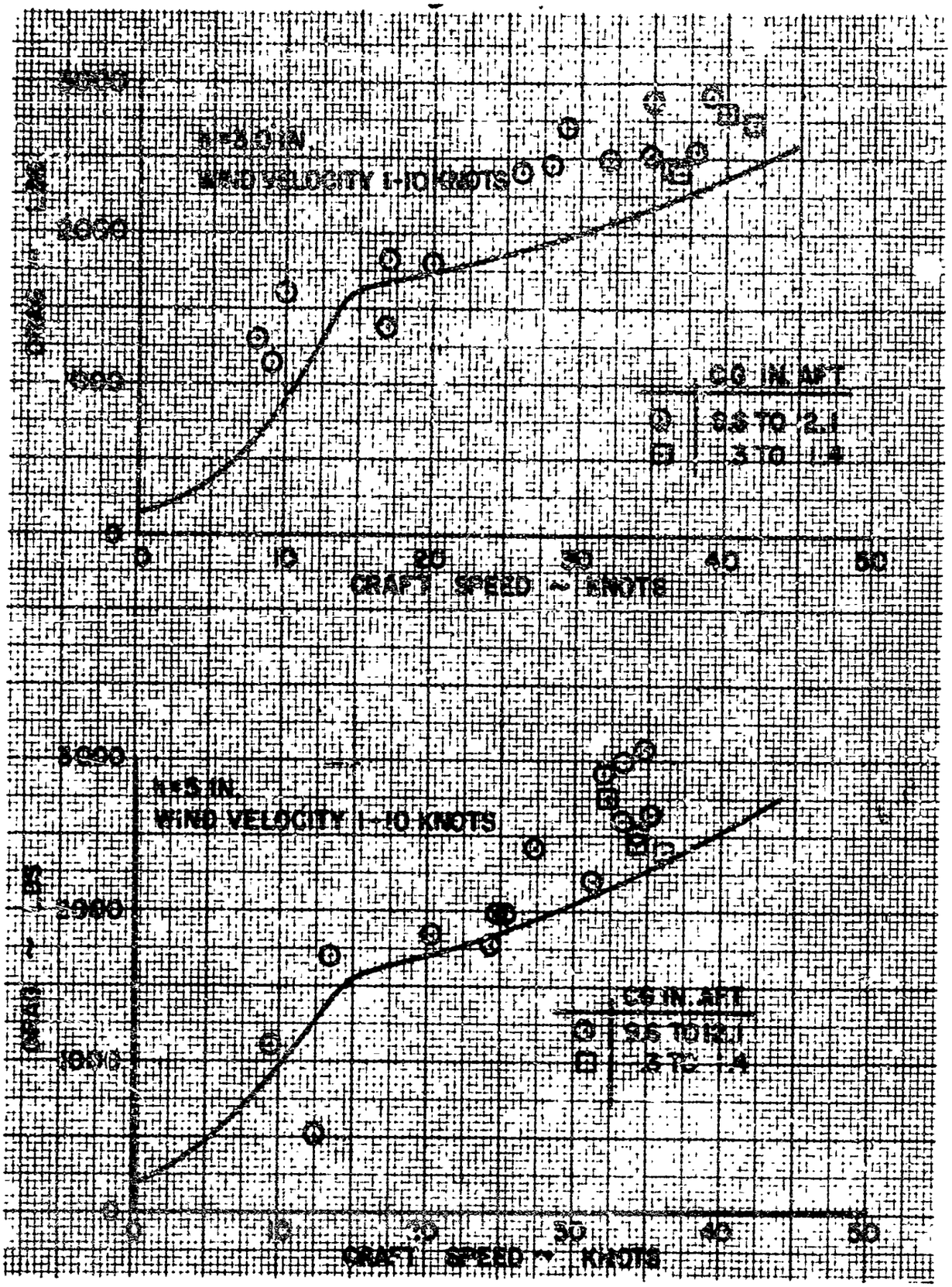

Figure 6-14. VA-3 Drag Data, Comparison of Test Data with Theory, Sea State 1, Headwind

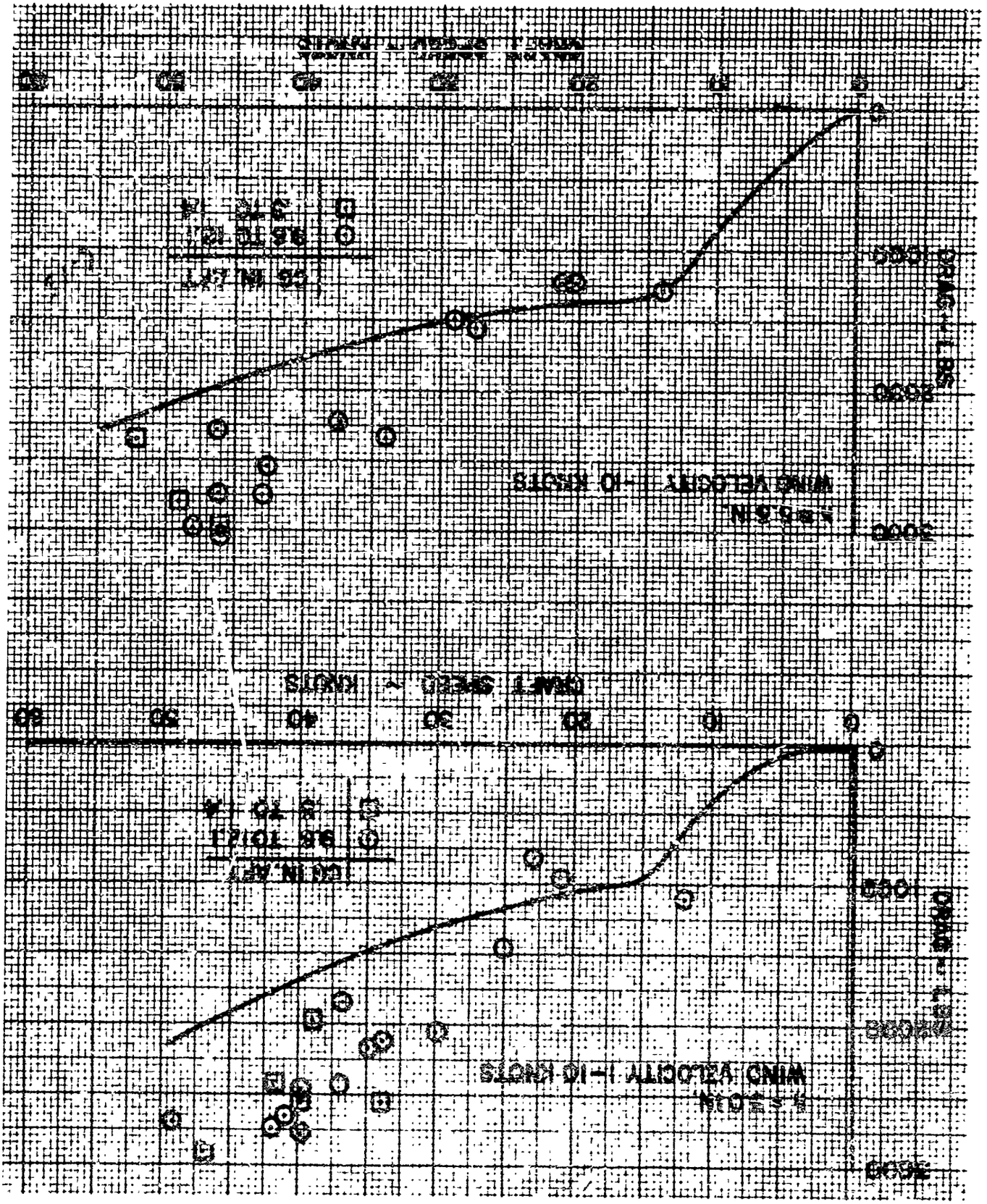

Figure 6-15. VA-3 Drag Data, Comparison of Test Data with Theory, Sea State 1, Tailwind

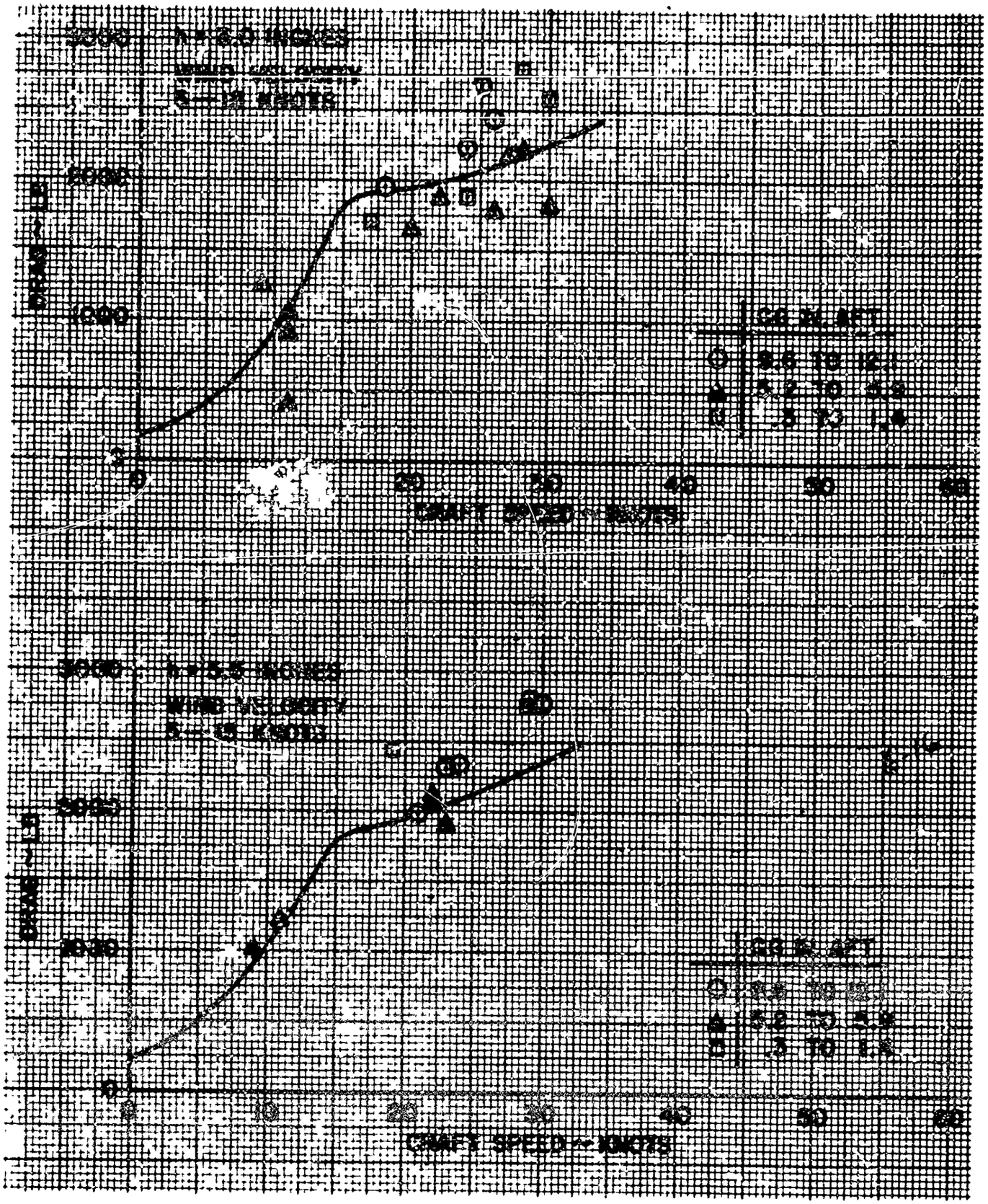

Figure 6-16. VA-3 Drag Data, Comparison of Test Data with Theory, Sea State 2, Headwind

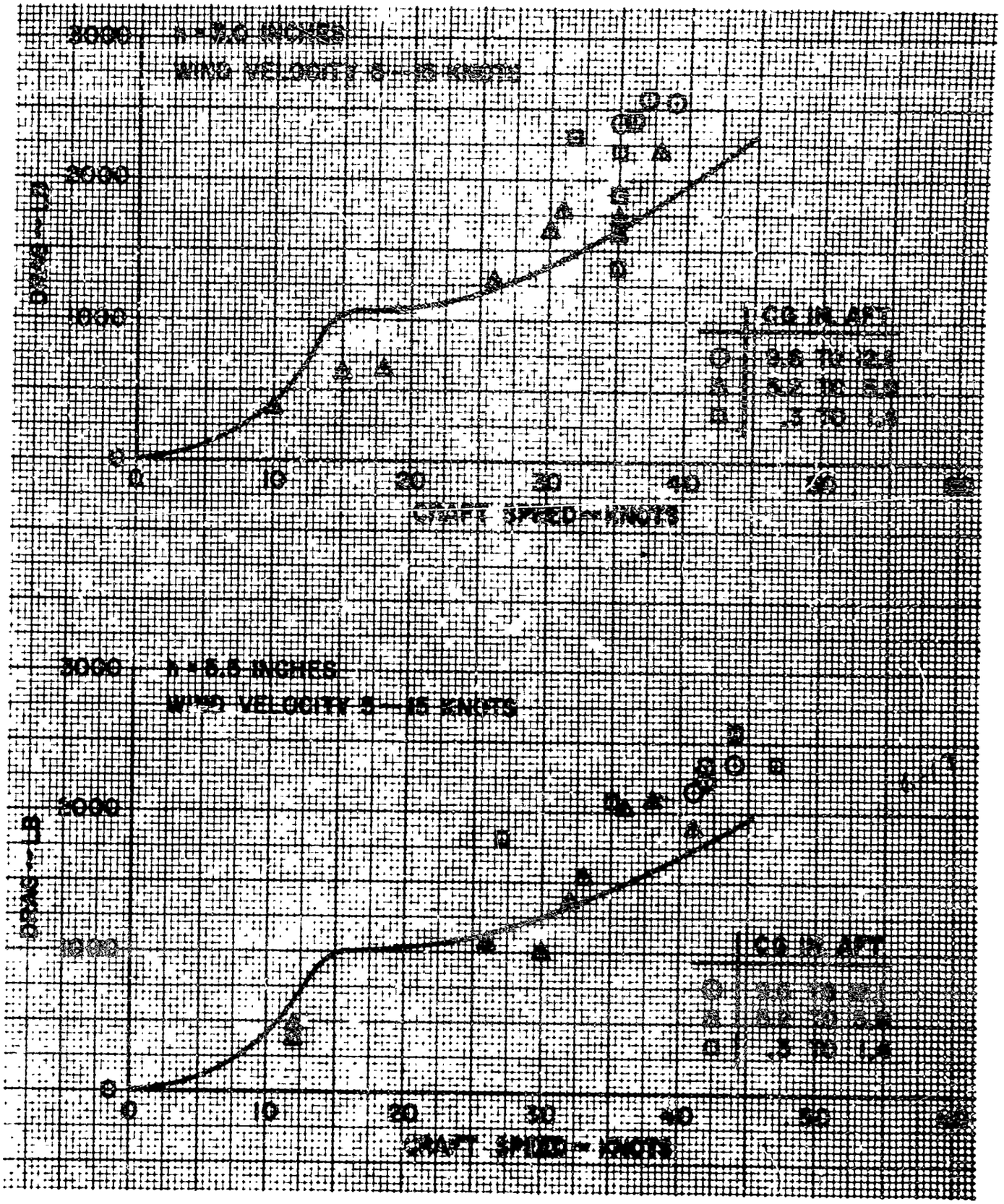

Figure 6-17. VA-3 Drag Data, Comparison of Test Data with Theory, Sea State 2, Tailwind

as high as 500 pounds for a 10-inch-forward center-of-gravity movement can be inferred from these data in view of the scatter. However, additional test points are required to confirm the influence of center-of-gravity movement on drag.

It will be observed that the above drag decrease can be considered as an incremental thrust. Section VID has

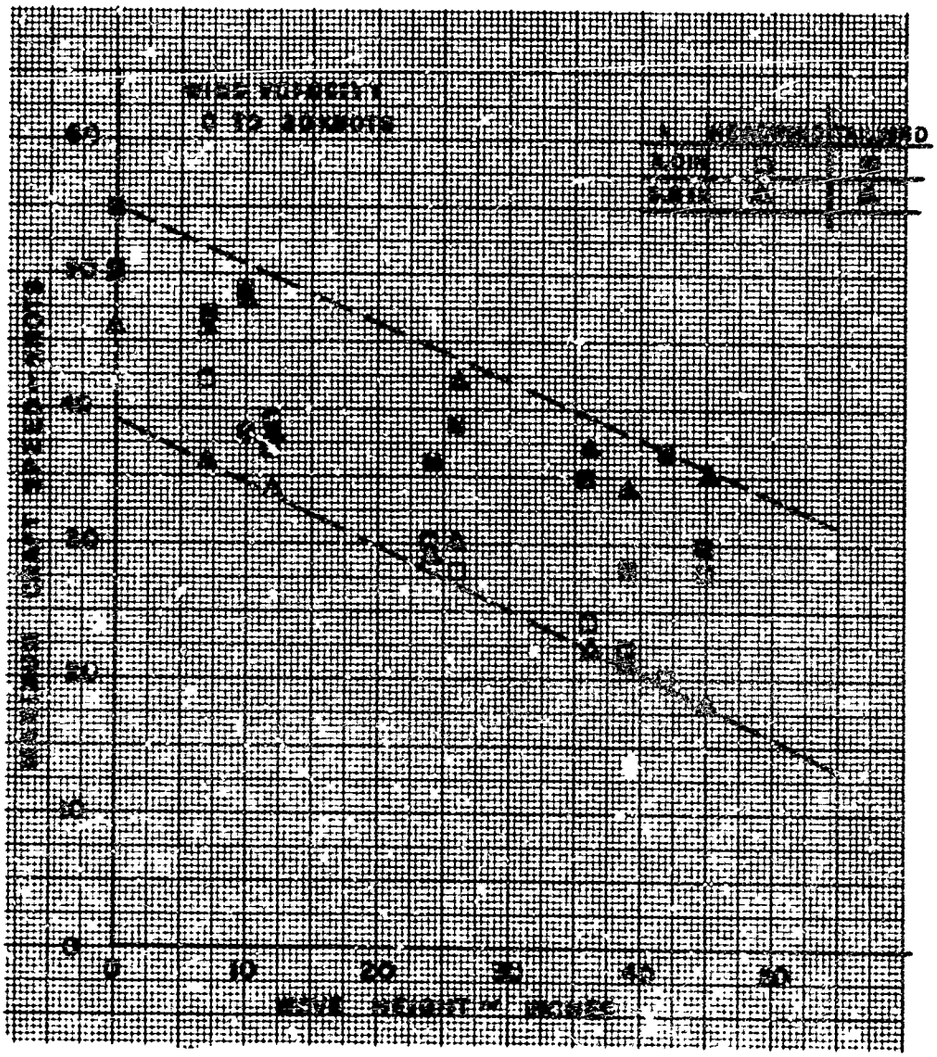

Figure 6-20. VA-3 Maximum Speed, Effect of Wave Height

shown that a center of gravity movement of 10 inches while hovering over water causes a pitch angle variation of ½ degree. Corresponding to a ½ degree pitch down, and assuming a discharge coefficient of 1.0, an incremental thrust of 529 pounds may be calculated due to assymetric outflow from the cushion. To realize this increment, the craft would have to be initially level and in calm sea to avoid drag from the skirts contacting the water. This was the case for the VA-3, for the results of Section VIE show that for a water speed between 40-50 knots the VA-3 has zero pitch angle.

To provide a valid comparison with the test data, the drag corresponding to each test point was estimated by the method given in the section on theoretical drag estimates. A resultant mean curve for the estimated drag is shown in the figures. The comparison shows that the estimated drag is lower than the experimental data.

An attempt was made to analyze the difference between the theory and the experimental data at sea state zero, by plotting the drag difference as a function of water speed (shown in Figures 6-21 and 6-22), and as a function of relative air velocity (shown in Figures 6-23 and 6-24). It is not clear

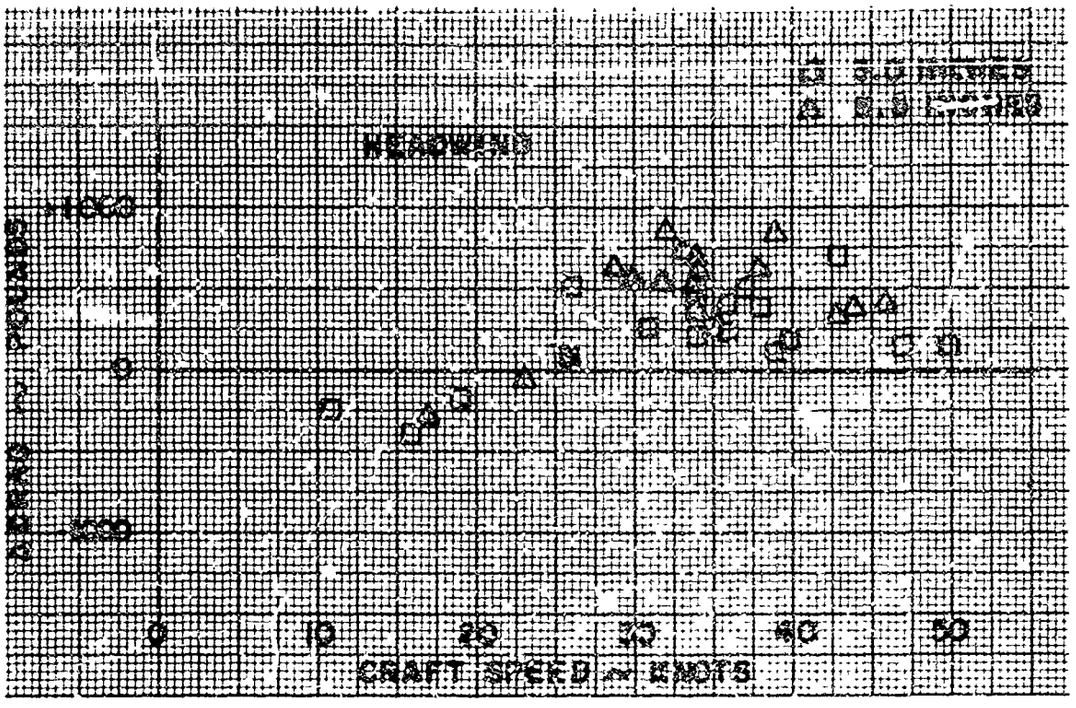

Figure 6-21. Deviation of Test Data from Theory, Sea State 0, Headwind, Drag vs Craft Speed

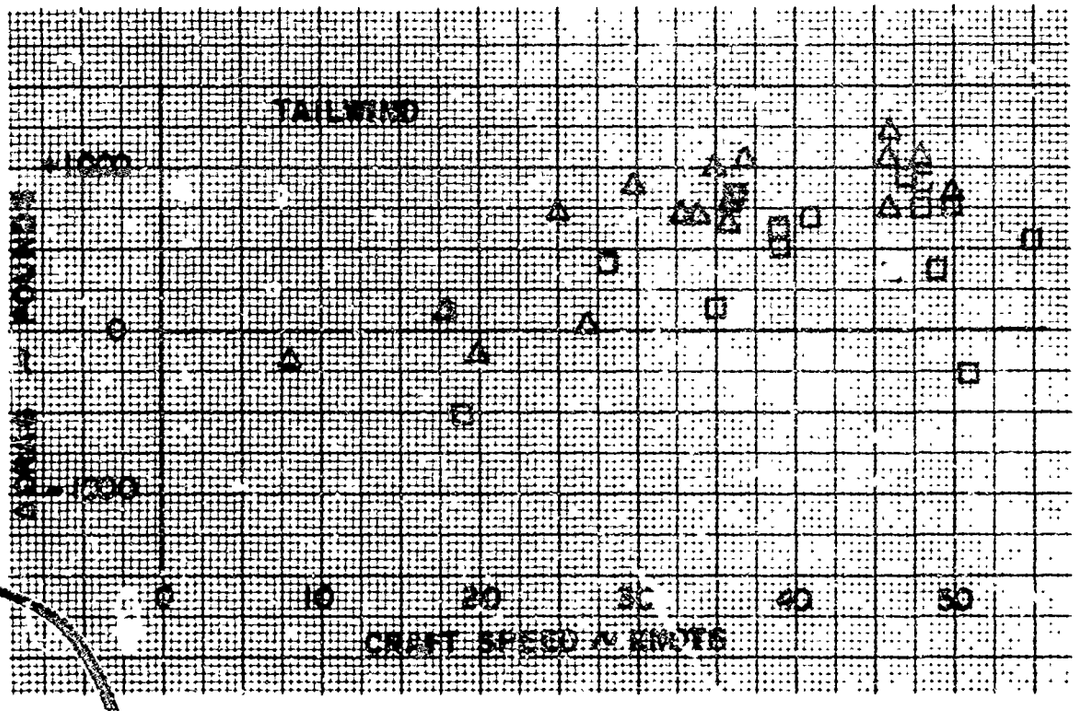

Figure 6-22. Deviation of Test Data from Theory, Sea State 0, Tailwind, Drag vs Craft Speed

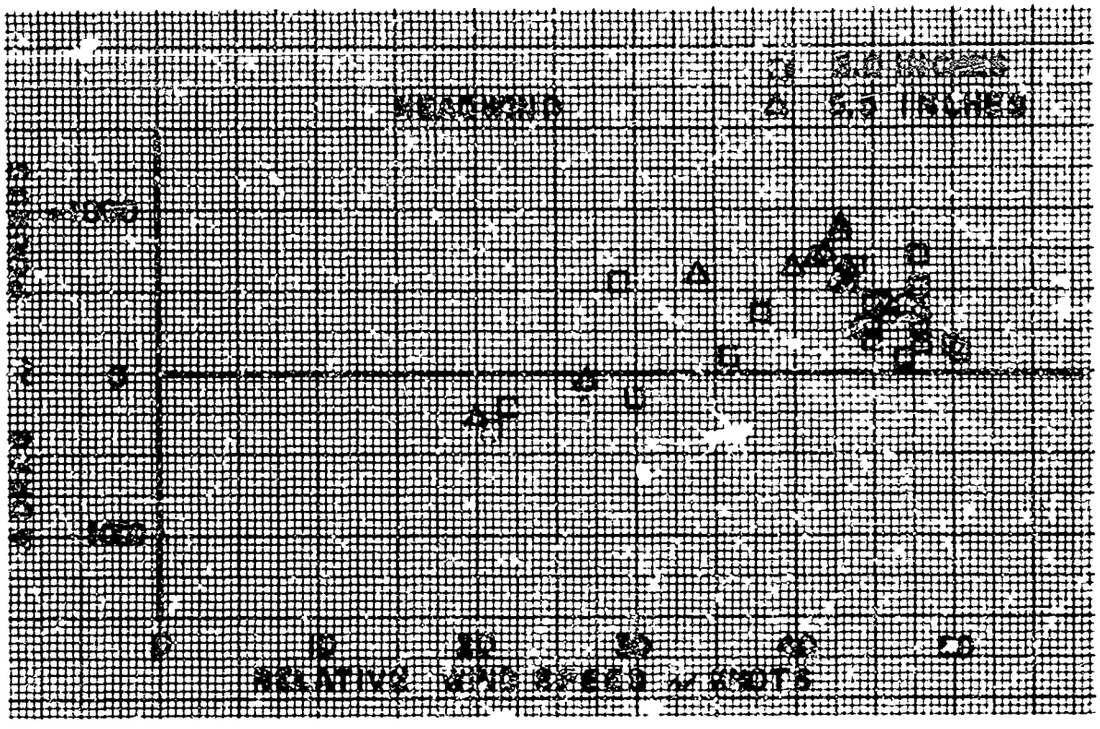

Figure 6-23. Deviation of Test Data from Theory, Sea State 0, Headwind, Drag vs Relative Wind Speed

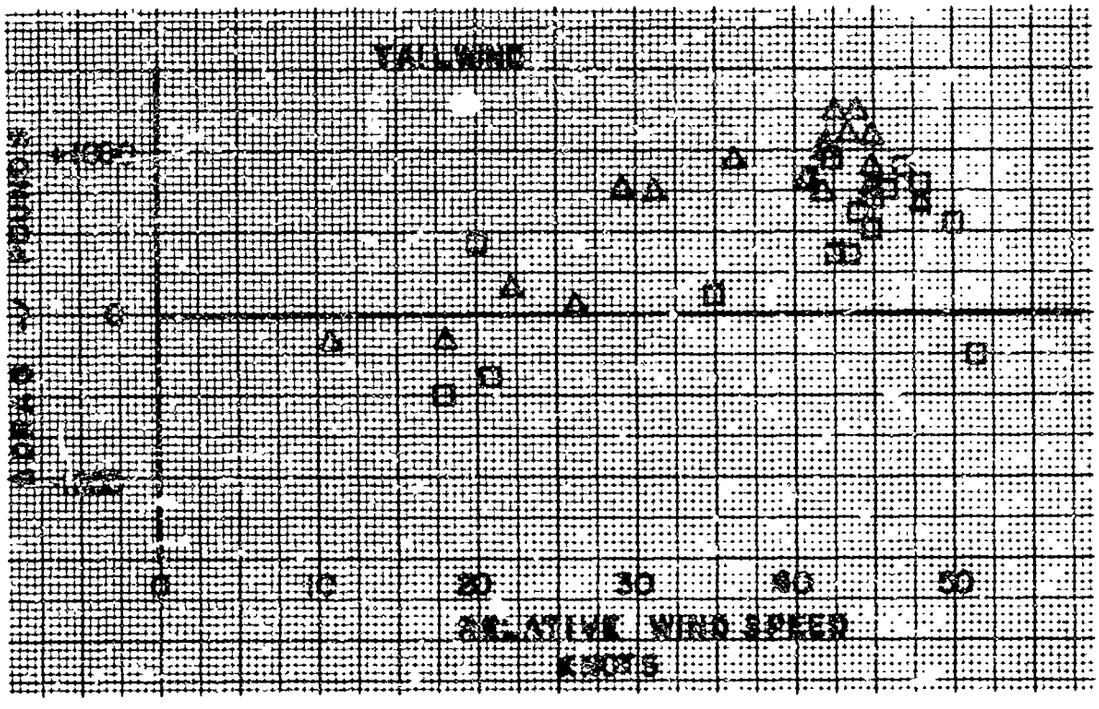

Figure 6-24. Deviation of Test Data from Theory, Sea State 0, Tailwind, Drag vs Relative Wind Speed

from the curves whether the difference in drag was a function of either the relative air velocity or the Doppler speed. However, it is apparent that the drag increment is greater for the tailwind than the headwind case, and the drag increment is greater for the 5.5 inch hover height case than the 3 inch hover height. The reason for the drag increase is not readily apparent; it could be due to errors in profile drag, craft interference with the propeller, or spray drag. Further detail analysis of the data collected during the program may provide additional drag data to clarify the above. To assist in defining the source of error, the craft should be run over level ground at speed so that spray drag effects are eliminated. The propeller thrust could also be verified by strain-gaging the propulsion engine mounts to determine the force transferred into the craft.

One conclusion that can be drawn from the error analysis is that the theoretical estimate for skirt drag is substantially correct. Because skirt drag varies with sea state (Figure 6-11), and the other theoretical drag terms are substantially independent of sea state (Figure 6-9), any deviation in actual skirt drag from the theory would have

caused the overall drag error to either increase or decrease with changing sea states. An error analysis at sea states 1, 2, and 3, corresponding to the analysis at sea state 0 referred to in the preceeding paragraph, revealed that the error was almost constant at any given forward speed. The theoretical skirt drag estimate can be assumed, therefore, to be substantially correct.

The drag results from the VA-3 program have shown that

1) Small variations in weight were not discernible within the data scatter

2) Skirt drag was estimated with reasonable accuracy

3) Pitch trim will affect the craft drag for small pitch angles

4) The drag was underestimated at 45 knots by 10 to 30 percent; further analysis and tests over smooth level ground are required to identify the source of additional drag

5) The craft maximum speed was overestimated by 5 knots

C. OPERATIONAL AND MODEL TESTS DURING THE VA-3 DEVELOPMENT

The VA-3 has undergone continuous development since its conception in 1961. The principal development effort has been to obtain clearance between the ground and the hard structure in the most efficient manner possible.

At the time of the preliminary design of the VA-3, the advantages of flexible skirts were not apparent. The preliminary design and models of the VA-3 were based on recirculation concepts (References 2 and 68). However, Vickers' subsequent experience with the VA-1 machine showed that the recirculation concept was not practical. The VA-3 design was then changed to a simple peripheral jet. Tests were conducted to establish the desirable jet width and the best configuration layout for stability both in pitch and roll (Reference 12) for a minimum of stability airflow. Model tests were also conducted on single-sided jet extensions (Reference 46) and spray deflectors (Reference 58), both of which were installed in the VA-3. The spray deflectors improved hoverheight but were removed after damage from high water loads. The jet extensions achieved only a limited success due to periodic damage sustained during operation. This damage was attributed to lack of flexibility.

In addition to the above tests on jet configuration, component tests were made on lift-fan air intakes (Reference 56 et al), installed centrifugal impeller characteristics (Reference 62 et al), and the aerodynamic characteristics including interference effects (Reference 51). Early water

tank model tests without flexible skirts were conducted to establish the ditching characteristics of the VA-3. These tests resulted in the shape of the bow being modified. Later tests were made at speeds up to 60 knots to establish the wave response to uniform waves and succeeded in the identification of the craft resonant frequency range. Operational experience, however, showed that resonance conditions never occurred, presumably because of the random nature of the sea and the craft damping characteristics.

The above model tests without flexible skirts concluded the VA-3 model test program.

The VA-3 was then put in fare-paying service for 2 months to obtain field maintenance experience and passenger reaction on noise and comfort levels. The fare-paying service ended after a gale caused the VA-3 to drag her moorings and be damaged against a sea-wall.

While the craft was being repaired, the pressure flow characteristics of the present VA-3 skirts were established by static tests (Figures 6-25 and 6-26). The VA-2 was used as a test vehicle for 2-foot skirts very similar to the proposed VA-3 skirts. After successful conclusion of these tests, 3-foot skirts were fabricated and installed on the VA-3.

In view of the skirt tests on the VA-2, no further model testing on the VA-3 was considered necessary to predict performance with 3-foot flexible skirts. The performance characteristics were based on the original VA-3 configuration tests, the flow tests of full-scale skirt sections, and the tests of VA-2. Therefore, no direct comparison can be made of full-scale VA-3 (with 3-foot skirts) tests with wind tunnel or water tank model tests.

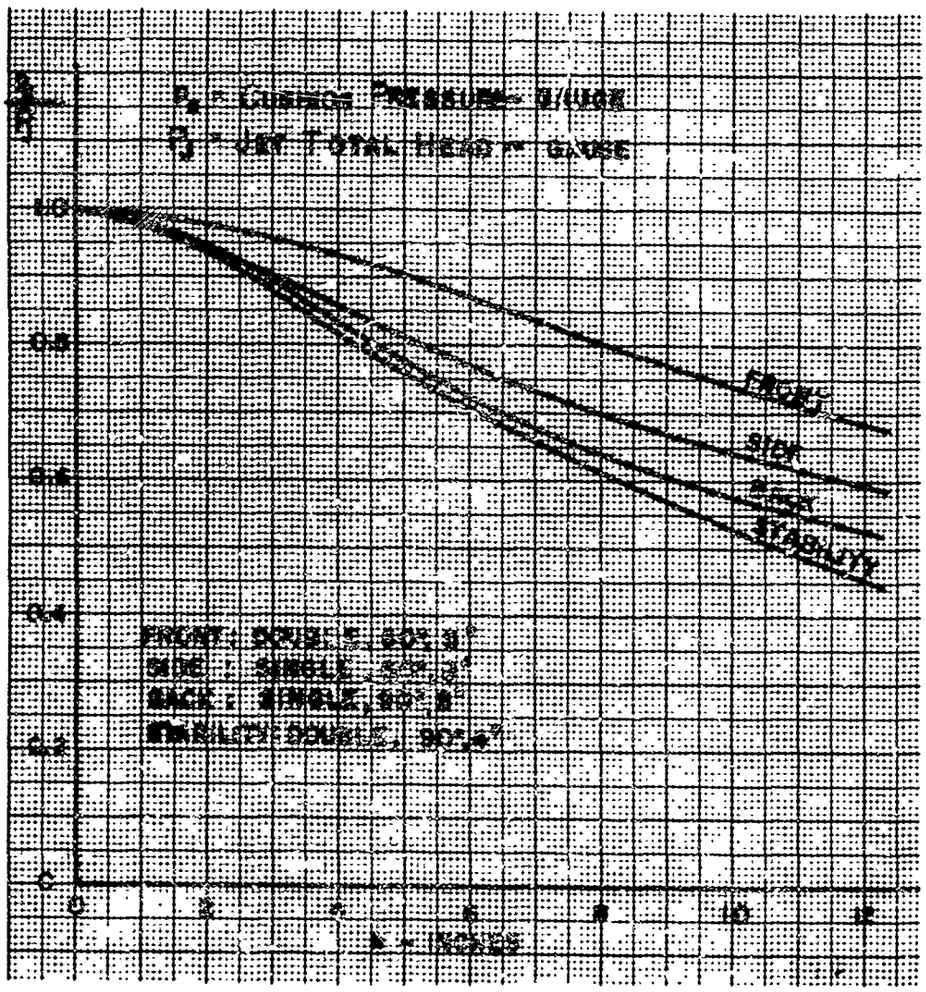

Figure 6-25. VA-3 Flexible Skirt Characteristics, Total Head

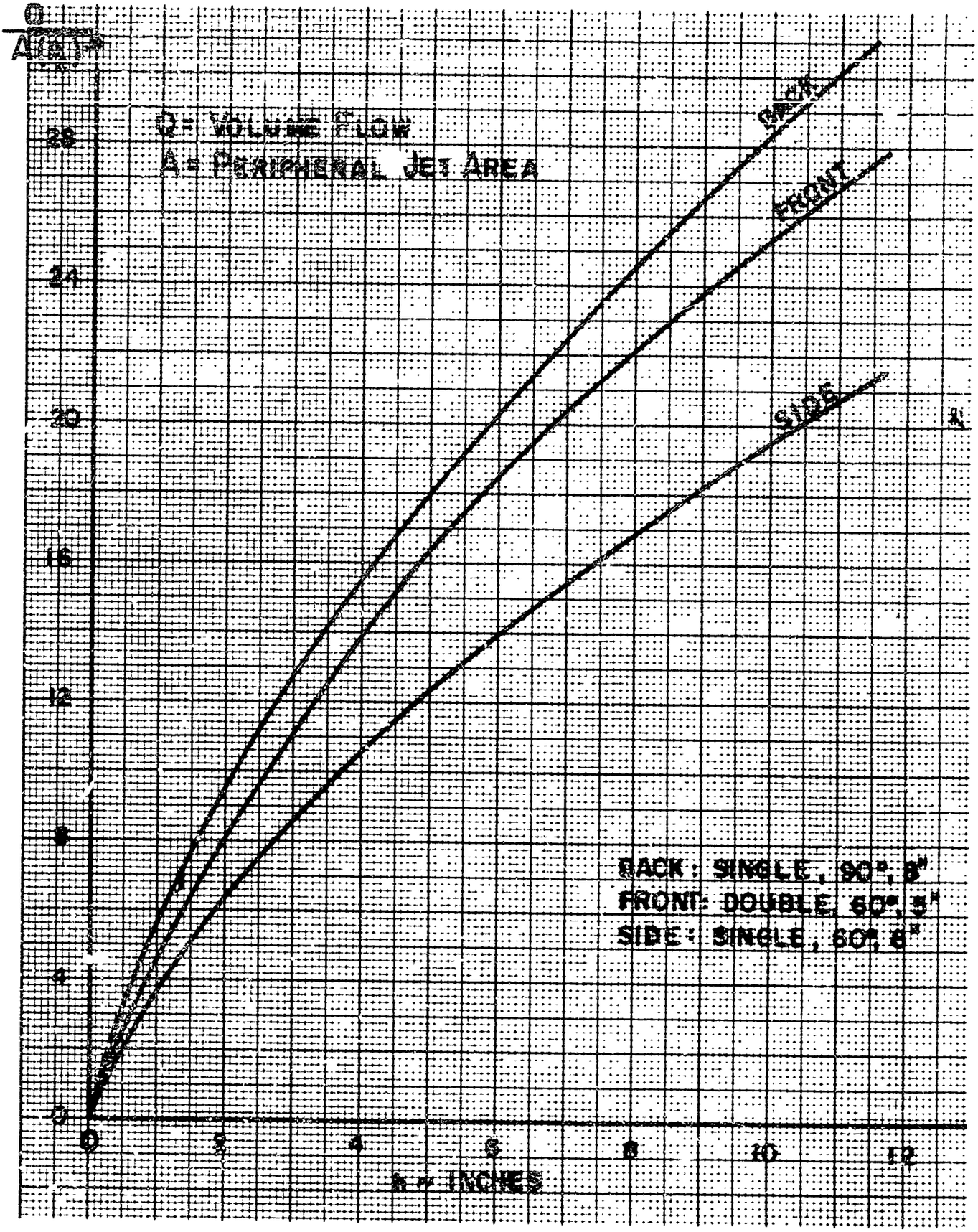

Figure 6-26. VA-3 Flexible Skirt Characteristics, Volume Flow

D. STABILITY AND CONTROL

1. Stability

a. Introduction

The static and dynamic stability characteristics were investigated during the three basic operating modes of the craft: as a displacement vessel, on cushion over land, and on cushion over water.

b. Displacement Mode

When floating, the craft acts as a normal displacement vessel; and conventional naval architectural concepts of stability can be applied. Tests were carried out to determine the metacentric heights in pitch and roll; these tests consisted of moving ballast fore and aft a known distance along the craft center line and measuring the resulting change in pitch angle. The test for roll was identical, except the ballast was moved across the craft. No dynamic stability tests were made for this mode.

c. Over-Land Mode

The static and dynamic stability characteristics for the over-land mode were determined with the craft tethered on a prepared concrete pad. The static stability tests consisted of measuring the craft stiffness in heave, pitch, and

roll with the lift-engine power being varied to cover the range between minimum power (lift-off) and the maximum available.

Dynamic stability was assessed by forcing oscillations in the roll and pitch modes, using the spoilers and propulsion engine thrust, and recording the decay of the resulting oscillations to calculate the degree of damping present.

No attempt was made to determine the effects of forward speed on the stability characteristics in this mode of operation because a suitable test area could not be easily obtained.

d. Over-Water Mode

The over-water mode tests consisted of forcing the roll mode of oscillation using the spoiler controls at various speeds. The tests were performed on a calm day in sheltered water.

e. Results

(1) Displacement Mode

The metacentric height is given by

$$GM = \frac{x_s \Delta w}{W \tan \gamma}$$

where: Δw = weight moved

x = distance weight is moved

W = gross weight of craft

γ = angular displacement of craft due to movement of Δw through x

The displacements γ were plotted against x for each case taken.

For roll case, $\Delta w = 2{,}370$ pounds

$W = 31{,}415$ pounds

From Figure 6-27, for $x = 200$ inches

$\gamma = 52$ minutes

and $\tan \gamma = 0.01512$.

Then, GM = 83.3 feet.

For the pitch case, $\Delta w = 2{,}370$ pounds

$W = 31{,}415$ pounds

Now, from Figure 6-28 for $x = 300$ inches,

$\gamma = 25$ minutes

and $\tan \gamma = 0.00727$.

Then, GM = 259.4 feet.

(2) Overland Mode

(a) Heave Tests

The results of the heave stiffness tests are shown in Figures 6-29 and 6-30. It can be seen that the

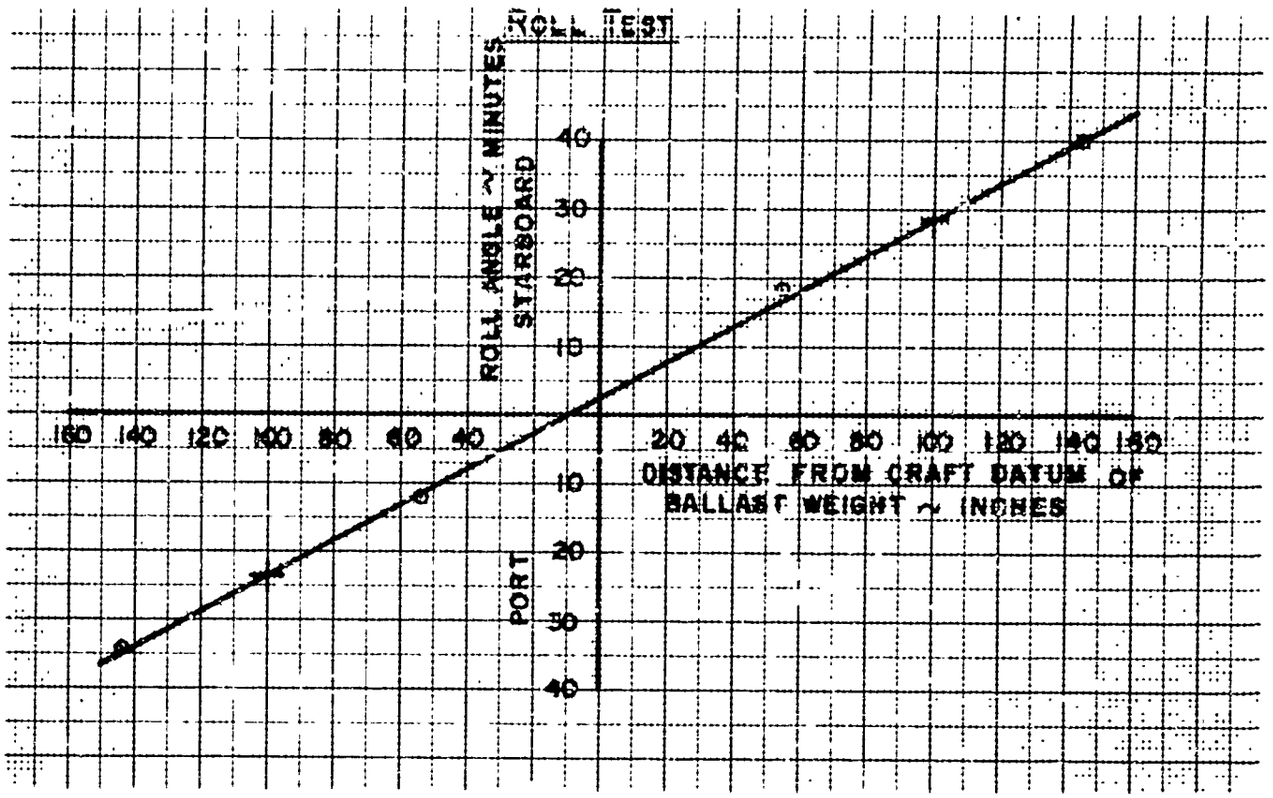

Figure 6-27. VA-3 Static Stability - Displacement Mode, Roll Test

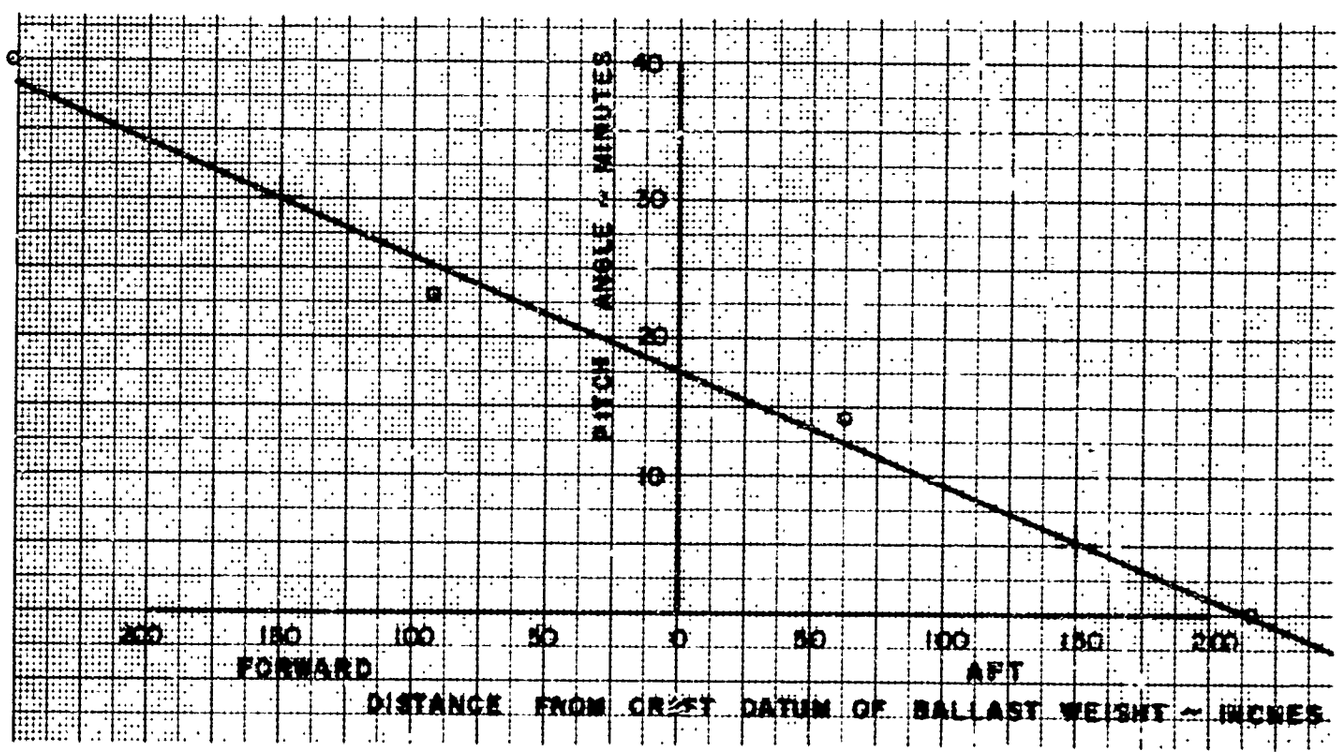

Figure 6-28. VA-3 Static Stability - Displacement Mode, Pitch Test

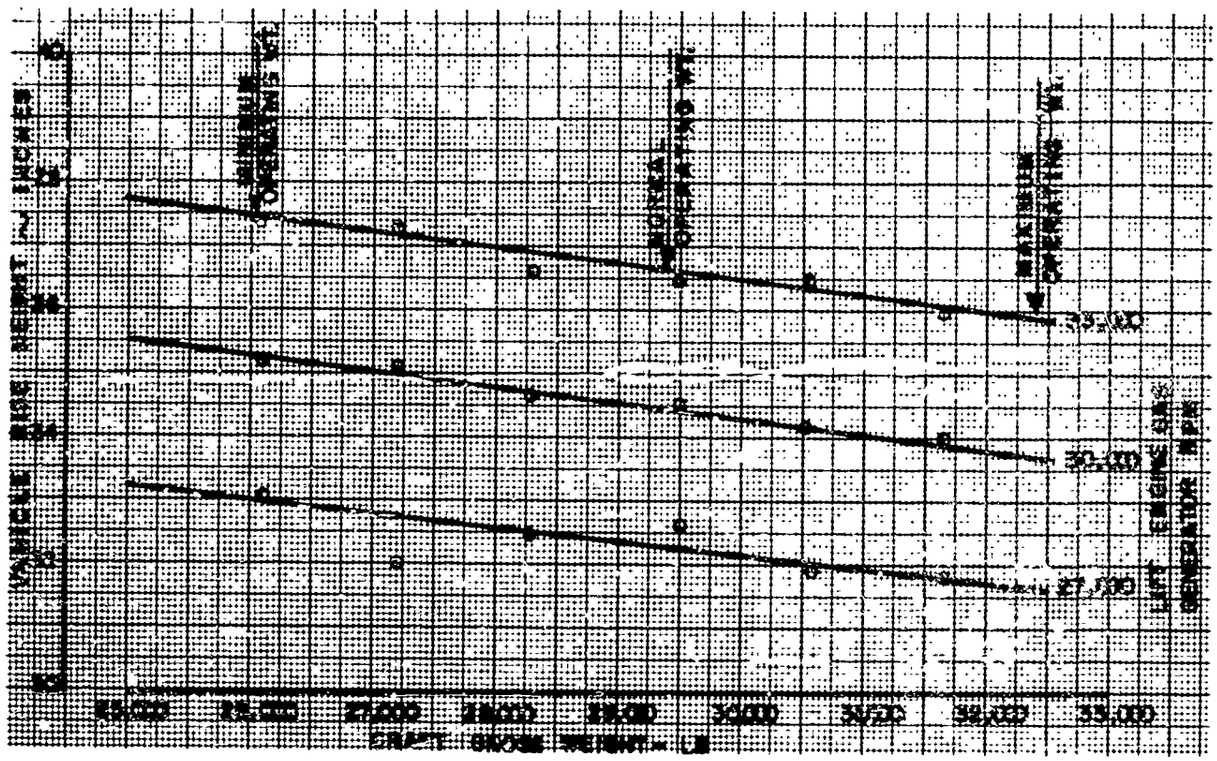

Figure 6-29. VA-3 Hovering Test -- Heave Stiffness

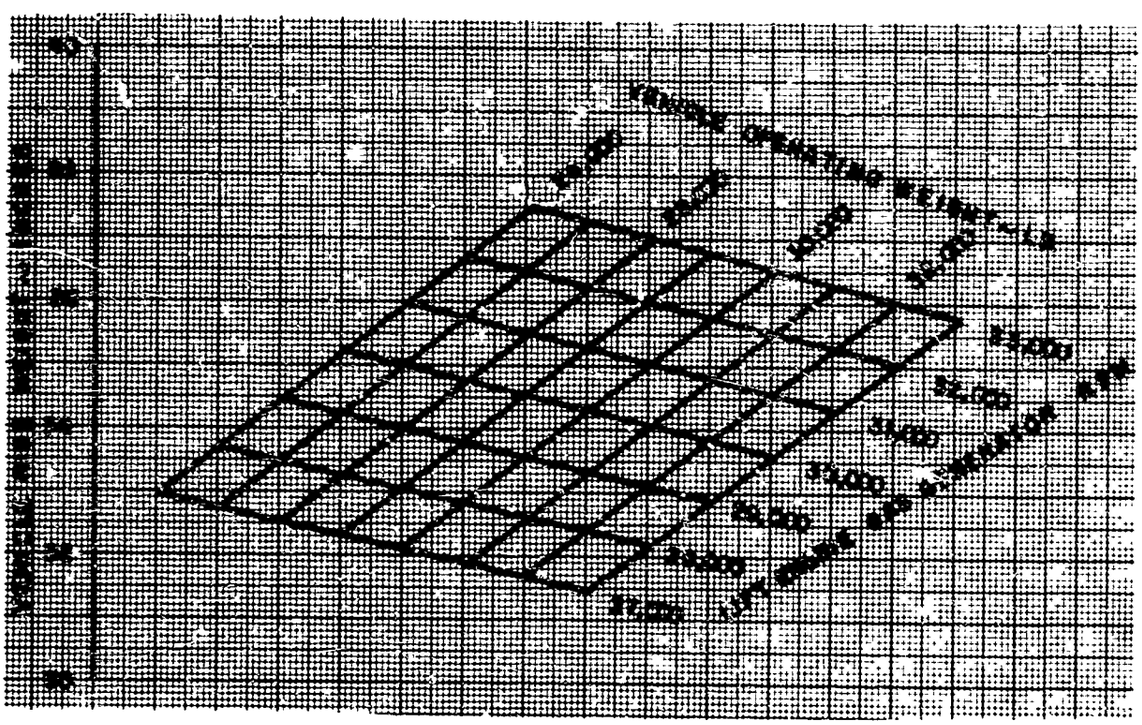

Figure 6-30. VA-3 Hovering Tests -- Vehicle Rise Height

changes in stiffness are negligible with lift engine power and craft weight in the normal operating range.

The curves show the heave stiffness, Kz, to be 48,552 pounds per foot. Thus, at the normal operating weight of 29,400 pounds, the rigid body heave frequency, f_z = 1.16 cps.

(b) Pitch Tests

The rotations about the pitch axis for various craft center-of-gravity positions relative to datum at a fixed craft weight are shown in Figure 6-31. The skirt was clear of the ground at all times, and the rise height at the center of gravity remained constant.

The pitch stiffness, signified by K_θ, is the moment required to rotate the craft by 1 radian, a value of K_θ = 3,396,278 lb-ft/rad is derived from Figure 6-31. Because the radius of gyration in pitch is 12.7 feet, then at an operating weight of 29,000 pounds, the pitch inertia, I_θ = 4,731,926 lb-ft^2. This gives a pitch natural frequency, f_θ = 0.76 cps; and, finally, the critical damping $(D_\theta)_{crit}$ = 1.406 x 10^6 lb/ft^4/sec. The data obtained from the damping tests proved to be unusable.

(c) Roll Tests

The roll attitudes taken up by the craft for various center-of-gravity displacements from the datum are shown in Figure 6-32. The roll stiffness can be expressed as

$$K_\phi = 0.4166 \times 10^6 + 82.82 \times 10^6 \phi^2 \text{ lb-ft/rad}$$

The system with the above spring characteristics has been analyzed in Appendix A and yields the following values of roll frequency, which are also shown in Figure 6-33.

TABLE 6-6. ROLL FREQUENCIES FOR VARIOUS ROLL ANGLES

Maximum Roll Angle, ϕ_M (degrees)	f_ϕ (cps)
0	0.426
0.5	0.428
1.	0.435
1.5	0.447
2	0.463
2.5	0.482
3	0.505

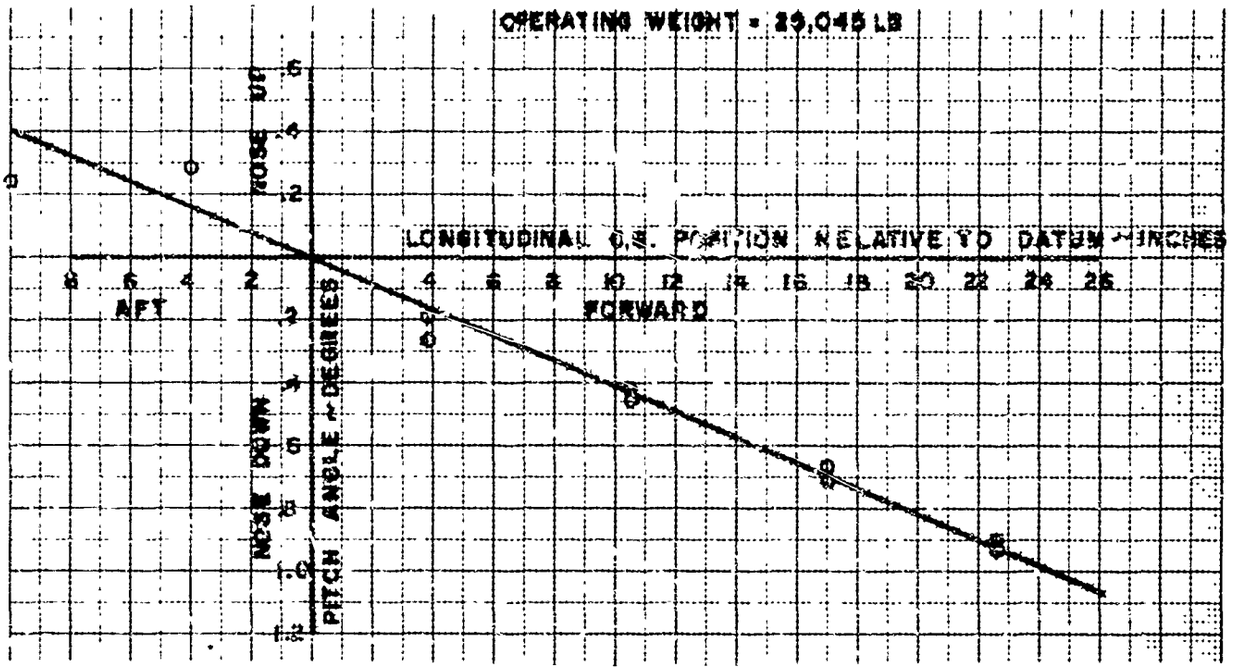

Figure 6-31. VA-3 Hovering Tests -- Pitch Stiffness

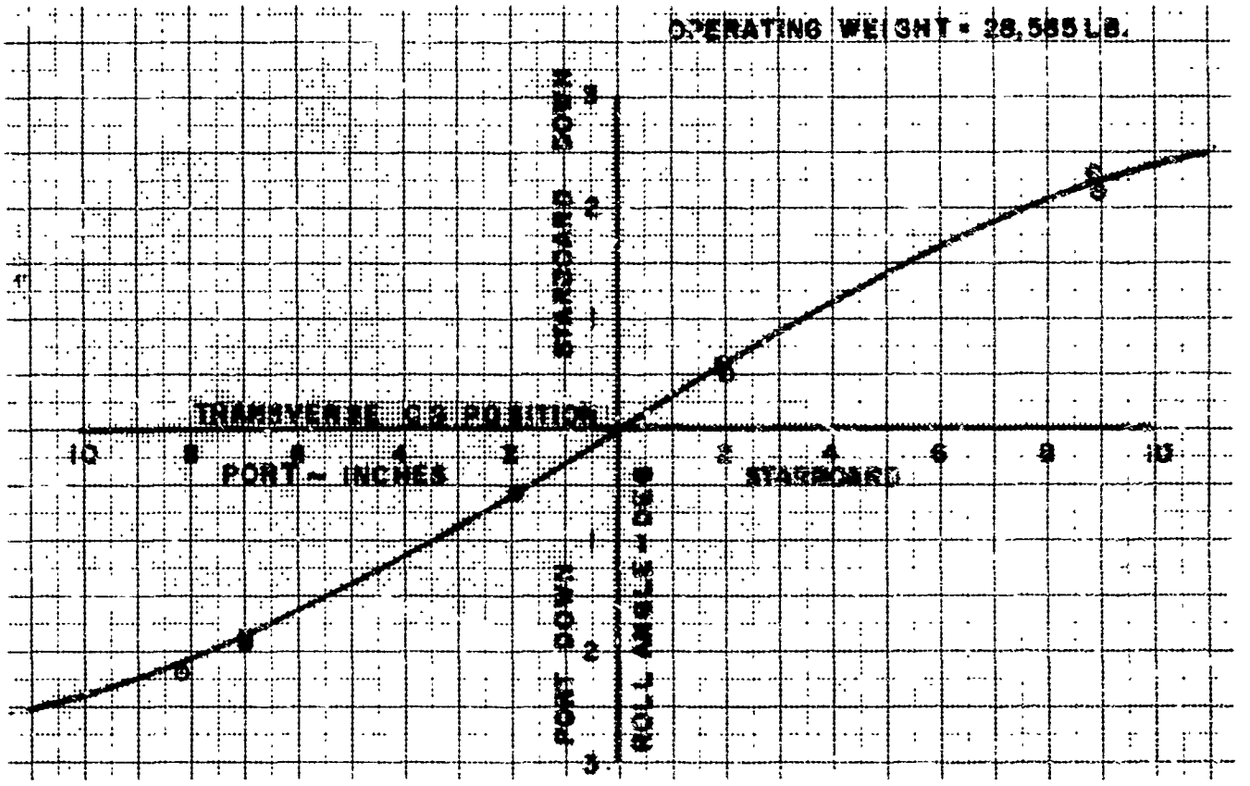

Figure 6-32. VA-3 Hovering Tests -- Roll Stiffness

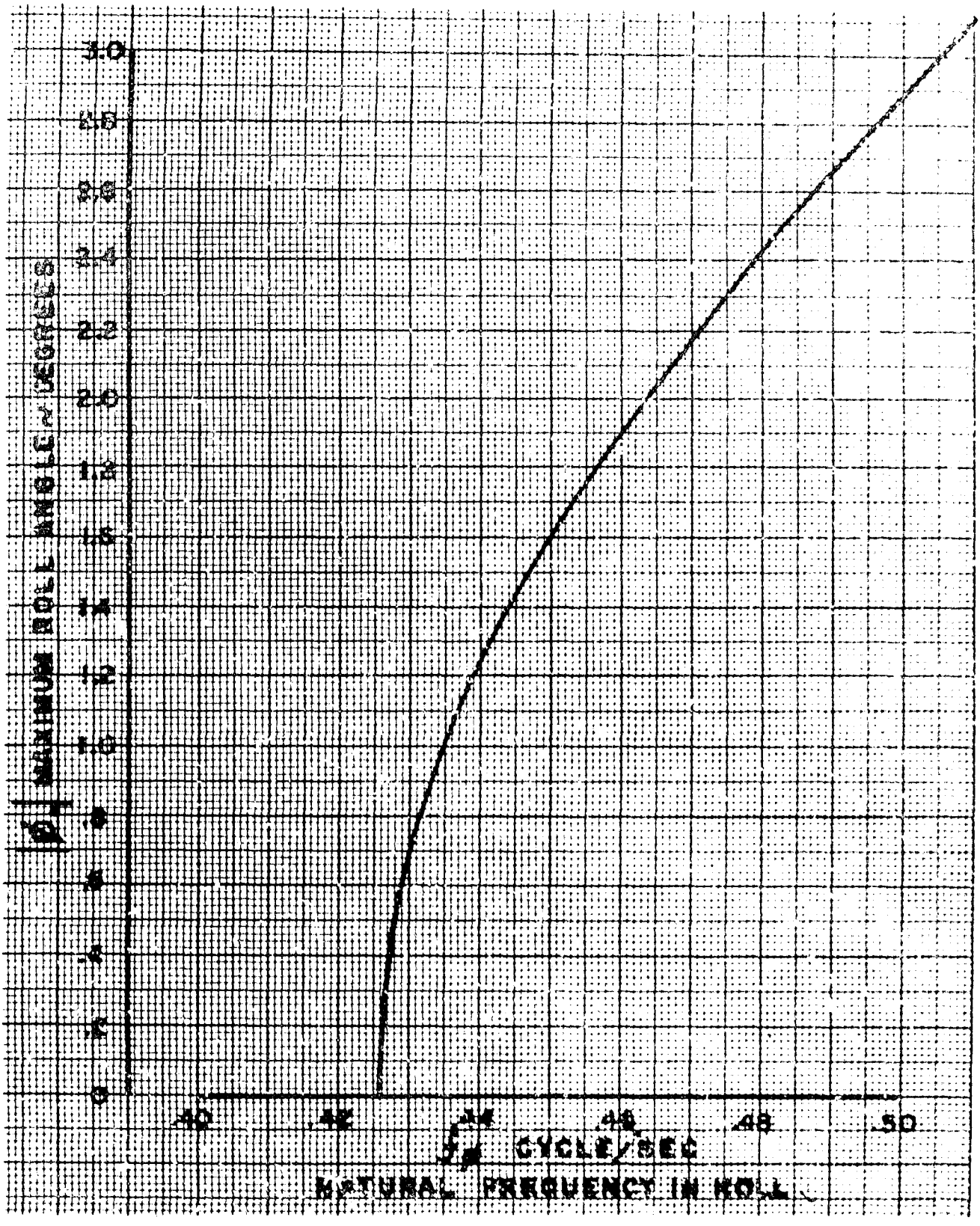

Figure 6-33. VA-3 Roll Natural Frequency

In the analysis of the roll damping, the reference value of damping $(D_\phi)_{crit}$ will be taken consistent with the zero roll angle.

Because

$$I_\phi = 1{,}875 \times 10^6 \text{ lb-ft}^2$$

$$(D_\phi)_{crit} = 0.73174\ f_\phi \times 10^6 \text{ lb-ft}^4/\text{sec}$$

Therefore,

$$(D_\phi)_{crit} = 0.3115 \times 10^6 \text{ lb-ft}^4/\text{sec}$$

Analysis of the damping records was carried out by the method shown in Appendix B and yielded the following results:

TABLE 6-7. DAMPING WITH PROPULSION ENGINES AT 75-PERCENT POWER

Lift Engine RPM	Spoiler Application	Damping Percentage Critical
33,000	Port	27.0
	Starboard	17.8
30,000	Port	30.0
	Starboard	15.0
27,000	Port	--
	Starboard	--

TABLE 6-8. DAMPING WITH PROPULSION ENGINES STOPPED

Lift Engine RPM	Spoiler Application	Damping Percentage Critical
33,000	Port	31.4
	Starboard	18.1
30,000	Port	36.3
	Starboard	26.3
27,000	Port	--
	Starboard	--

(3) Over-Water Mode

Only damping tests were performed for the over-water mode; the method of analysis is given in Appendix B. The results of this analysis are as follows:

TABLE 6-9. DAMPING WITH MINIMUM LIFT POWER (27,000 RPM)

Doppler Speed (knots)	Spoiler Application	Damping Percentage Critical
10	Port	8.0
	Starboard	31.0
25	Port	9.6
	Starboard	11.5
36	Port	16.1
	Starboard	24.7
45	Port	--
	Starboard	16.6

TABLE 6-10. DAMPING WITH MAXIMUM LIFT POWER (33,000 RPM)

Doppler Speed (knots)	Spoiler Application	Damping Percentage Critical
10	Port	--
	Starboard	--
25	Port	10.1
	Starboard	8.8
30	Port	10.3
	Starboard	6.1
38	Port	10.2
	Starboard	25.4

f. Discussion

(1) Displacement Mode

The metacentric heights determined are very large, certainly many times those common in ship design practice. These values stem in part from the very wide beam of the VA-3. One consequence of the large metacentric height is that the roll and pitch periods will be very short, making a synchronous pitch or roll condition highly unlikely. The short-period waves necessary to achieve frequency coincidence would be of small amplitude compared to the dimensions of the craft, making the extraction of energy difficult.

In practice, the VA-3 behaves like a raft, always taking up roll and pitch angles consistent with the local slope of the waves whenever the wavelength is more than twice the craft length.

(2) Overland Mode

The stiffness tests show the craft to be statically stable over the normal operating range. In heave, the effects of weight and lift engine power on the stiffness are negligible. In roll, the craft exhibits pronounced non-linear "hard spring" characteristics. The natural frequencies in heave, pitch, and roll are well separated and give ride characteristics more akin to those of a domestic automobile than to those of a planing-hull displacement craft.

Attempts to force the heave and pitch modes of oscillation to obtain decay records proved to be abortive. The amplitudes of the oscillation forced with the means available proved to be so small (and damped out so quickly) as to negate any analysis. The roll mode was forced by applying the full spoiler angle on one side of the craft as quickly as possible and then returning to neutral immediately; this resulted in a

pulse-like forcing function. Even so, the roll mode proved difficult to force, particularly at the minimum lift power settings where the amplitudes were of the order of 0.25 degree and decayed within a cycle.

Substantially higher damping was shown in cases in which the initial disturbance rolled the port side of the craft downward (that is, when the port spoiler was in use). Initially this was assumed to be due to the torque reaction of the propulsion units, both propellers of which rotate in the same direction. However, a repeat of the tests with the propulsion engines stopped gave closely similar results. These results cannot be explained satisfactorily in the light of the symmetry of the roll stiffness characteristics.

(3) Overwater Mode

No static stability measurements were taken during the present series of tests while hovering over water; however, some Vickers data is available that shows (Figure 6-34) the pitch stiffness over water to be of similar order to that over land. This is confirmed by the accelerometer records taken during the over-water trials; generally, the craft responded in

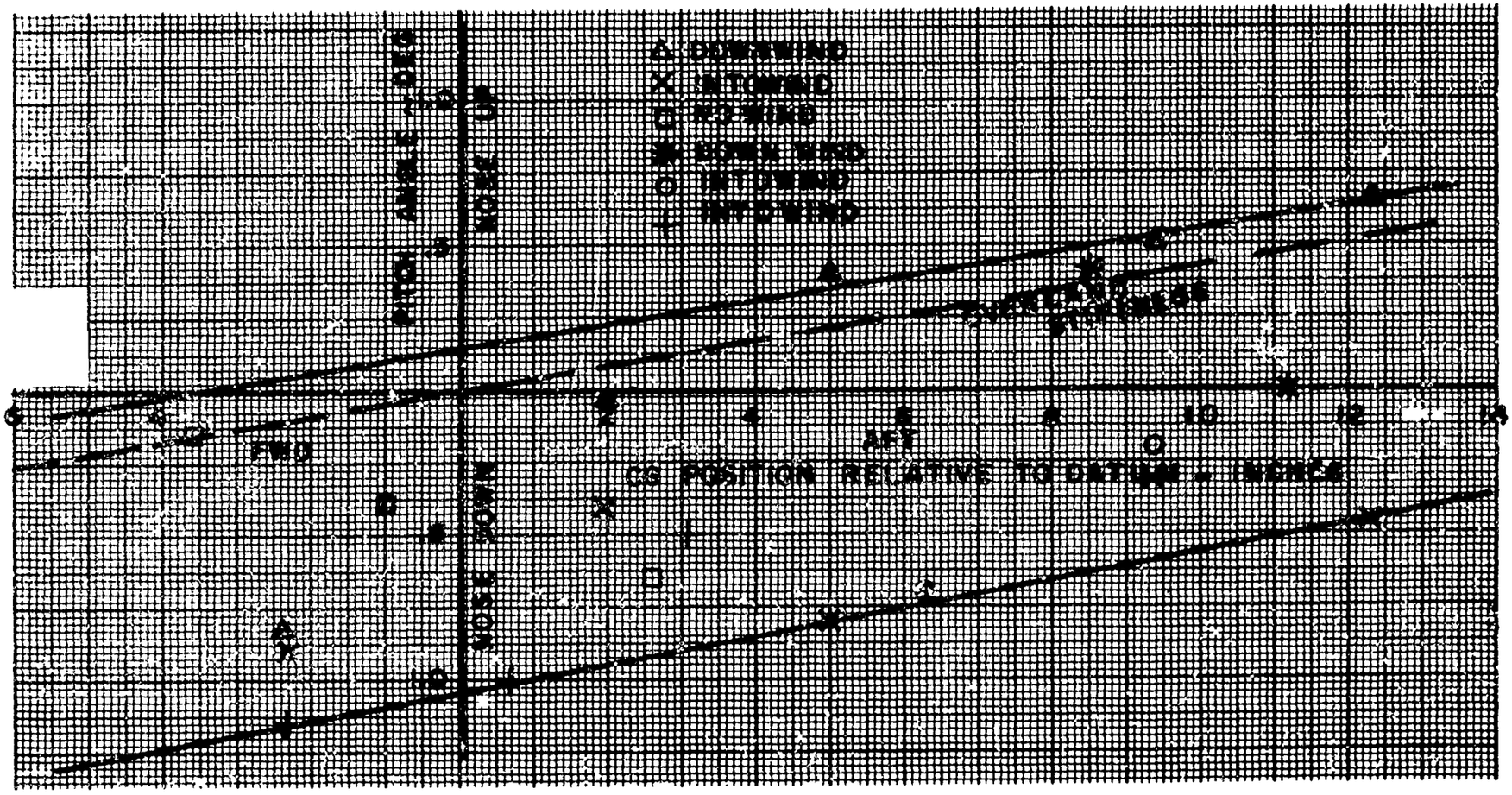

Figure 6-34. VA-3 Static Stiffness in Pitch, Overwater Test

roll and pitch at approximately those frequencies calculated from the hovering stiffness results. No significant response at the heave natural frequencies was noted. For future trials, Republic recommends that a spectrum analysis be conducted on the response-time history; this will establish the differences in cushion characteristics between land and water and enable any stiffness degradation with forward speed to be determined.

The damping computed during the over-water runs proved to be erratic. Even though the tests were conducted on a calm day in sheltered water, low-frequency forcing of the roll mode was evident. Because the roll excitation from the spoilers was not large, selection of the forced response components on the record was difficult. Within these limitations and over the range of speeds tested, no apparent correlation between damping and forward speed is evident.

2. Control and Maneuvering

a. Phase A - Over-Water Runs

During the testing, it was concluded that the best method of operation in sea states 0 to 1 was to run at minimum hover height; while in sea state 1 to 3, running at

maximum hover height proved superior. The reason for this is that in low sea states, the momentum drag can be reduced with little or no increase in wave drag. In higher sea states, the increase in wave drag is not offset by the reduction in momentum drag.

GEM craft are very susceptible to side wind loads. In coastal water, wind velocity and direction continually change due to land mass interference. Therefore, a good yaw and roll control system is required. It was found that both the rudder control and spoiler control of the VA-3 are adequate, but there are parts of the systems that can be improved.

For example, the rudder pedal forces were excessive, and it was noted that the drivers continually overcorrected in attempting to steer a course. In some runs, 10 to 30 changes of rudder position per minute were recorded. Rudder control was most effective during beam sea operation. The combination of high pedal forces and the numerous changes employed were extremely exhausting for the driver. Therefore, either an alternate method of yaw control should be used in the future, or the system should be improved by the use of

boosters and servos. It should be noted that all drivers preferred to employ differential propeller pitch in making turns, although the rudder control system could have been used.

A number of times during this phase of testing, there was a tendency of the bow to be drawn down into the water while the craft was traveling at speeds above 40 knots. Once, because of this phenonenon, the craft actually ditched while traveling downwind at 46 knots. Further investigation of this situation should be conducted with additional thrust provided to allow investigation at increased maximum operating speeds.

b. Phase B - Surf Tests

The best method for driving to shore over breaking surf was to employ minimum hoverheight and at the same time to adjust the forward propulsion speed to the apparent forward velocity of the breaking surf. The craft should come directly across the surf line, with the longitudinal center line of the craft and the surf line at approximately 90 degrees. Some extra forward thrust is recommended to prevent the craft from slowing down as it approaches the beach.

In re-entering the surf, maximum hoverheight should be employed, and the angle between the longitudinal center line of the craft and the surf line should again be 90 degrees. The speed of the craft should be at least 15 knots and should be adjusted to minimize the pitching of the craft. It was found that the initial wave encountered does not impose as much a problem as subsequent waves, especially when the waves are closely pitched (35 feet or less), because the first wave encountered tends to put the craft in a nose down attitude in relation to oncoming waves. One method to minimize this effect is to cross the surf line at a slight angle off 90 degrees (no more than 10 to 15 degrees off). An attempt should also be made to maneuver the craft to minimize the number of waves negotiated at the point where they break.

c. Phase C - Long-Crested Wave Runs

Long crested swells in the radius of the test area never exceeded 150 feet. Tests were therefore conducted within this wavelength. It is noted that the pattern was an octagon. Therefore, part of the test was conducted with the wave fronts at 45 degrees to the craft longitudinal. This made the effective wave lengths 210 feet. It was found that

the craft negotiated 4-foot waves in this type of sea with little or no impacts.

c. Phase D - Over-Land Runs

Over level terrain the craft is extremely sensitive to wind velocity and direction. The best method for maneuvering is to employ minimum lift power and allow the skirts to drag. This imposes controllability at the expense of skirt wear. Cushion exhaust presented no problem to nearby observers.

E. SEA KEEPING

1. Acceleration Data

The accelerometer records taken during Phase A trials in sea states 2 and 3 were analyzed. The amplitudes traced on these records were random, so statistical methods were used to describe them quantitatively.

The technique used was as follows: Periods during which the craft speed and heading remained constant were determined. The number of times the trace crossed a given acceleration threshold level over each such period was counted. The frequency of occurrence of maxima in any acceleration band

could thus be computed, together with the cumulative probability (the probability of achieving an acceleration equal to or greater than a given level) and the probability density.

The major part of the analysis was conducted using records from the bow accelerometer, because the greatest levels were achieved there, and they could be assessed more conveniently. However, for comparative purposes, a limited amount of data from the accelerometer near the center of gravity was analyzed, because this provides information as to the relative comfort in the passenger cabin.

In long-crested waves, the craft executes a coupled heave and pitch motion as it "contours" the waves (similar to a hydrofoil). The bow and center-of-gravity accelerometers were in phase while the stern accelerometer was out of phase. This situation was found whenever the sea state was well defined with a predominant wave direction.

In short-crested waves, the craft tended to plow through succeeding wave crests with small pitch changes. This was accompanied by longitudinal accelerations of the craft; however, these rarely exceeded 0.1g.

The craft was taken out off Montauk Point in a 9- to 12-foot confused sea, which would correspond to sea state 5, with wave lengths (35 feet) much shorter than those consistent with such a sea. On this run quite pronounced pitch and roll was experienced, with bow normal accelerations of 1.5g being encountered, together with longitudinal accelerations of up to 0.6g in the aft direction. The rearward-facing seating proved to be particularly good in those seas.

The results of analysis on the acceleration time histories are shown in Figures 6-35 to 6-45. Figures 6-35 and 6-36 show the effect of lift engine power when operating in sea states 2 and 3, respectively. In sea state 2, the maximum lift power setting tended to give the smoother ride, while in sea state 3 the minimum lift power setting reduced the probability of experiencing severe accelerations. In some cases, the curves are not comparable because a speed differential exists; these differences occurred because the driver made way at the maximum speed that he felt to be consistent with safe operation during a given test. (This is the manner in which the craft would normally be operated.) His judgment was subjective; and, because little impression of forward speed is

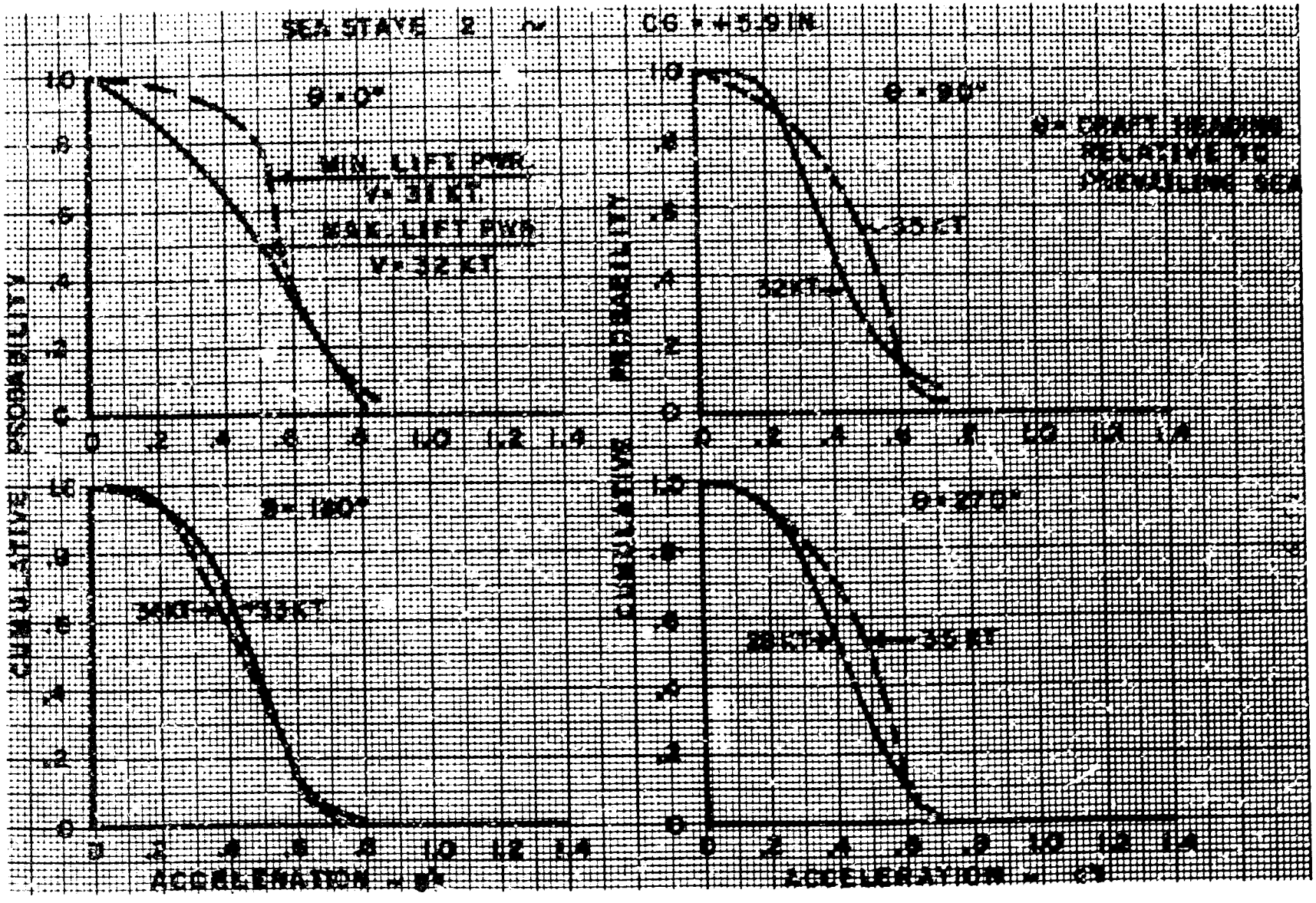

Figure 6-35. Effect of Lift Engine Power on Cumulative Probability of Bow Acceleration, Sea State 2, cg = 5.9 inches

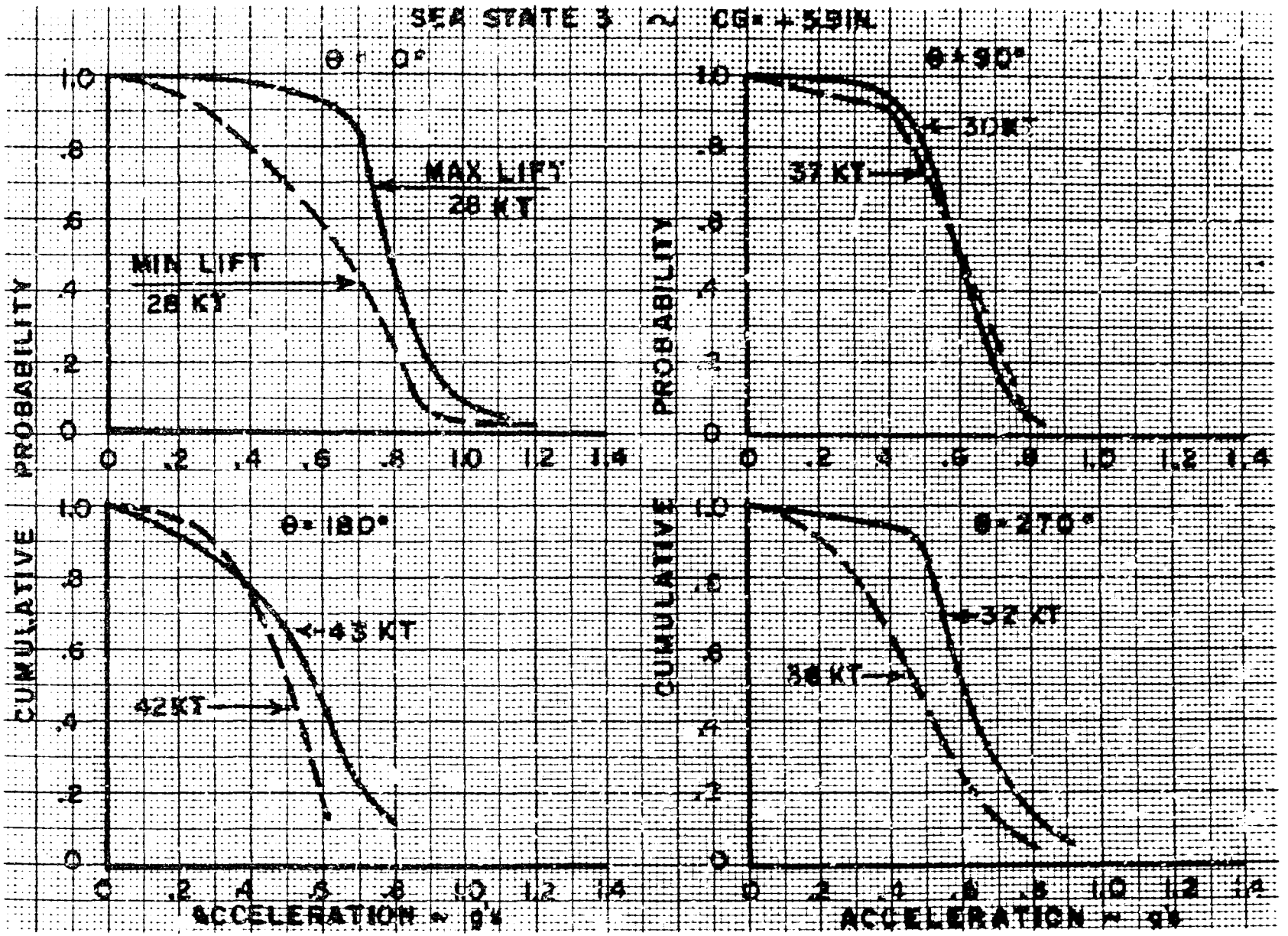

Figure 6-36. Effect of Lift Engine Power on Cumulative Probability of Bow Acceleration, Sea State 3, cg = 5.9 inches

gained from the driver's position, he tended to judge the severity of the conditions by the accelerations he experienced. If the driver's judgment had been consistent from day to day, analysis of the records would yield the same result whatever the conditions, subject to the craft performance limitations. Obviously, in future tests a more objective approach will be made, such as holding the speed constant. However, this could not be done in this series of tests due to the conflicting data requirements on the runs carried out and the desire to take maximum advantage of the infrequent days during which the sea state was high.

Figures 6-37 and 6-38 show the effect of operating in sea states 2 and 3 at minimum and maximum lift power and the mid-cg position. The curves demonstrate the expected result that operation in sea state 3 is more severe than in sea state 2, the disparity between the two sea states being worse at maximum lift power. Figures 6-39 and 6-40 show similar data for operation at the aft-cg position. The same broad conclusions can be drawn as in the previous case; however, the differences are less pronounced, because data for the two center-of-gravity positions was obtained on two separate occasions as were the

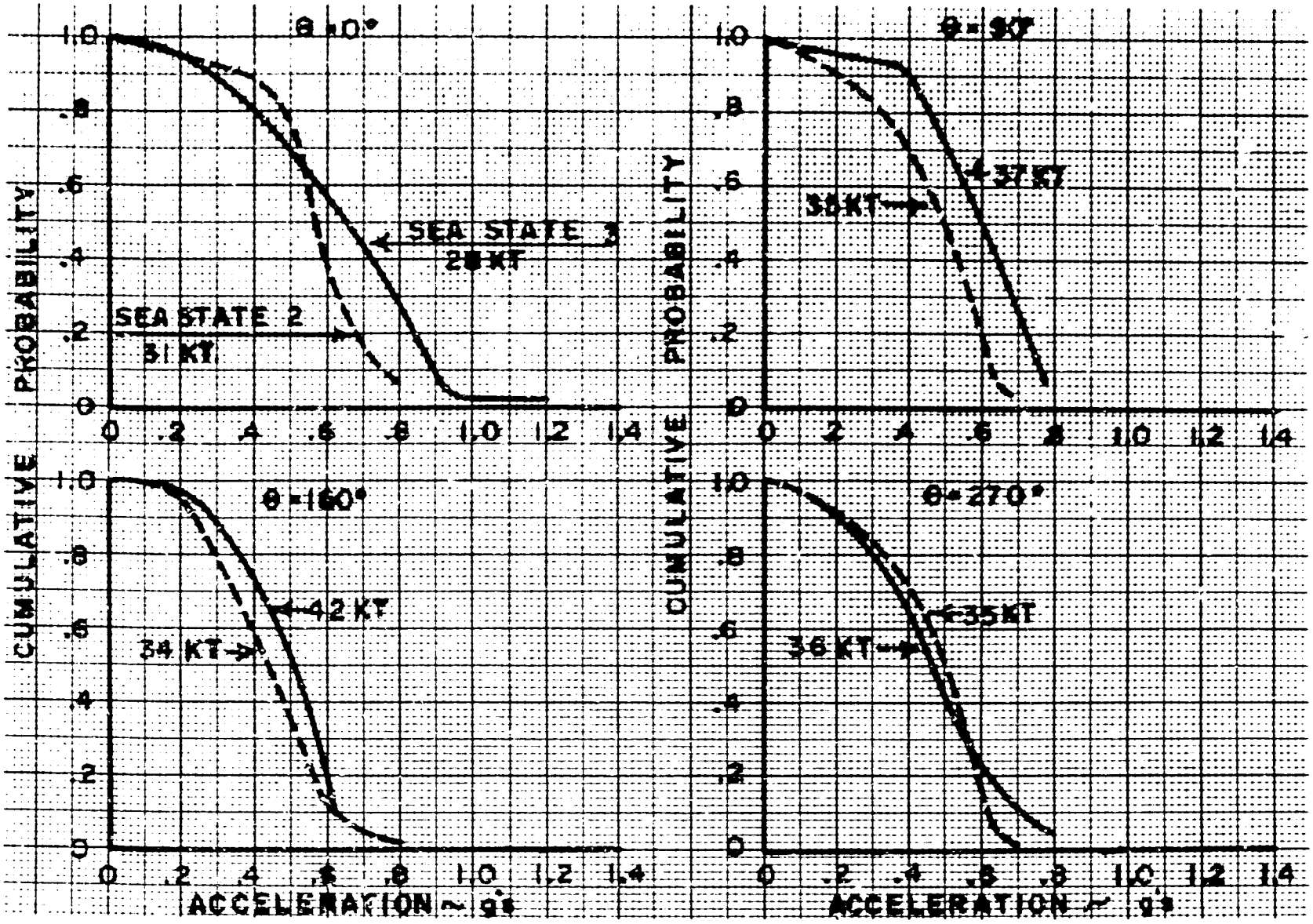

Figure 6-37. Effect of Sea State on Cumulative Probability of Bow Acceleration, Minimum Lift Power, cg = 5.9 inches

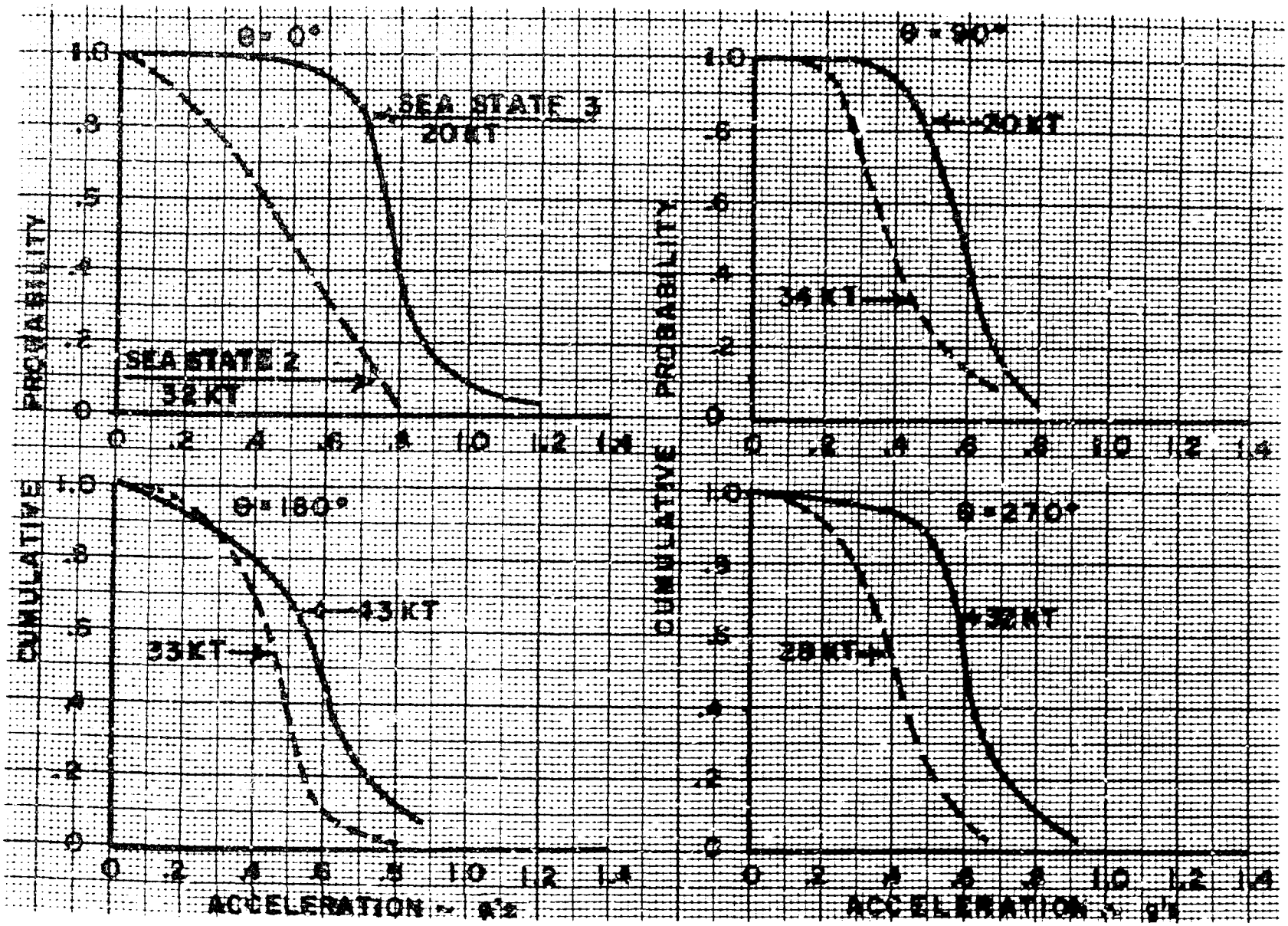

Figure 6-38. Effect of Sea State on Cumulative Probability of Bow Acceleration, Maximum Lift Power, cg = 5.9 inches

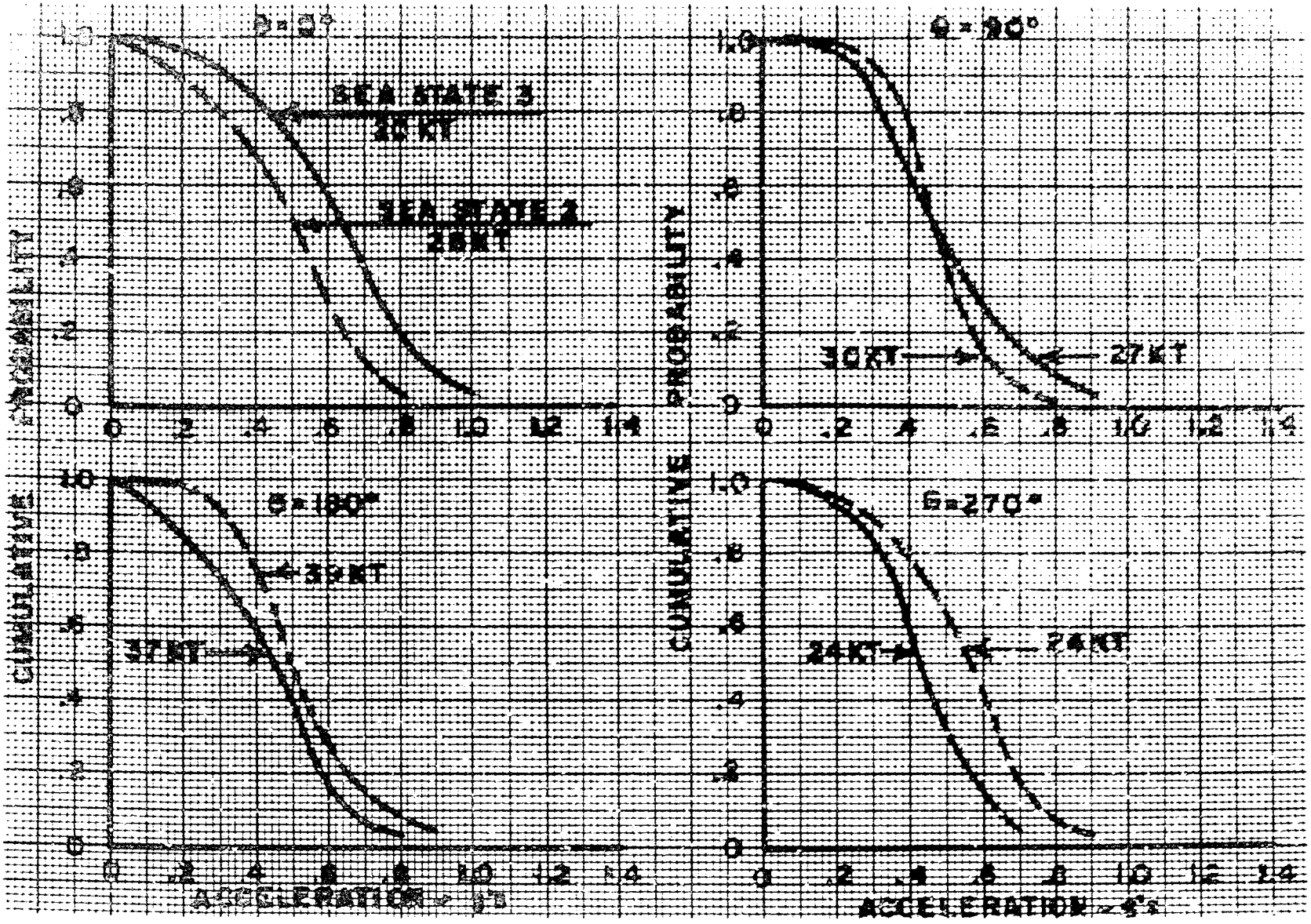

Figure 6-39. Effect of Sea State on Cumulative Probability of Bow Acceleration, Minimum Lift Power, cg = 12 inches

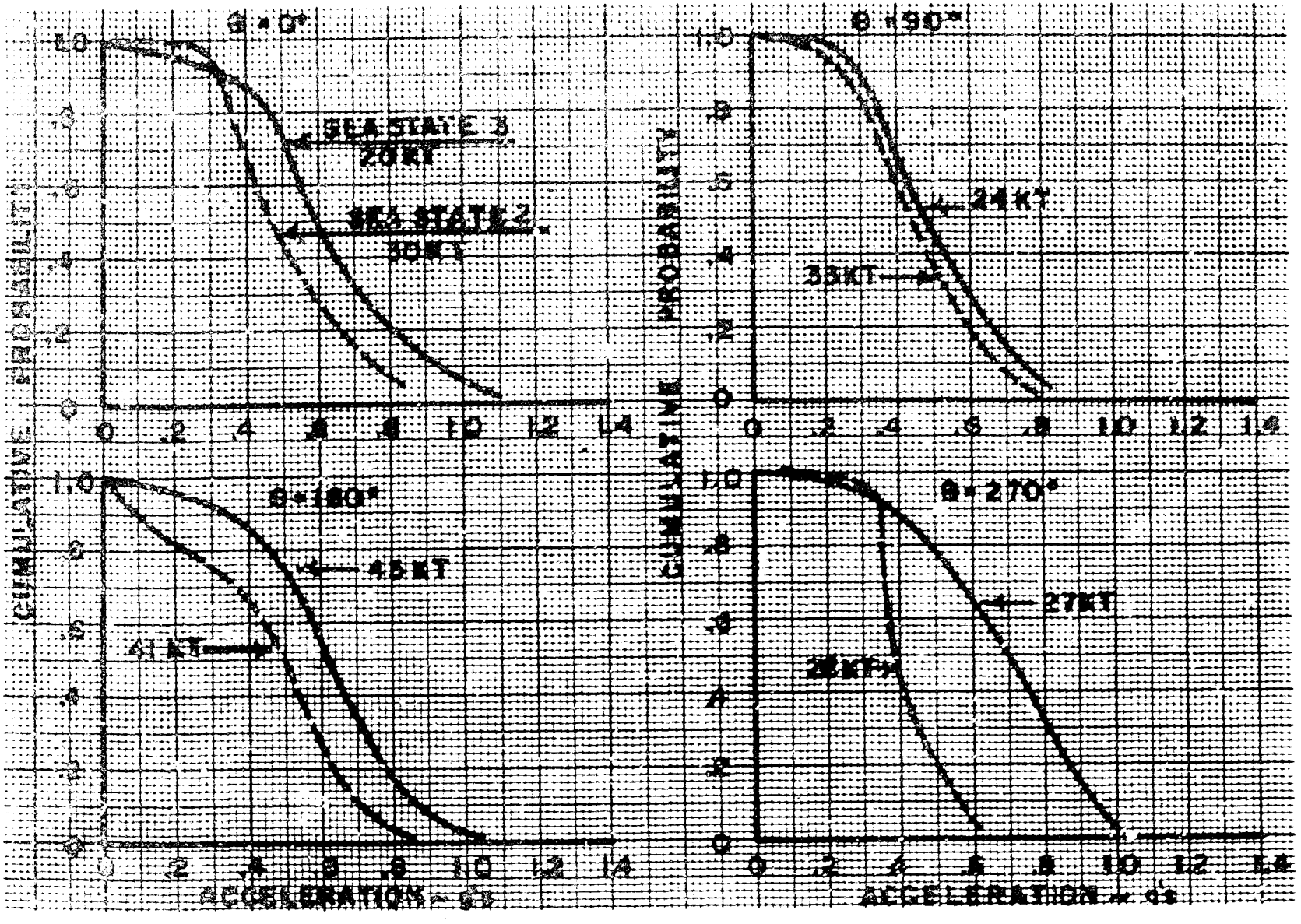

Figure 6-40. Effect of Sea State on Cumulative Probability of Bow Acceleration, Maximum Lift Power, cg = 12 inches

data for the different sea state conditions. Furthermore, contributing to the lack of correlation was the imprecise definition of wave conditions specified by sea state numbers. It was also found in practice that wave conditions could vary over the test area at any given time.

Figure 6-41 shows the effect of operation in sea state 3 at various center-of-gravity positions. When running upwind and downwind, the forward center-of-gravity position gives the worst condition, this probably being due to the nose-down pitch attitude adopted. No plausible explanation is offered for the differences between the two runs conducted cross sea, but the large speed difference between the mid-cg condition and the remaining conditions should be noted.

Figure 6-42 shows the probability density and cumulative probability distributions for operating in sea state 3 and a 9- to 12-foot confused sea described earlier. The data from the confused sea run shows a broader distribution of density than the data taken at sea state 3. The cumulative probability shows only small increases, considering the relative severity of the two conditions.

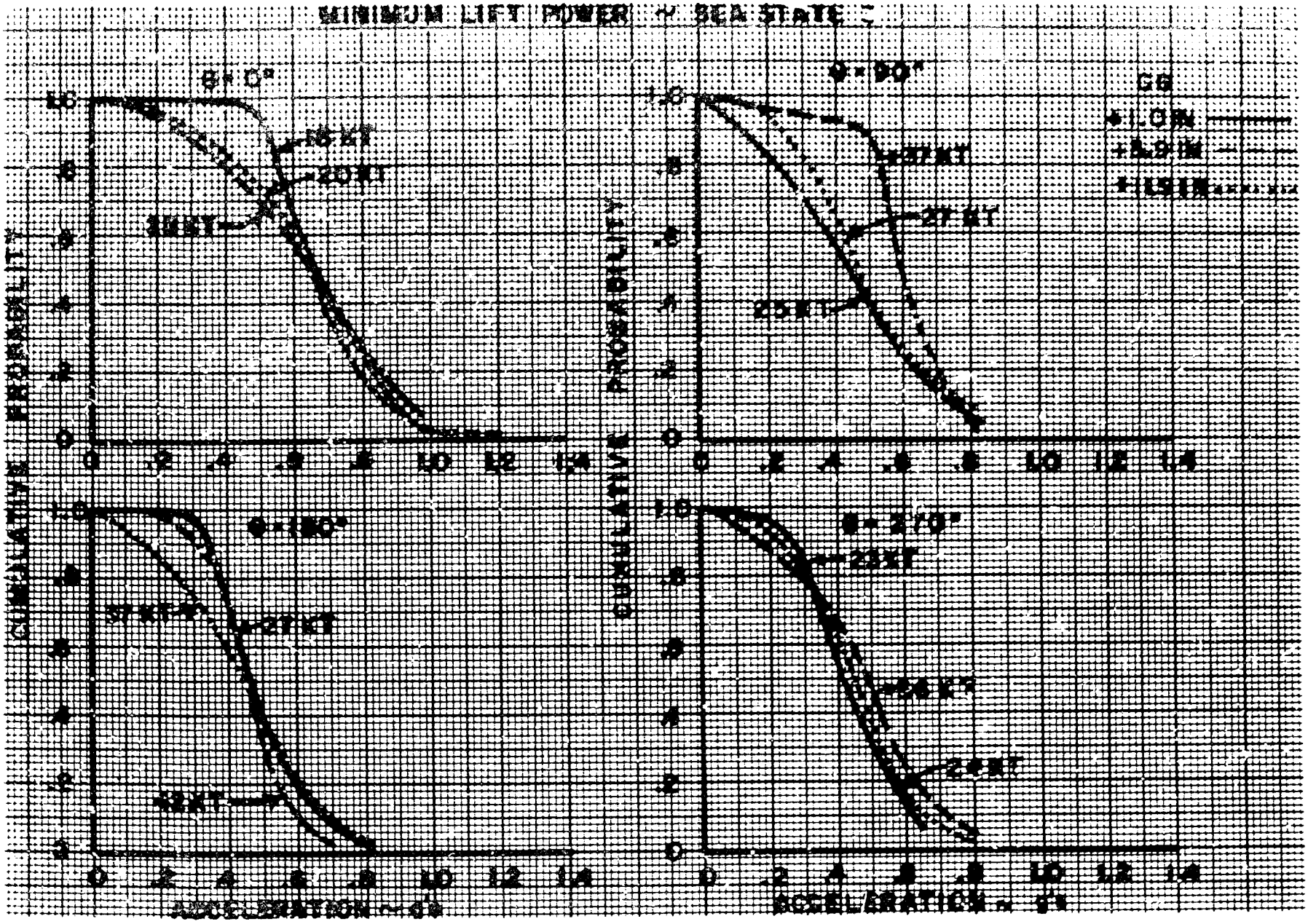

Figure 6-41. Effect of Center of Gravity Postion on Cumulative Probability of Bow Acceleration

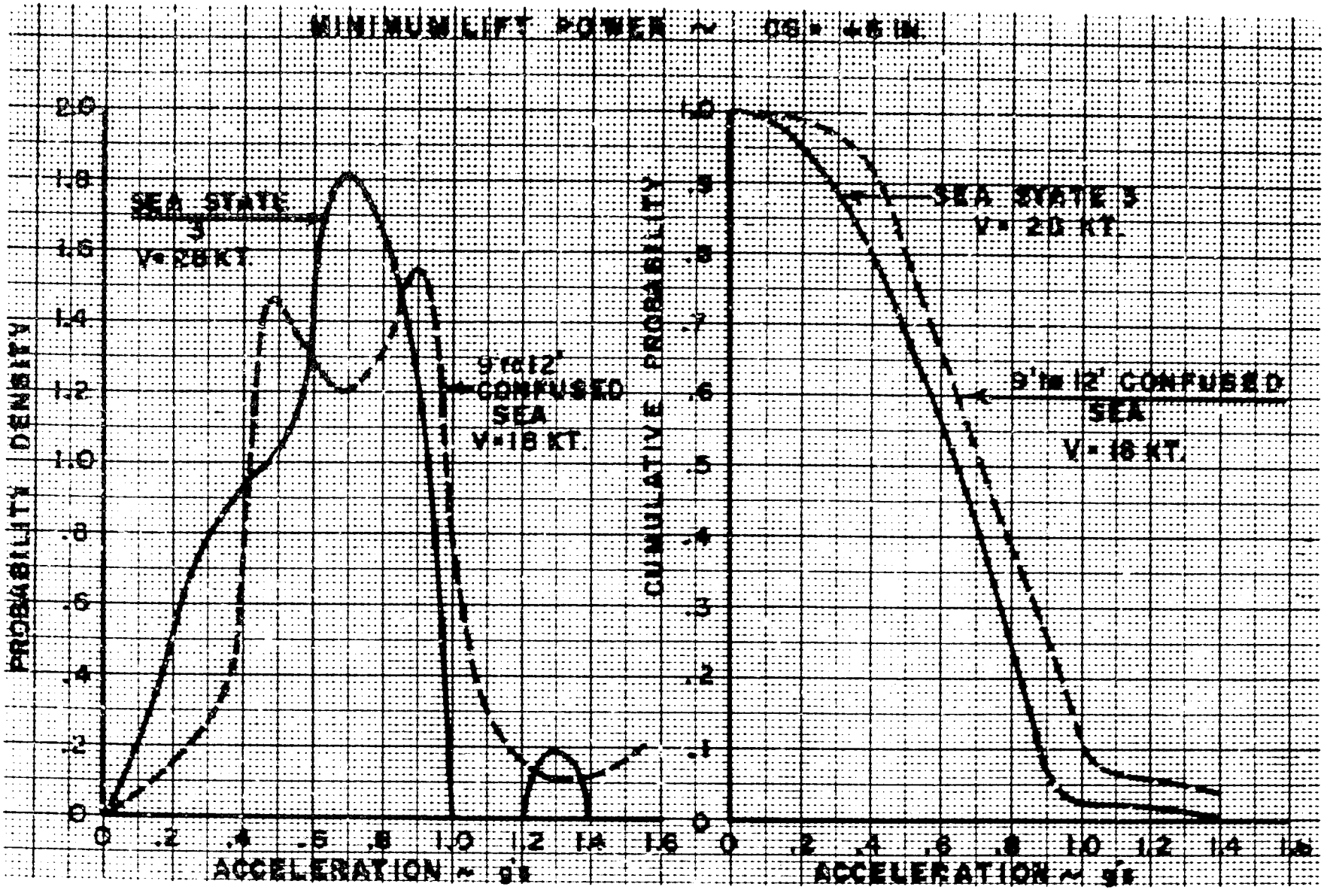

Figure 6-42. Comparison of Bow Acceleration Data for Sea State 3 and 9- to 12-foot Confused Sea

Figure 6-43 shows the probability distributions of low acceleration for operations in sea state 3 at the aft-cg position. The peaks in the curves occur at the rms acceleration levels, and it should be noticed that most of the density is concentrated between 0.4g and 0.7g, which accounts for the steep rise in the cumulative probability in these regions.

Figure 6-44 shows data read simultaneously from the bow and center-of-gravity accelerometers. This shows the relative smoothness of the ride experienced by occupants of the cabin; acceleration levels of 0.5g in this area are exceeded infrequently. Figure 6-45 shows the probability density distribution for the run heading into the prevailing sea. The contributions of the heave and pitch modes are clearly evident in the distribution of bow acceleration, the contribution of the heave mode to the low acceleration correlating well with the center-of-gravity acceleration data.

2. Pitch Data

The mean pitch angles in sea state 0 are shown in Figure 6-46 for various forward speeds. The data indicates that the VA-3 experiences a progressive pitch down with forward speed. This is due to the craft pressure wave creating an

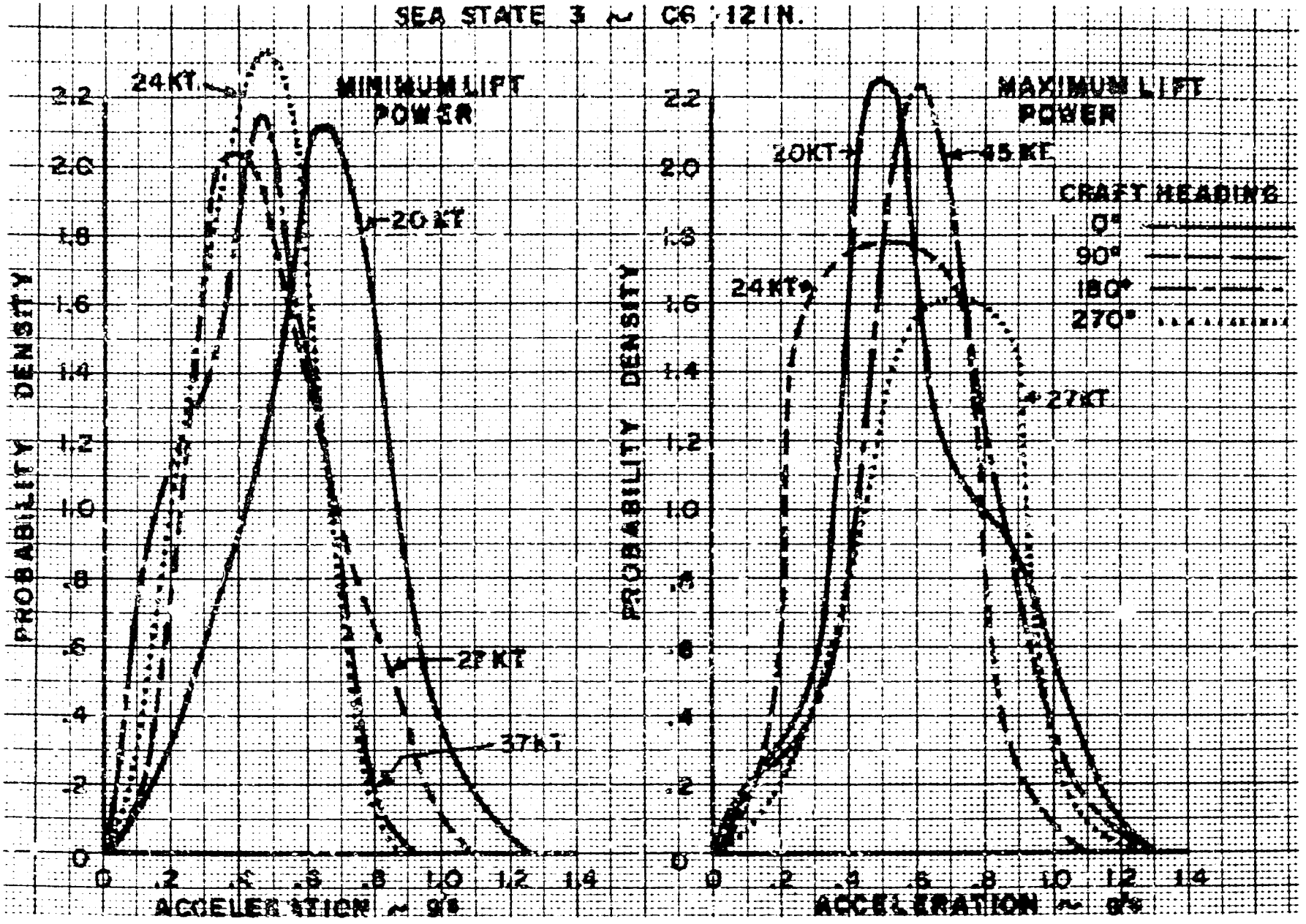

Figure 6-43. Probability Distribution of Bow Acceleration, Sea State 3

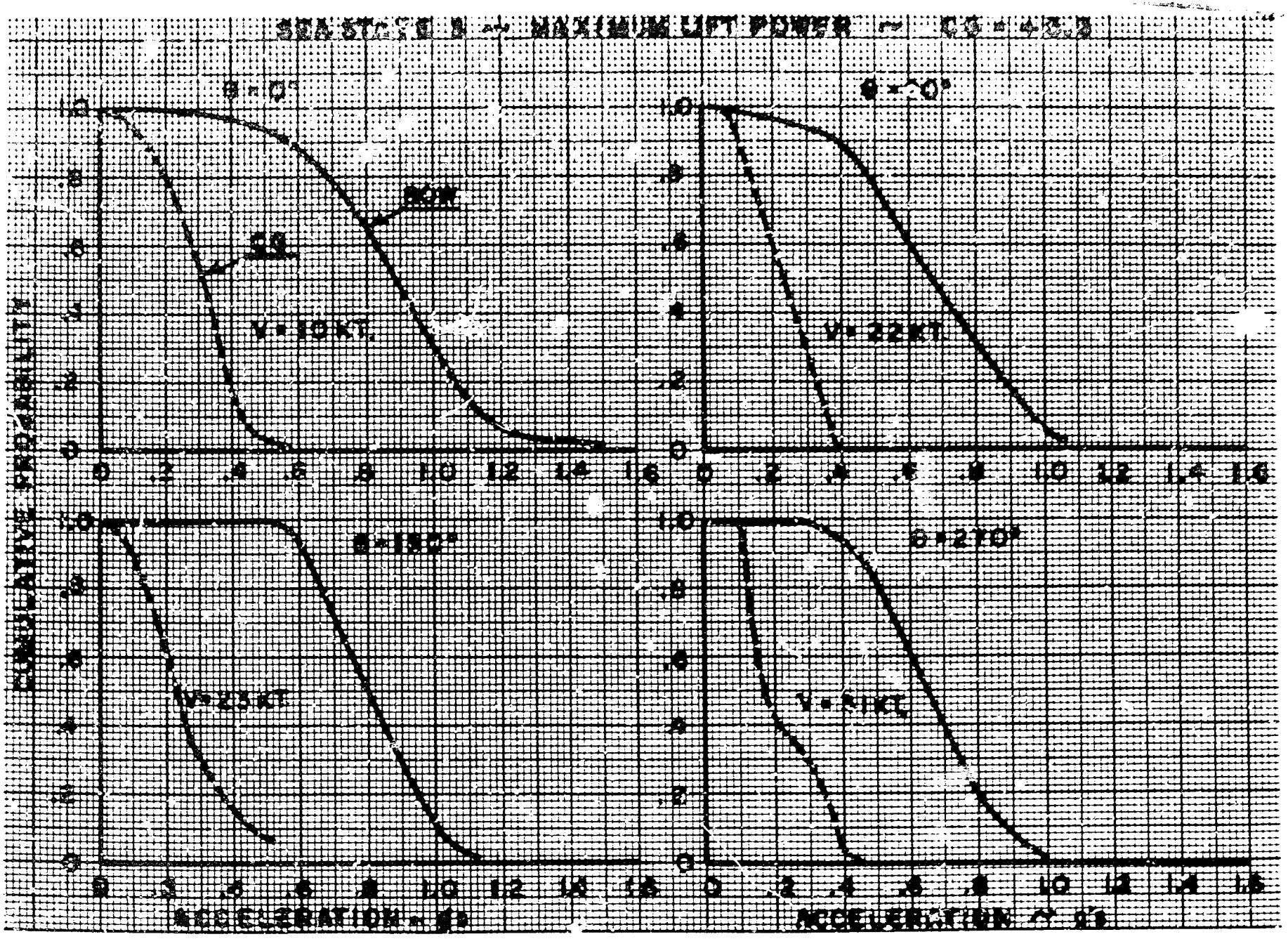

Figure 6-44. Comparison of Acceleration Data Measured at Bow and Center of Gravity

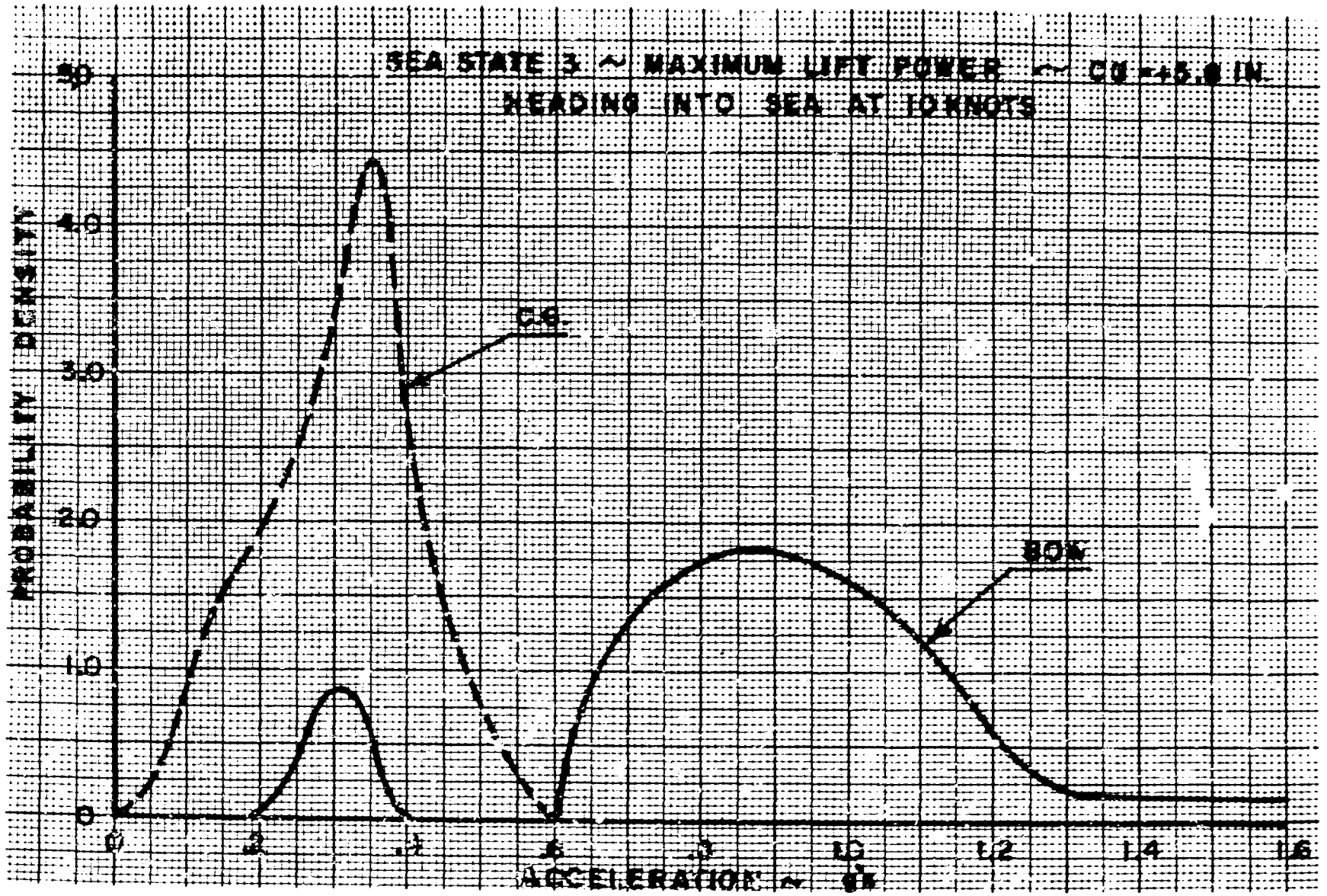

Figure 6-45. Comparison of Probability Distribution of Bow and CG Acceleration

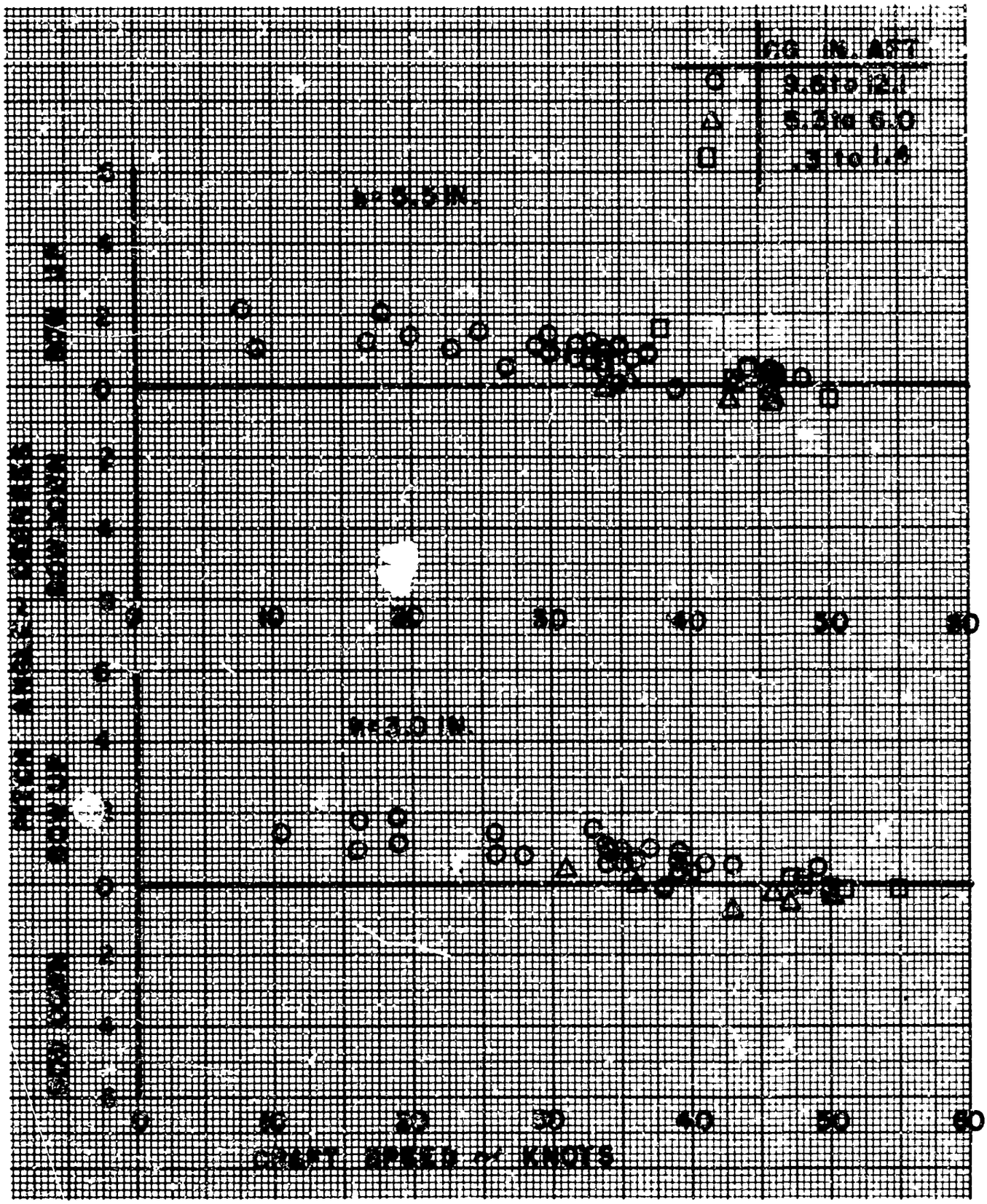

Figure 6-46. VA-3 Average Pitch Angle, Sea State 0

initial nose-up condition which decreases with increases in forward speed. The effect of the raised propulsion thrust line is to further increase the crafts nose-down attitude. Pitch angle corrections, however, can readily be made by differential rpm settings of the forward and aft lift fans.

3. Roll Data

The pronounced starboard list of the craft is shown in Figures 6-47 through 6-50. The degree of list is attributable to the additive propeller torques. An analytical estimate of the roll produced by this source compares favorably with the results. The envelope of maximum roll angles in all test conditions is shown in Figures 6-47 through 6-50 and also exhibits a starboard bias.

4. Spray and Wake Characteristics

The spray generated by an air cushion vehicle is dependent upon the cushion pressure and the air gap between the skirts and the water surface. Each craft will therefore create its own characteristic spray pattern. The VA-3, while hovering as shown in Figure 6-54, is enveloped in its spray.

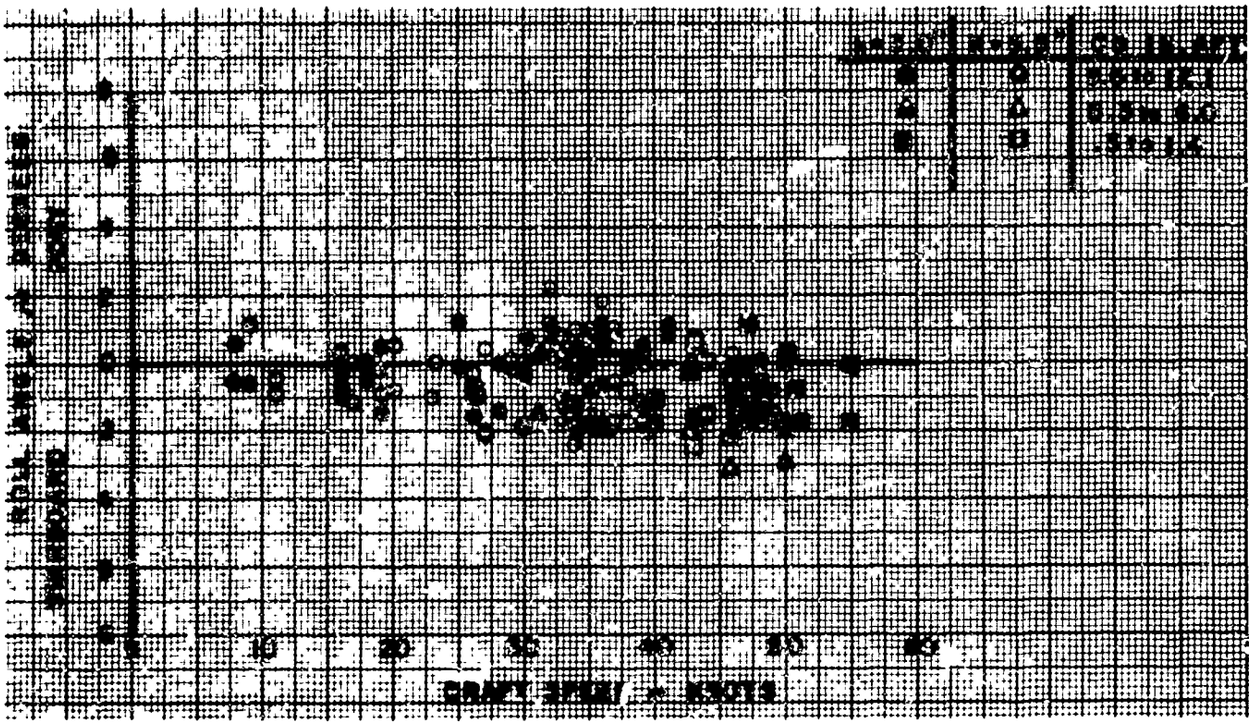

Figure 6-47. VA-3 Maximum Roll Angle, Sea State 0

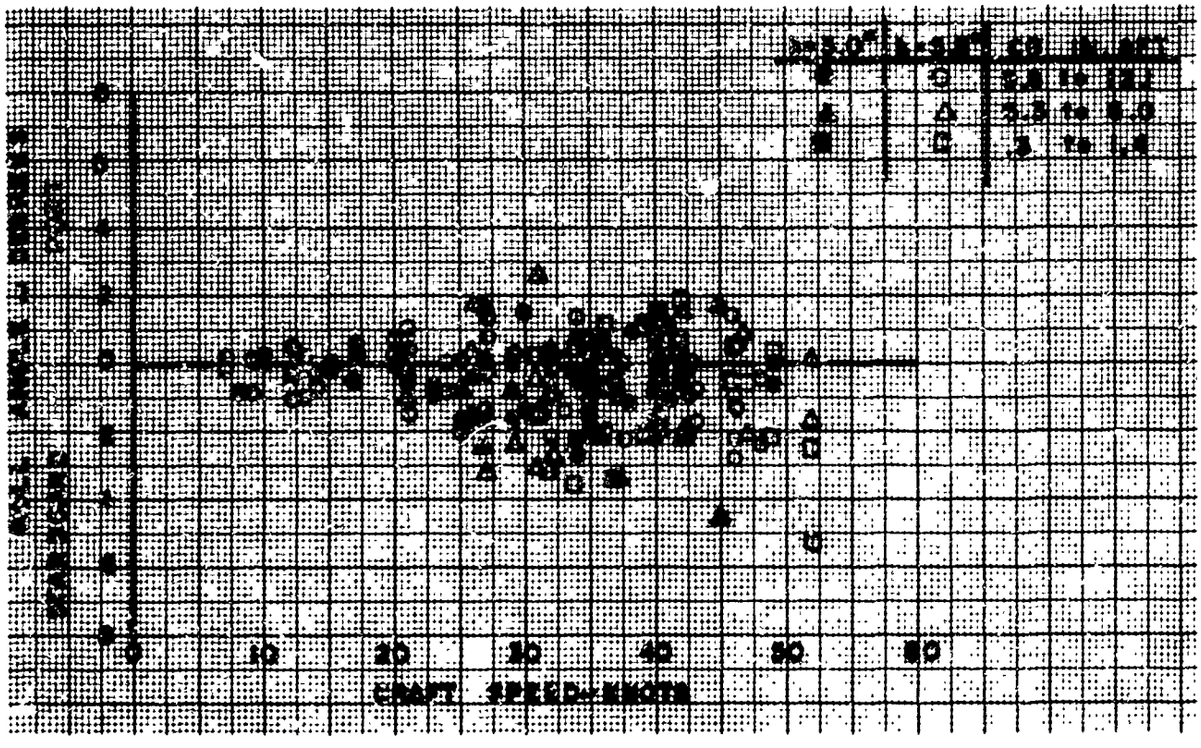

Figure 6-48. VA-3 Maximum Roll Angle, Sea State 1

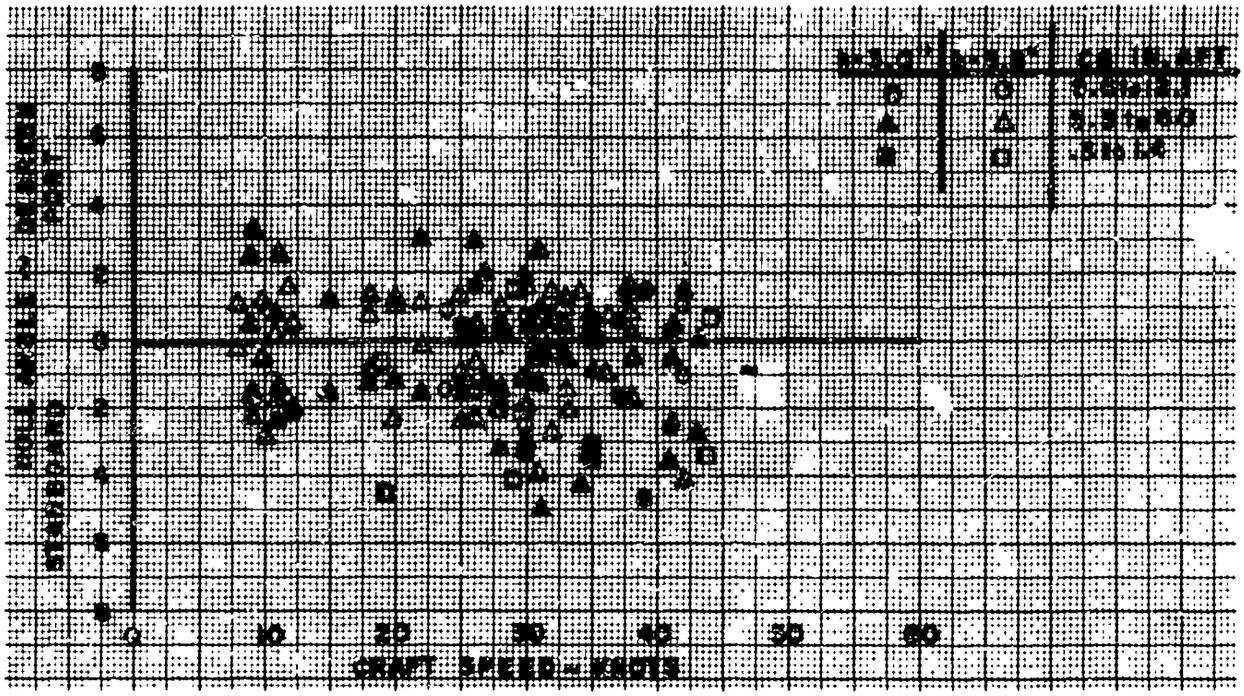

Figure 6-49. VA-3 Maximum Roll Angle, Sea State 2

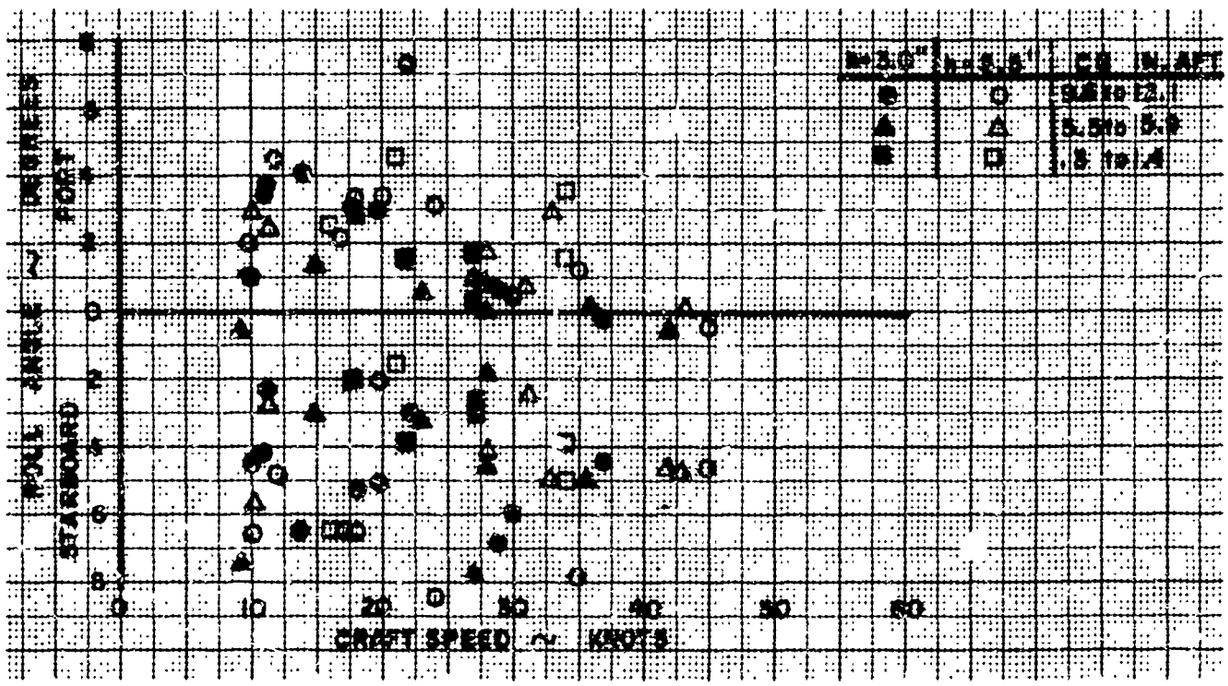

Figure 6-50. VA-3 Maximum Roll Angle, Sea State 3

During acceleration, the spray is swept sideways along the craft, as is shown in Figures 6-51 to 6-56. At speed, the figures show that the spray is projected essentially parallel to the water surface unti it loses its momentum, and then the bow causes the spray to be swept sideways and rearwards along the craft.

The wake shows the small degree of disturbance produced by the craft when above hump speed. The characteristic "keel" effect of the single-sided jets is clearly shown.

F. OPERATION IN SURF

1. Surf Test Diagrams

Each surfing test run consisted of an approach from the open sea through the surf, transition to the beach, turnaround on the beach, and return against the surf to the open sea. The runs were performed in surf ranging from that of near-calm conditions to that having 7-foot breakers.

Data are presented in the diagrams (Figure 6-57) as follows: An arrow directed to the beach represents a surf run from open water to the beach. A second arrow,

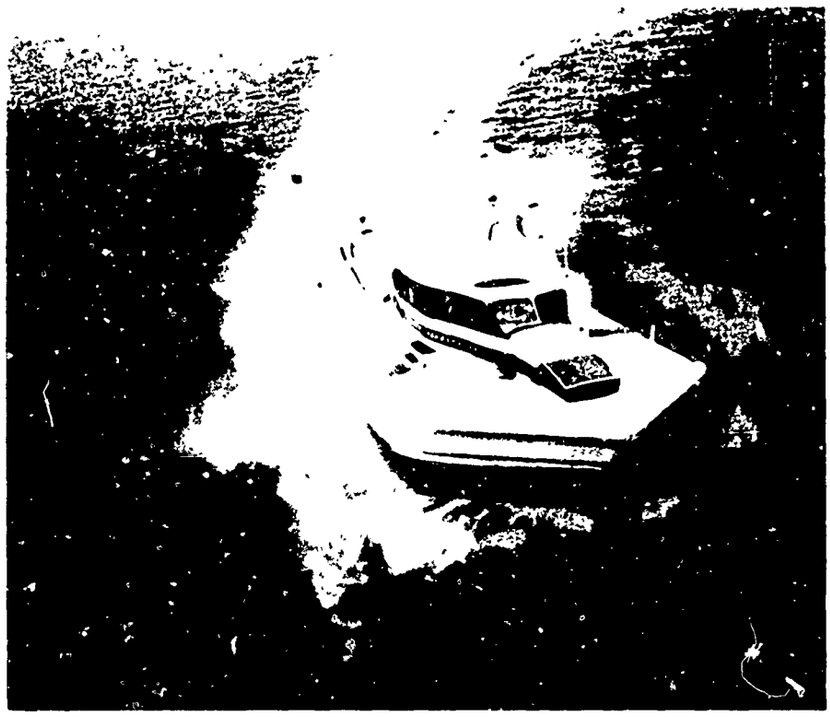

Figure 6-51. Spray and Wake Pattern in a High-Speed Turn

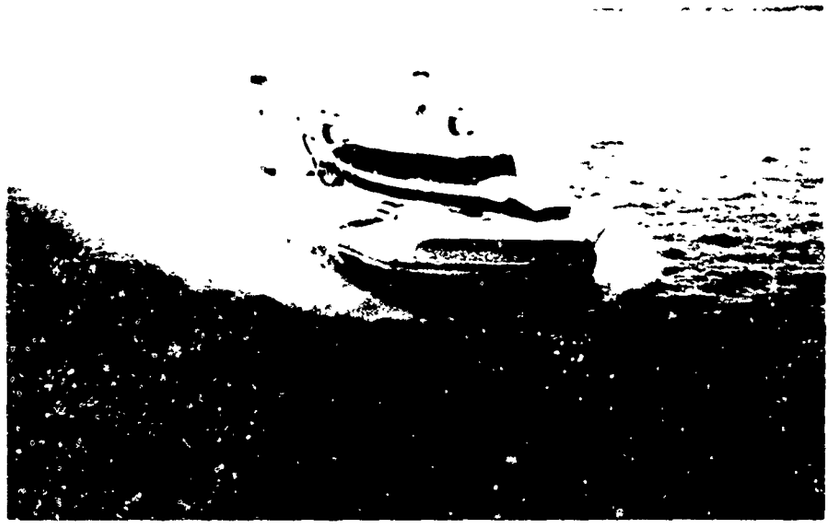

Figure 6-52. Spray and Wake Pattern at High Speed

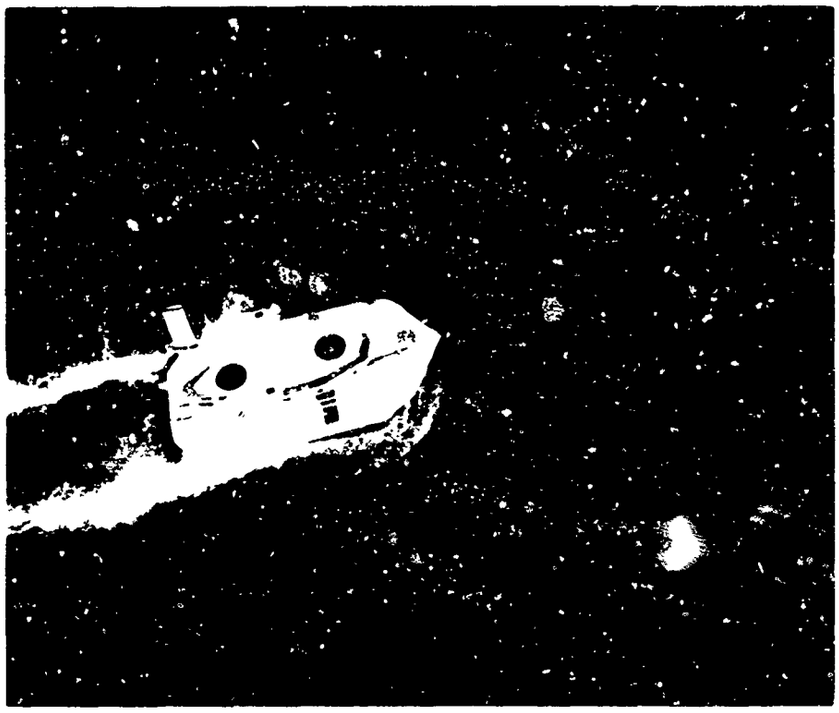

Figure 6-53. Spray Pattern, from Overhead

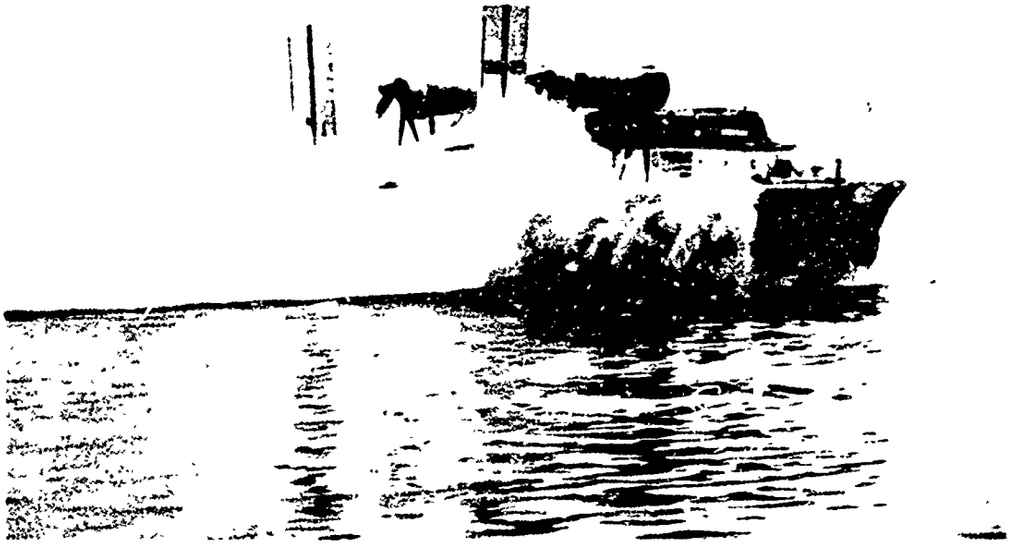

Figure 6-54. Spray and Wake Pattern During Intermediate Speed Run

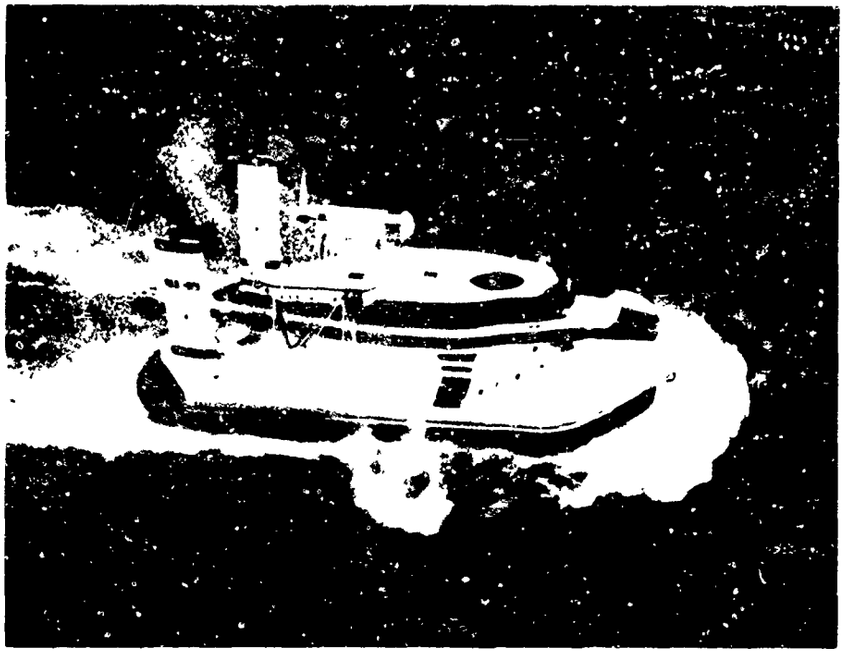

Figure 6-55. Spray Pattern at Intermediate Speed

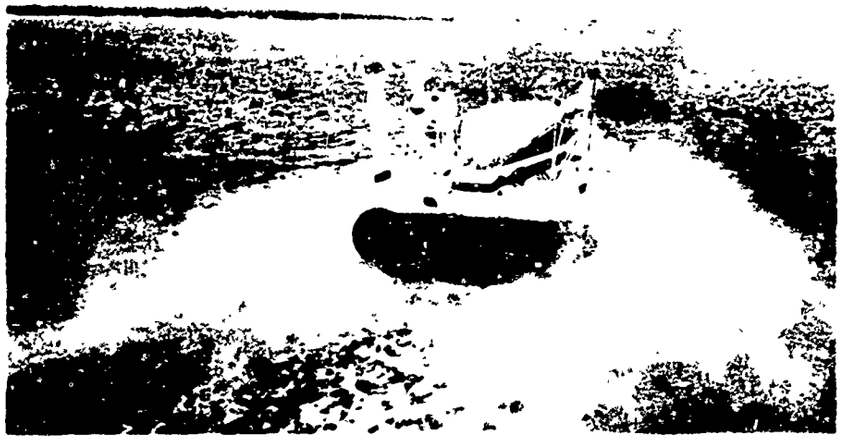

Figure 6-56. Spray and Wake Patterns at High Speed

Sea Conditions: 2-foot swells, 30 to 50 feet apart
Surf Conditions: Calm to 1-foot breakers

Maximum g at cg = +0.70
-0.75

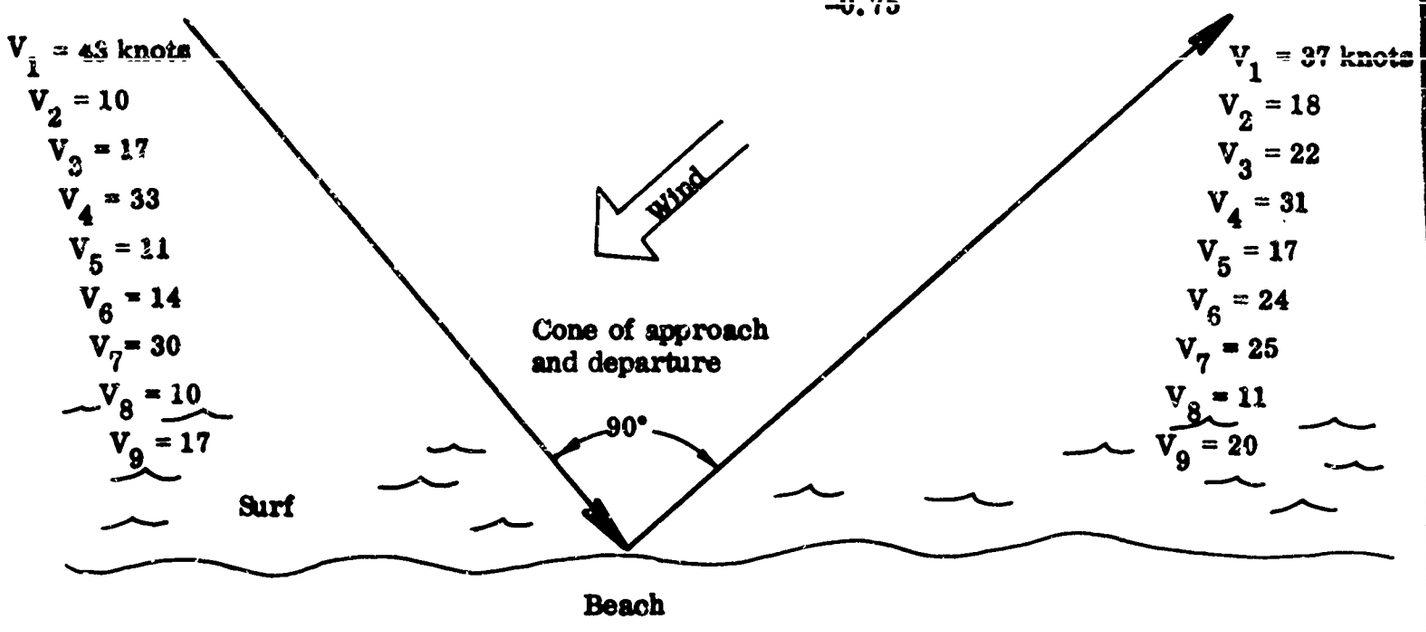

	In			Out		
	Bow g	Pitch (Degrees)	Roll (Degrees)	Bow g	Pitch (Degrees)	Roll (Degrees)
V_1*	+0.5 -0.6	+3.8 -0.5	+0.9 -3.8	+1.0 -0.8	+2.0 -2.4	+2.0 -4.3
V_2	+0.1 -0.2	+1.7 -0.1	+0.2 -2.3	+0.8 -1.0	+4.8 -4.8	+0.1 -2.4
V_3	+0.2 -0.2	+2.9 -0.1	+0.3 -1.8	+1.5 -1.25	-3.0 -6.0	+2.1 -4.5
V_4	+0.3 -0.35	+3.8 -1.8	+0.4 -2.5	+0.5 -0.9	+4.2 +2.0	+1.1 -3.9
V_5	+0.1 -0.1	+2.0 -0.3	-0.8 -1.5	+0.5 -0.75	+5.3 -4.3	+3.7 -5.5
V_6	+0.1 -0.1	+1.6 -1.0	-0.4 -1.4	+0.9 -0.9	+4.7 -3.8	+3.7 -3.6
V_7	+0.5 -0.3	+2.9 -2.0	0 -3.4	+0.6 -0.5	+4.5 -1.9	0 -6.9
V_8	+0.1 -0.1	+3.0 -2.7	-0.7 -1.8	+0.7 -0.6	+5.9 -4.3	+1.5 -2.9
V_9	+0.25 -0.20	+4.0 -1.2	-0.7 -3.4	+0.7 -0.6	+3.4 -5.5	+2.3 -5.0

* Run number referred to from Figure

Figure 6-57. Surf Test Diagrams

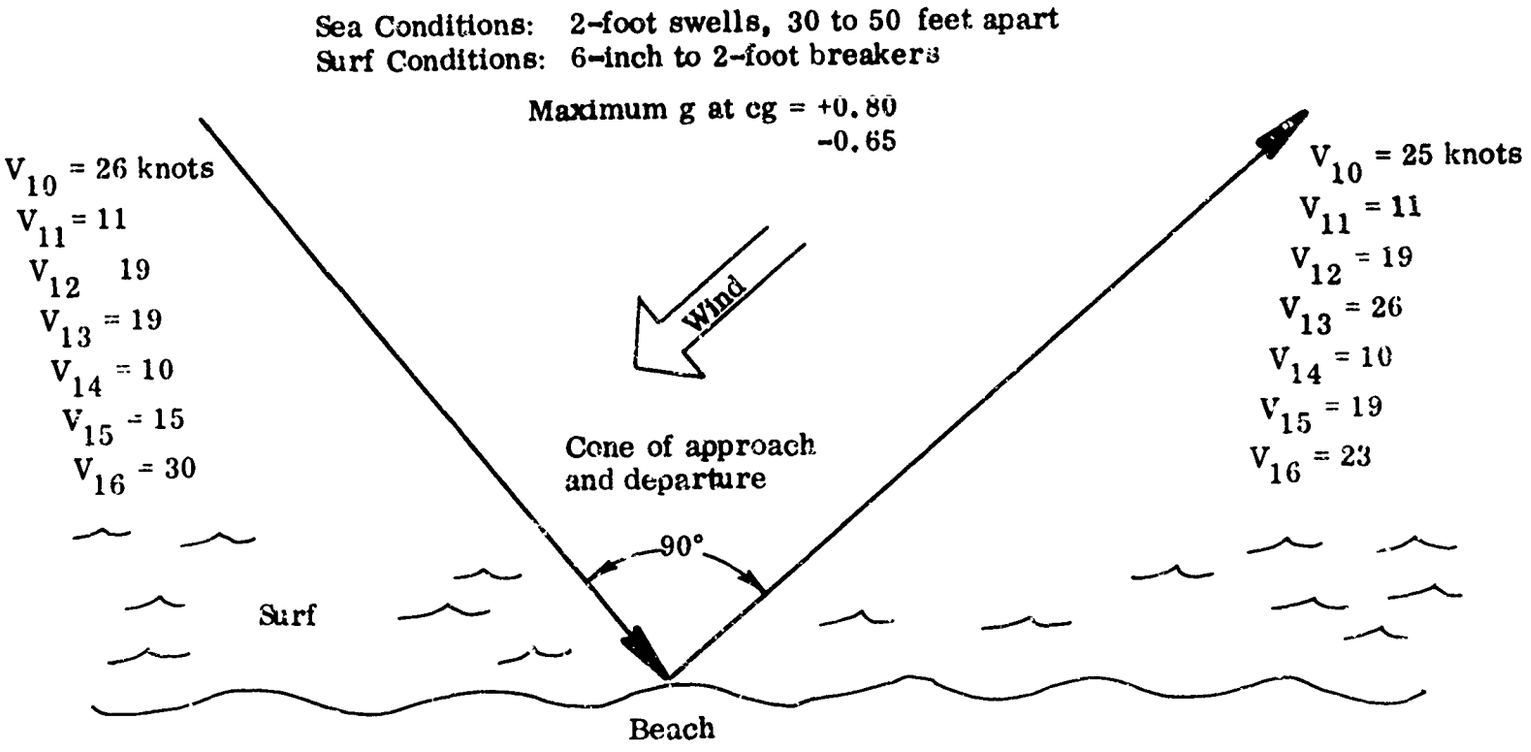

	In			Out		
	Bow g	Pitch (Degrees)	Roll (Degrees)	Bow g	Pitch (Degrees)	Roll (Degrees)
V_{10}	+0.5 -0.4	+4.5 -1.1	+0.5 -2.8	+0.6 -0.5	+4.6 -1.7	+1.8 -4.0
V_{11}	+0.2 -0.15	+1.7 -1.0	-0.2 -2.2	+1.0 -0.7	+7.2 -3.7	+1.0 -2.5
V_{12}	+0.25 -0.25	+4.6 -1.7	-0.1 -2.5	+0.5 -0.4	+4.3 0	+1.9 -3.8
V_{13}	+0.3 -0.25	+1.8 -0.3	-0.4 -2.3	+0.6 -0.75	+5.0 -3.0	+0.6 -3.4
V_{14}	+0.1 -0.15	+1.3 -1.7	-0.2 -2.3	+0.3 -0.35	+4.2 -2.3	0 -3.0
V_{15}	+0.25 -0.25	-2.6 -3.7	-1.9 -0.5	+0.6 -0.75	-3.7 -4.5	+0.5 -3.5
V_{16}	+0.3 -0.25	+1.3 -1.7	+0.3 -1.9	+0.7 -0.8	+4.1 -5.6	+1.7 -3.5

Figure 6-57. Surf Test Diagrams (Cont'd)

Sea Conditions: 6-foot to 7-foot swells, 100 feet apart
Surf Conditions: 5-foot to 7-foot breakers, 50 feet apart

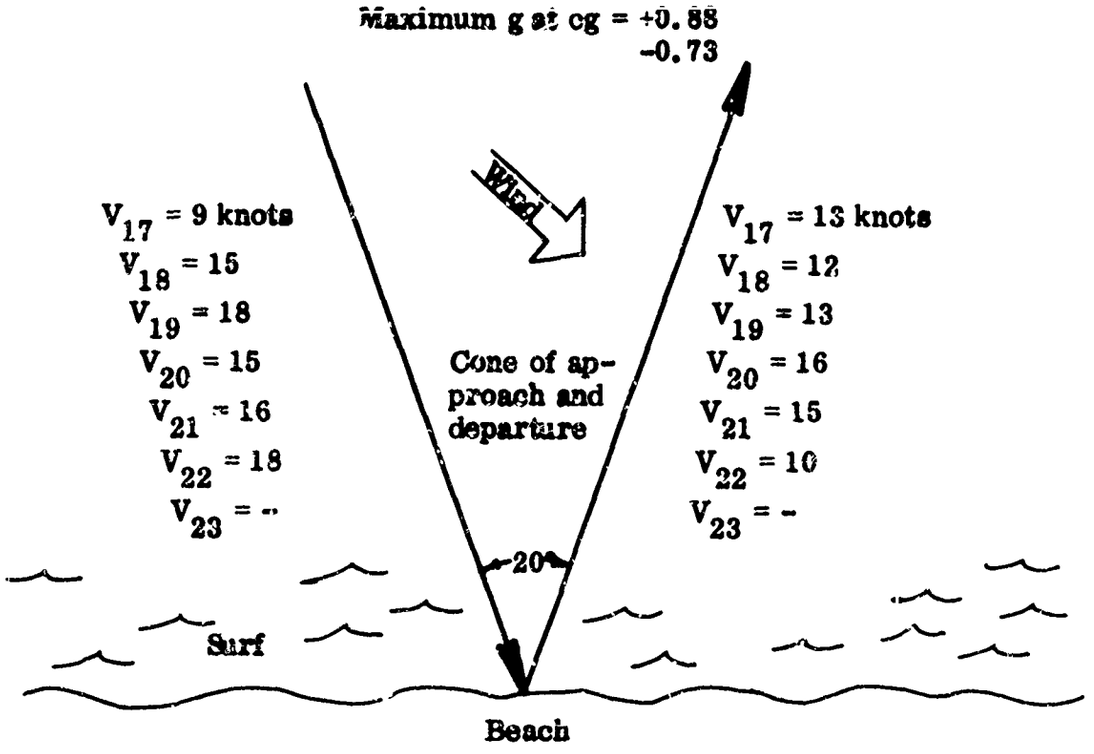

	In			Out		
	Bow g	Pitch Degrees)	Roll (Degrees)	Bow g	Pitch (Degrees)	Roll (Degrees)
V_{17}	+1.6 -1.3	+1.8 -0.5	+1.0 -4.5	+1.6 -1.3	+7.4 -6.5	+0.2 -4.3
V_{18}	+1.6 -1.4	+2.6 -0.7	+0.9 -2.7	+1.6 -1.3	+10.2 -9.7	+2.2 -5.9
V_{19}	+1.6 -1.9	+6.8 -2.7	+2. -2.8	+1.6 -1.9	+8.1 -8.5	+2.1 -3.9
V_{20}	+1.6 -1.45	+6.5 -1.5	+0.4 -3.2	+1.6 -1.45	+9.4 -6.5	0 -3.2
V_{21}	+1.6 -1.4	+5.3 -1.7	+1.8 -2.1	+1.6 -1.4	+10.2 -7.5	+3.8 -5.9
V_{22}	+1.6 -1.4	+3.2 0	+2.0 -1.2	+1.6 -1.4	+7.7 -7.2	+2.7 -0.8
V_{23}	-1.5 -1.35	-	-	+1.5 -1.35	-	-

Figure 6-57. Surf Test Diagrams (Cont'd)

Sea Conditions: 6-foot to 7-foot swells, 35 feet apart
Surf Conditions: 4-foot to 5-foot breakers, 35 feet apart

Maximum g at cg = +0.45
-0.50

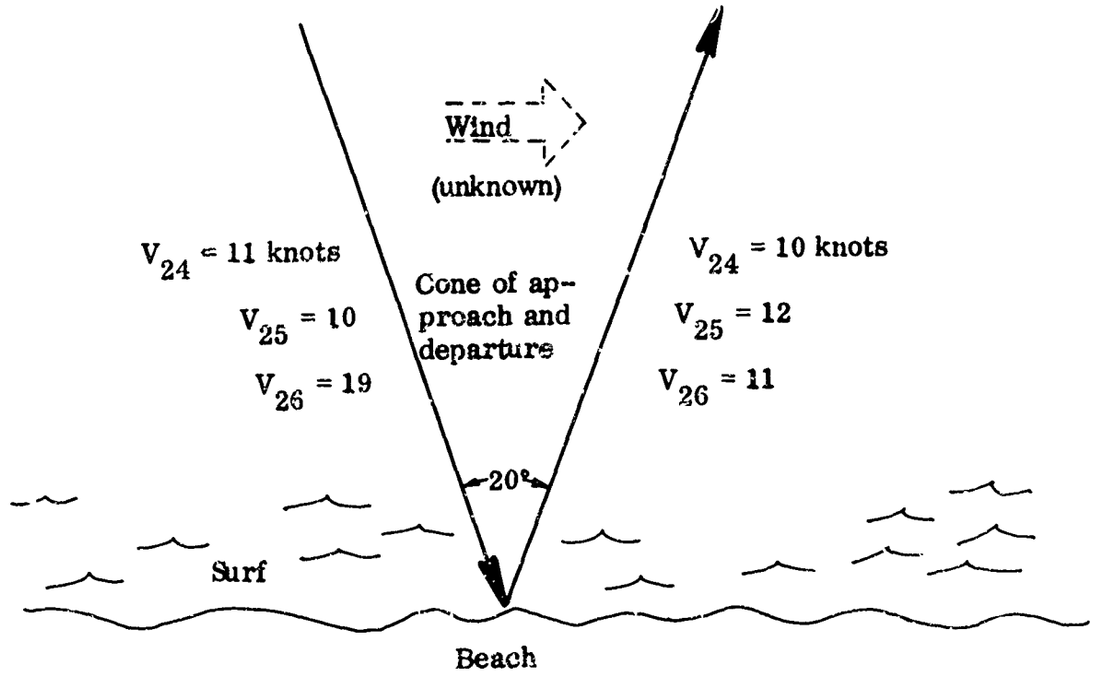

	In			Out		
	Bow g	Pitch (Degrees)	Roll (Degrees)	Bow g	Pitch (Degrees)	Roll (Degrees)
V_{24}	+0.2 -0.1	-	-	+0.35 -0.43	-	-
V_{25}	+0.3 -0.35	-	-	+1.05 -1.00	-	-
V_{26}	+0.6 -0.35	-	-	+1.6 -1.5	-	-

Figure 6-57. Surf Test Diagrams (Cont'd)

Sea Conditions: 6-foot swells, 50 feet apart
Surf Conditions: 6-foot breakers, 50 feet apart

Maximum g at cg = +0.55
-0.25

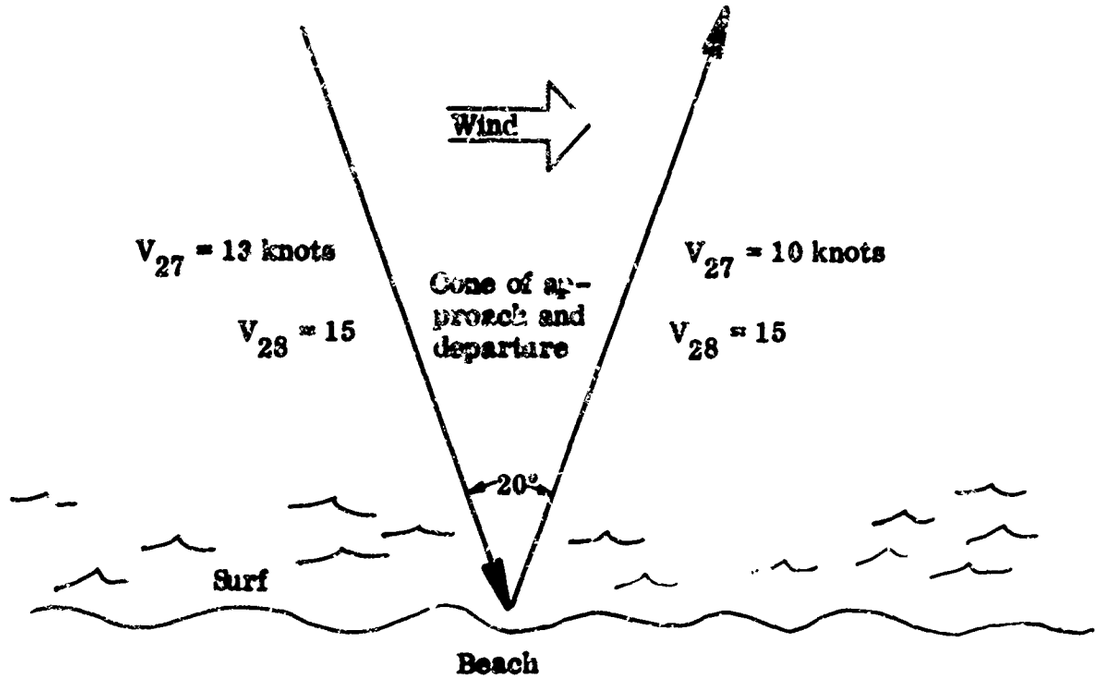

	In			Out		
	Bow g	Pitch (Degrees)	Roll (Degrees)	Bow g	Pitch (Degrees)	Roll (Degrees)
V_{27}	+0.4 -0.53	-	-	+1.15 -1.15	-	-
V_{28}	+0.45 -0.55	-	-	+1.6 -1.45	-	-

Figure 6-57. Surf Test Diagrams (Cont'd)

directed from the beach, represents the return from the beach to the open water. The runs are grouped according to the sea and surf conditions that prevailed during the runs. The bow vertical acceleration, craft pitch angle, craft roll angle, and Doppler speed presented represent the data obtained while traveling through the most severe breakers during each run. The approximate angles of approach and departure to and from the beach are not drawn to scale but are noted.

2. Discussion of Surf Tests

Surf negotiation can be divided into two parts:

1) Negotiating surf from the open sea toward the beach

2) Negotiating surf from the beach toward the open sea

Traveling to sea was found to be much more difficult than travelling to the beach when the breakers were higher than 5 feet.

No special techniques were required to negotiate surf while heading toward the beach (Figures 6-58 through 6-60) when the surf was near calm (2.5-foot waves or less), but surf producing breakers higher than 2.5 feet was best negotiated by maintaining the craft centerline near 90 degrees to the breaker fronts and running at minimum hover height.

Figure 6-58. Beach Approach, In Outer Surf

Figure 6-59. Beach Approach, Entering Inner Surf

Figure 6-60. Beach Approach, Moving onto Beach

Figure 6-61. Going to Sea, Across Surf, Crossing Wave Crest

The best control and smoothest ride were obtained when the craft speed was adjusted to be equal to or near the speed of the wave fronts, so that the craft traveled as far as possible in one trough between two waves, thereby cutting across as few breakers as possible. As the waves began breaking, they also decreased in speed, necessitating a comparable reduction in craft speed. However, crossing breakers did not appear to present any great problems. Unfortunately, available beach areas facing the ocean within operating range of the base were narrow (approximately 100 feet), with bluffs rising sharply from the inland portion of the beach. Therefore, it was impossible to approach the beach at high speeds; however, from open water tests in heavy seas it is felt that the craft could negotiate 4- to 5-foot breakers at higher speeds without undue control difficulties.

In like manner, no special techniques were required to negotiate surf while heading toward open water from the beach (Figures 6-61 through 6-63) as long as the breakers did not exceed 2.5 feet. However, as the breakers increased in height, the best techniques generally were to employ maximum hover height and a heading of near 90 degrees to the

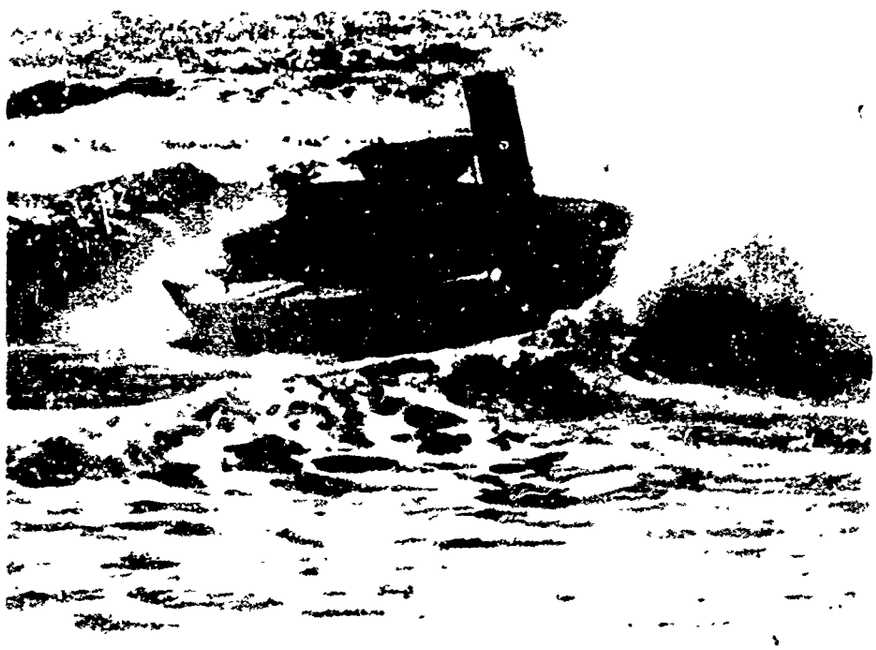

Figure 6-62. Going to Sea Across Surf, Riding Down Back of Wave

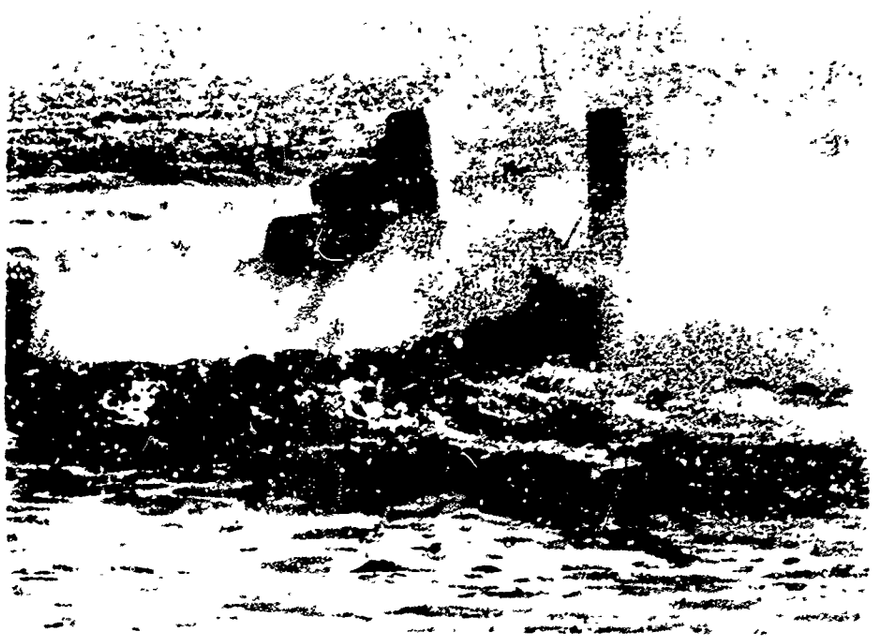

Figure 6-63. Going to Sea Across Surf, Heading into Following Breaker

breaker fronts. Special problems and techniques follow: Travelling against breakers of 5- to 7-feet could produce high water impacts, especially when crests were relatively close together. The most severe condition resulted when the craft impacted a succeeding breaker while still in the nose-down attitude produced by the sea side of the preceeding breaker. This resulted in the bow actually being buried into the succeeding breaker. A condition such as this on one occasion produced damage to the starboard bow of the VA-3. (The design of the VA-3 bow presents a large flat concave surface that is undoubtedly not the optimum bow design for operation in these surf conditions.) It was noted that each breaker rarely produced a continuous front over a great length. It is therefore felt that the optimum method of navigating such surf is to attempt to maneuver the craft so that a minimum number of waves are negotiated at the breaking point. The speed should also be adjusted to meet breakers when level or at positive pitch angles.

When travelling from open water to the beach, the craft can negotiate surf considerably higher than that negotiated during tests. The surfing capabilities while departing from the beach to open water where large breakers are present, could probably be improved by one or more of the following:

1) A bow design that does not present a wide flat surface to the breaker front, as does the VA-3 bow

2) A higher skirt

3) An inflatable bow to obsorb impact loads

G. OPERATION OVERLAND

The overland capabilities of the VA-3 were evaluated by determining its general handling characteristics over varied land terrain such as sand bars, sandy soil, marshland crossed with irrigation ditches, undulating surfaces, areas containing obstacles such as logs, stones, and miscellaneous debris, and shear drops. A brief description of the specific land tests conducted is given below:

1) Operation over a sand bar, 30 feet wide and sloping to 3 feet high at the center, at a speed of 25 knots

2) Operating in 4- to 5-foot scrub-covered dunes

3) Operation over marshland crossed with irrigation ditches at speeds up to 25 knots

4) Operation over a sand bar containing a 1-in-7 slope at Doppler speeds of 15, 25, and 30 knots

5) Operation over a sandy slope of 1-in-5 at Doppler speeds of 28 and 30 knots

6) Operation over a scrub-covered dune with a slope of 7-in-30, coupled with a transverse slope

7) Operation off a shear drop of 5 feet at 5 to 10 knots (Figure 6-64).

8) Operation over a 4- to 6-foot drop off a scrub-covered dune onto the beach

9) Traversing a small island containing a steep, scrub-covered approach rising up to 8 feet elevation

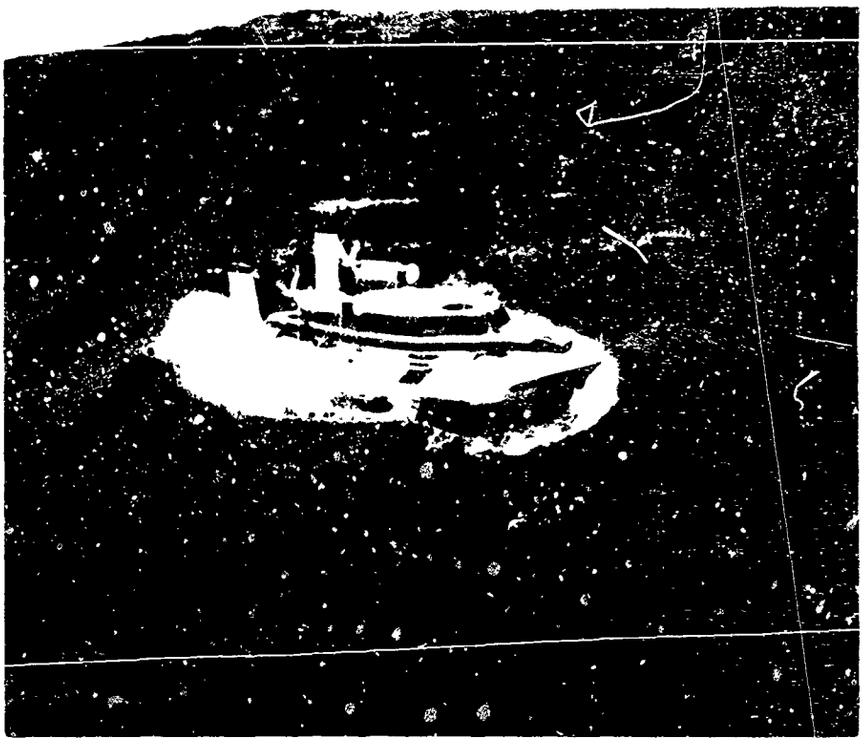

Figure 6-64. Transition from Land to Water

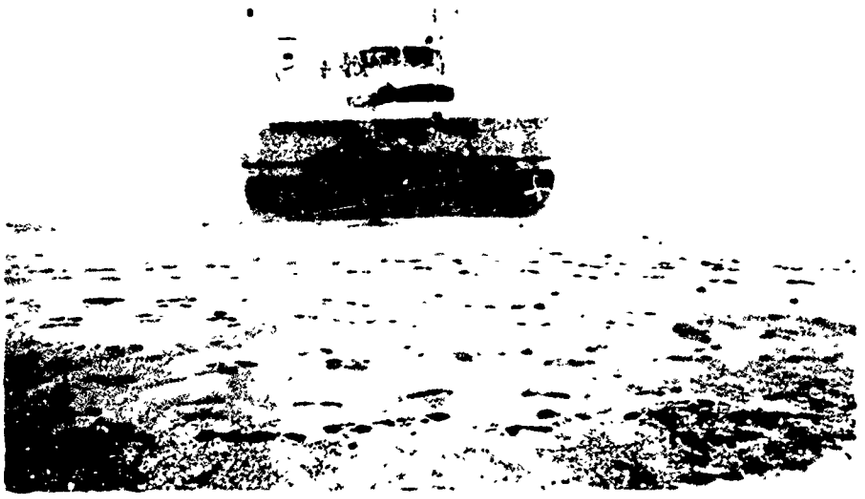

Figure 6-65. Operation over Sand

10) Operation over a sand bar containing a steep slope on one side and a shallow slope on the other at speeds of 5, 15, and 20 knots

11) Measurement of minimum turn radii at various speeds over land

Sand bars and tidal flats offered no problems in handling. Exposed sand bars (Item 1 above) approximately 30 feet wide and sloping to 3 feet high at the center were crossed at speeds in excess of 25 knots. During the course of testing the VA-3 also crossed sand bars (Items 4 and 5) at speeds up to 30 knots. It should be noted that a rider in the craft felt no sensation whatsoever when crossing bars. One sandy section in particular (Item 9) was quite rough, with large hammocks and a slope down to the water's edge. Viewing the terrain from the craft window left the passenger with a feeling that the ride would be quite rough with a decided thump at the water's edge. However, the actual sensation was quite the opposite, the ride being smooth with no sensation whatsoever of the transition back to water. It should be noted that the craft left no tracks when crossing sand, the only disturbance being the blowing around of a relatively minor amount of sand (Figure 6-65).

The marsh area (Item 3) had a growth of approximately 3 feet and was criss-crossed with irrigation ditches approximately 2 feet wide. At low water, the ditches were approximately 2 feet below the bog surface. The craft was operated at speeds of 20 to 25 knots over this terrain with no difficulty. The irrigation ditches did affect the cushion pressure and a small loss of hover height was experienced, but insufficient to cause contact of hard structure. Again no imprint was left in the marsh by the VA-3, but loose debris and a small amount of marsh grass was dislodged (Figure 6-66.

Runs in undulating terrains were performed in an area having scrub-covered shallow sloped dunes approximately 4 to 5 feet high (Item 2). The areas were traversed at speeds of 10 to 15 knots. Spoilers were used frequently in an effort to counteract side slopes and to maintain a straight heading. Although the general operation in this terrain was satisfactory, directional control was found to be difficult, especially during downwind runs, when the craft was actually moving sideways at times.

During testing in rough terrain (Figure 6-67 the craft was driven over a log approximately 2 feet in diameter. The

Figure 6-66. Riding over Marshland

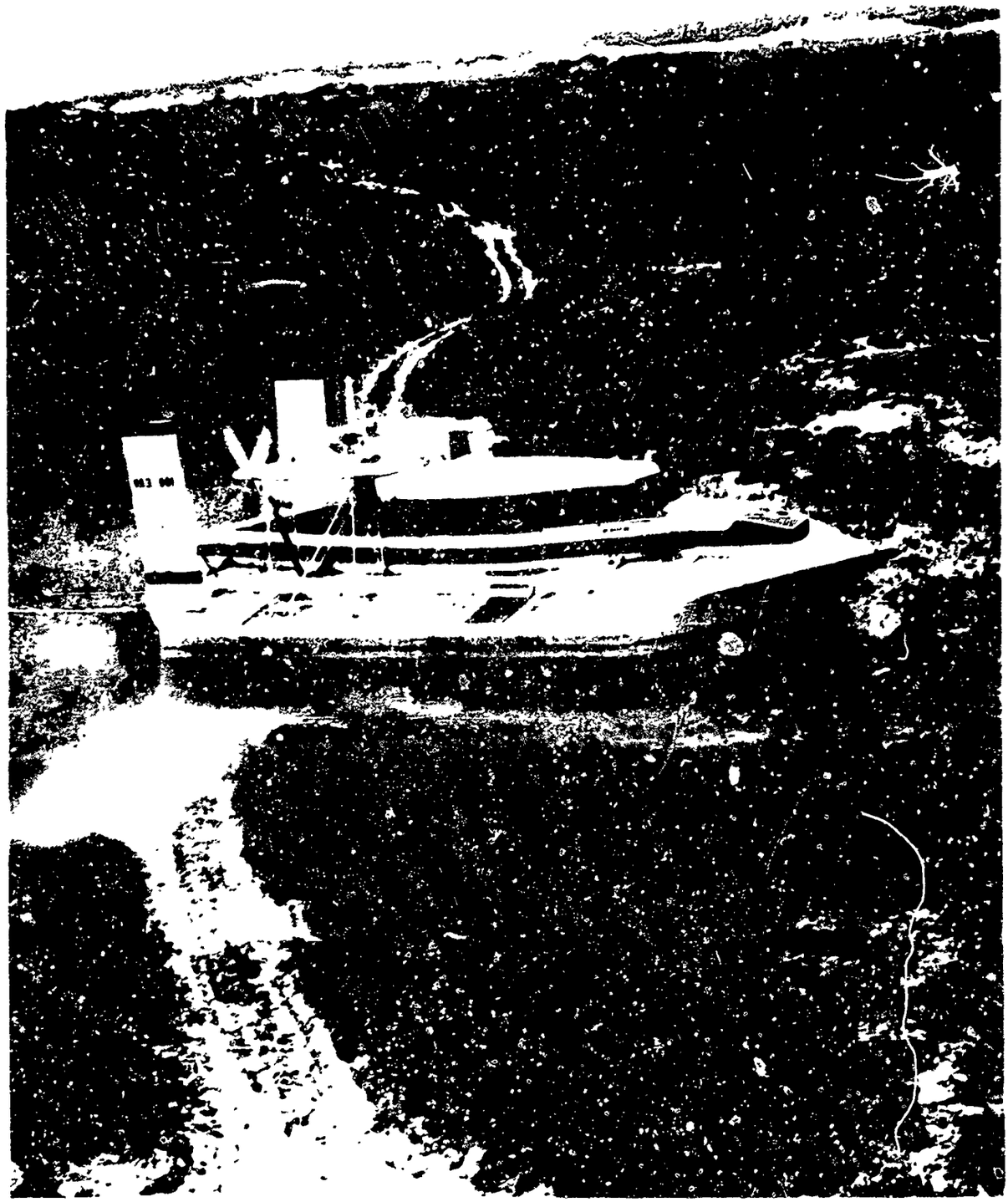

Figure 6-67. Traversing Rough Terrain

VA-3 was also tested over a shear drop (Item 7) of 5 feet at 5 to 10 knots. The contour map of this location is presented in Figure 6-68. The area below the shear was packed sand, which would reveal any contact. No hard structure imprint was found, although skirt drag was evident. It was found during this test and during subsequent operation off steep slopes (Item 8) that, when the bow pitched down, the cushion absorbed the impact and prevented the craft's hard structure from touching the ground. Several other steep slopes (Item 6) were negotiated at various speeds, but at no time during the overland tests did the VA-3 become stuck, although once when crossing a sharp ridge crest (Item 9) at about 5 knots the center of the craft was felt to scrape, giving the impression that the craft could be lodged on the ridge.

Minimum turn radii at various speeds were measured using rudders only (Item 11) (Figure 6-69). Differential propulsion pitch would have decreased the turn radii but would have introduced other factors outside the scope of this test. Stakes were placed 150 feet apart in a line. The craft approached the outboard stake at various speeds and started a 180-degree turn as the stake line was crossed.

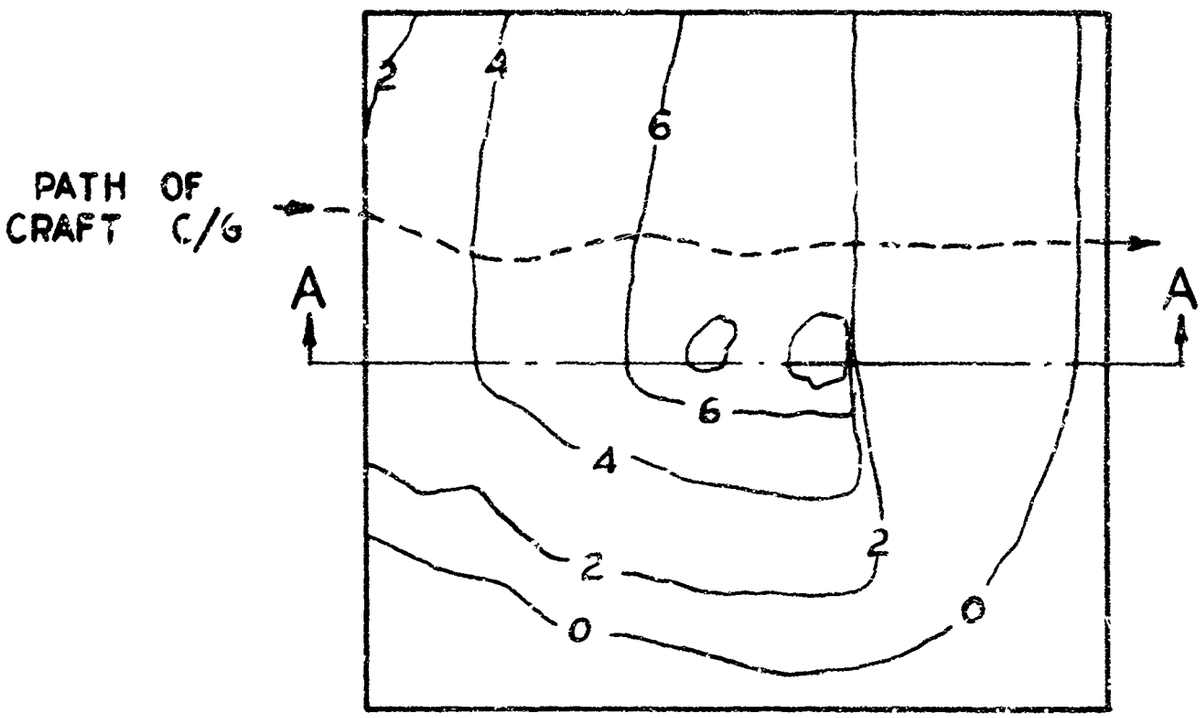

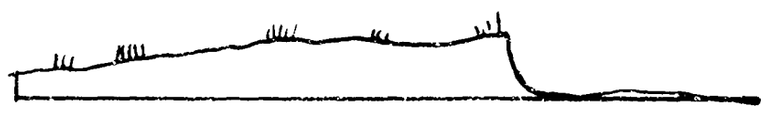

SECTION A-A

Figure 6-68. Contour Map

SCALE IN FEET 0 4 8 20

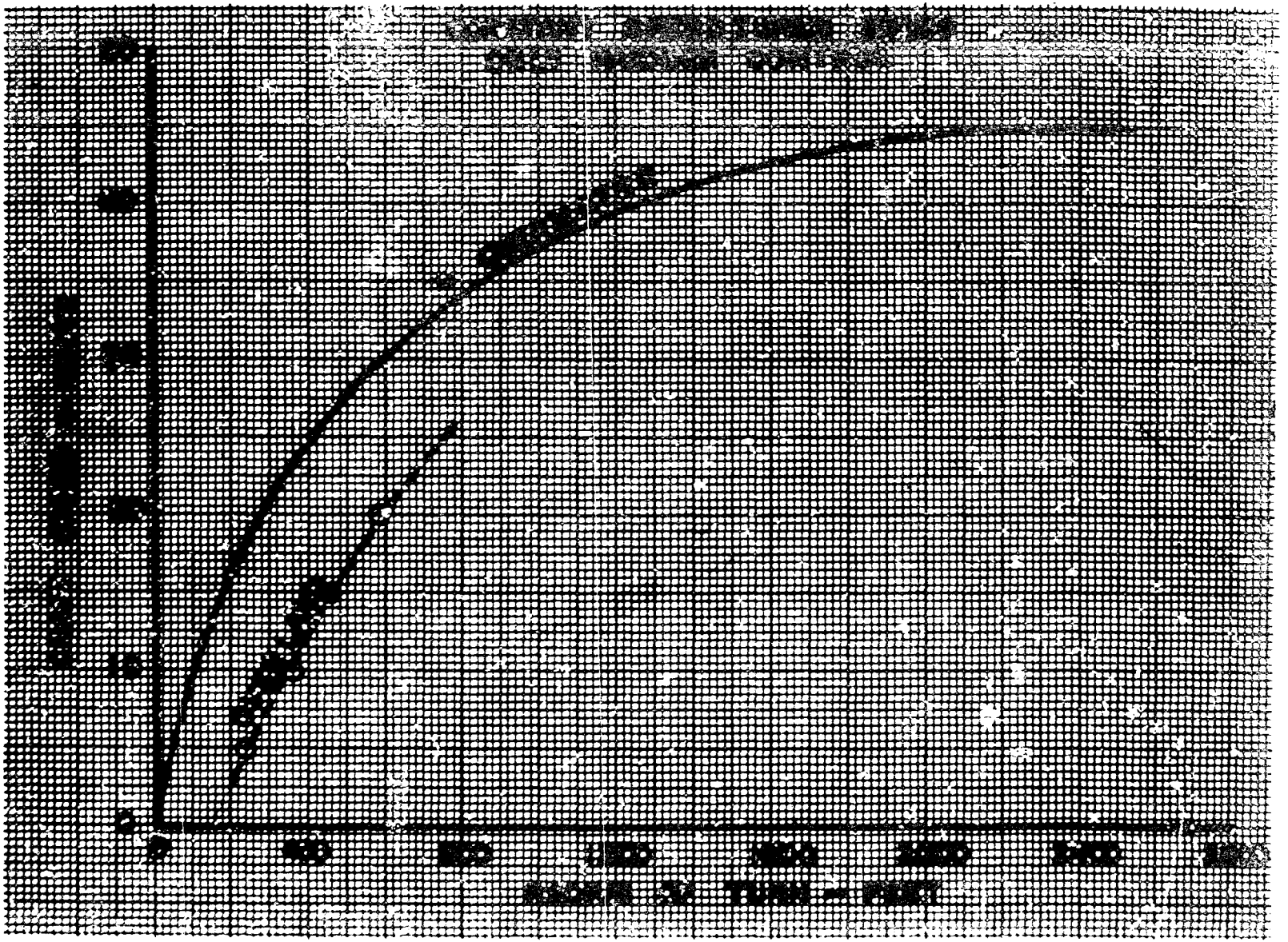

Figure 6-69. VA-3 Radius of Turn

In general, the VA-3 operated over all test terrain satisfactorily. The major problem encountered was the directional controllability, especially downwind and over undulating surfaces. One surprising fact was its ability to travel over shear drops with no resultant contact of the hard structure. Its ability to travel over a land surface leaving little or no imprints is also another interesting side advantage.

During these extensive overland tests, ingestion of foreign materials such as grass, marsh reeds, sand, and drift material did not cause any measurable erosion of centrifugal lift fan surfaces. Propeller tips were subjected to these same foreign materials without damage. It would appear, therefore, that these craft can be programmed to traverse beach and tidal areas without undue consideration for fan and propeller protections.

SECTION VII

RECOMMENDATIONS

A broad program of future air cushion vehicle development should be supported by additional sea keeping trials of the VA-3 in sea states 1, 2, 3, and higher. Such a comprehensive test program would supplement information currently available from this report and attainable from other programs. Specific recommended areas for development follow:

1) Continue development of operational techniques and handling over water, land and in conjunction with amphibious shipping. This can be accomplished best in an exercise with the Naval Amphibious Forces in the Norfolk area

2) Use the VA-3 as a test bed for development of flexible skirts. Fabric wear characteristics, fabrication and attachment methods, and fabric strength requirements cannot be satisfactorily derived from laboratory tests

3) Establish dynamic stability criteria for stiffness and damping in the natural environment, especially in short-crested waves. These stability criteria would be generally applicable to all air cushion vehicles. The use of magnetic recording equipment would permit more sophisticated methods of analysis

4) More accurate definition of drag and engine thrust can be achieved by consideration of the problems and improvements in the measuring techniques discussed in the drag analysis (Section VIB)

5) Establish structural integrity levels by strain-gaging critical areas such as panels and joints, especially in the bow sections. The structural flexibility of the VA-3, in contrast to that of the heavier, less flexible Skimmer I, represents a lighter design approach to impact load relief. Additional data is necessary to support the concept.

6) Install high-power propulsion engines to extend the data acquisition to higher speeds. Optimization of power required for control and maneuverability can also be achieved.

7) Evaluate existing water separation methods by measurement of performance in the actual air cushion vehicle environment rather than through laboratory simulation

SECTION VIII

REFERENCES

A. INTRODUCTION

These references are Vickers reports on the design and development of the VA-3. In the titles of these reports the VA-3 is sometimes referred to as the Type 3031.

B. AERODYNAMICS AND HYDRODYNAMICS REPORTS

1.	V/3031/AERO/01	Estimation of Directional Stability of Hovercraft
2.	V/3031/AERO/04	Type 3031 Modified for Open Circulation
3.	V/3031/AERO/05	Hovercraft VA-3 Performance
4.	V/3031/AERO/06	Hovercraft Test Program - Installation, and Functional and Initial Tests
5.	V/3031/AERO/07	Notes on Visit of Mr. J.R. Bowles of S. Smith & Sons (England) Ltd, to Discuss VA-3 Cabin Heating
6.	V/3031/AERO/08	The Elementary Theory of Hovercraft, Stability Analysis of Single Jets

7.	V/3031/AERO/10	Hovercraft Test Program - Detailed Test Schedule
8.	V/3031/AERO/11, Issue 2	The Performance of the VA-3 Hovercraft Over Sinusoidal Waves
9.	V/3031/AERO/12	Note of Preliminary Survey of Passenger Reactions to Travelling on VA-3 on 25-27 June 1962
10.	V/3031/AERO/13	On the Theory of Two Dimensional Hovercraft
11.	V/3031/AERO/15	A Survey of the Rhyl-Wallasey Ferry Service
12.	A/3031/16	Type 3031. Tests of Various Stability Jet Configurations
13.	DES/EJ/AR/14814	Technical Report on VA-3 - During the Rhyl-Wallasey Ferry Service
14.	F/3031/13	Final Report on Rhyl Exercises
15.	F/3031/14	Handling with Flexible Skirt Fitted
16.	Memo 12	Summary of Static Tests
17.	Memo 13	Additional Static Tests
18.	H1/3031/AERO/TR01 and 02	Performance of VA-3 Hovercraft
19.	V/3202/AERO/01	VA-3 Development - Estimates of Hoverheight for Various Arrangements of Peripheral Jet Nozzle
20.	ISH/3031/3	Prediction of Maximum Wave Heights Between Wallasey and RHYl
21.	V/3031/HYDRO/01	Hovercraft Seakeeping Trails
22.	V/3031/HYDRO/02	Notes on Visit to the Headquarters of the British Ship Research Association, London

23.	V/3031/HYDRO/03	Some Brief Notes on a Visit to the Tidal Institute
24.	V/3031/HYDRO/04 and 05	Wave Measurements in Liverpool Bay

C. STRESS ANALYSIS, WEIGHTS, AND NOISE REPORTS

25.	H/3031/STR/TR01	Analysis of Deck Frames Between Lift Engine Beams
26.	H/3031/STR/TR02	Analysis of Lift Engine Side Beams
27.	S/3031/3, Issue 2	Hovercraft Type 3031 Stressing Assumptions
28.	S/3031/1	Hovercraft Type 3031 Proposed Loading Cases
29.	V/3031/W/03	Type 3031 Hovercraft Weight Breakdown
30.	DS/3031/00/01, Issue 2	Engineering Specification for Type 3031 Hovercraft
31.	F/3090/1	Hovercraft Type 3090 VA-2
32.	H/3031/TO/TR01	VA-3 Weight Breakdown
33.	V/3031/00/PHY01	Hovercraft Noise Measurements
34.	V/3031/PHY02	Noise Measurements on VA-1
35.	V/3031/PHY03	Noise Measurements on VA-3
36.	V/3031/PHY04	Noise Measurements on VA-3

D. DOWTY ROTOL STRUCTURES REPORTS

37.	SDR1205	Propeller Stresses

38.	SDR1206	Drive-System Torsional Frequency
39.	SDR1317	Analysis of Lift-Fan Gear Bases
40.	SDR1318	Analysis of Propeller Gear Bases
41.	SDR1501, Issues 2 and 3	Analysis of Lift Fan
42.	SDR1502	Weight Analysis of Lift Fan

E. TEST REPORTS

43.	F/3031/1 through 12	Hovercraft Series of Reports from Operations Manager, Mr. L.R. Colquhoun
	———	The Development of Flexible Skirts for Air Cushion Vehicles
44.	DES/RTO/US/32S	VA-3 Test Program
45.	Report 2, 4, and 5	Hovercraft Operation - Montauk
46.	3031 Test Memo WT/3 to WT/8	Variable Stability Curtain Model Tests
47.	3031 Test Memo WT/6	1/10th Scale Tank Model Stability Tests Over Ground
48.	3031 Test Memo WT/9, 12, and 15	Two-Dimensional Rig
49.	3031 Test Memo WT/18	1/12th Scale Tunnel Model, Stability Results
50.	3031 Test Memo WT/21	Tank Model Tests Over Ground
51.	3031 Test Memo WT/27,28	Tests During January and February 1961 - Wind Tunnel Model 6, Series 6
52.	3031 Test Memo WT/40	Static Stability and Cushion Pressure Distribution of 1/12th Scale Model of Hovercraft

F. MODEL TESTS REPORTS

53.	A/91	Description and Calibration of the South Marston 7- foot x 5.5-foot Low-Speed Wind Tunnel
54.	WT/02	Intake Distribution Tests on 1/12th-Scale Model of Hovercraft Type 3031
55.	WT/03	Wind Tunnel Tests on 1/12th-Scale Working Model of Hovercraft Type 3031 Fitted with a Modified Bow
56.	WT/04	Static Stability Tests on 1/12th-Scale Working Model of Hovercraft Type 3031
57.	WT/06	Hovercraft Type 3031 - Results of Tank Tests on 1/10-Scale Dynamic Model with Modified Bow
58.	WT/07	Hovercraft Type 3031 - Two-Dimensional Spray Tests
59.	V/3126/WT/02	Reynolds Number Effects on Hovercraft - Simple Curtain Systems
60.	V/3126/WT/03	Further Two-Dimensional Tests on the Effect of Nozzle Size on the Performance of Simple Curtain Systems -- Performance of Two-Dimensional Deep Cushions
61.	A/3031/1	Thrust and Drag of Hovercraft Type A/3031/1
62.	A/3031/4	"Four-Spring Model" Analysis of Hovercraft Motion Over Waves
63.	A/3031/5	Heave Analysis
64.	A/3031/6	Hovercraft Type 3031 - Model Test of Centrifugal Impeller First Stage
65.	A/3031/7	Hovercraft Type 3031 - Model Tests of Centrifugal Impeller First Stage

66.	A/3031/8	Hovercraft Type 3031 - Model Tests of Centrifugal Impeller Second Stage
67.	A/3031/9	Type 3031 - Note on Operating Performance of a 7-ton Hovercraft, and Addendum 1 - Note on Operating Performance of a 10-ton Hovercraft
68.	A/3031/10	Preliminary Tests on Double Ended Two-Dimensional Recirculation Rig
69.	A/3031/11	Hovercraft Type 3031 - Model Tests of Centrifugal Impeller Third Stage
70.	A/3031/14	Hovercraft Sideforce and Roll Stability

APPENDIX A

ANALYSIS OF ROLL PERIOD

If the rolling moment, M_ϕ, is stated as $M_\phi = 28,585\ \bar{y}$ lb-in, $\bar{y}$ being the distance of the center of gravity relative to datum, then an approximation to the curve is

$$M_\phi = 87,178\ \phi + 5284\ \phi^3$$

where M_ϕ is in lb-in units and ϕ is the roll angle in degrees. Translating to the more familiar and convenient lb-ft/rad units yields

$$M_\phi = 0.4166 \times 10^6\ \phi + 82.83 \times 10^6\ \phi^3 \text{ lb-ft } (\phi \text{ in radians})$$

Now, stiffness has no real meaning in this situation, except that, for a small displacement about the equilibrium position,

$$K_\phi = 0.42 \times 10^6 \text{ lb-ft/rad}$$

The radius of gyration in roll is 8.1 feet, so at the test weight of 28,585 pounds,

$$I_\phi = 1.875 \times 10^6 \text{ lb-ft}^2$$

The equation of motion can thus be written as:

$$\frac{I_\phi}{g}\ \ddot{\phi} + M_\phi = 0$$

Then $\ddot{\phi} + \dfrac{32.4}{1.875 \times 10^6}\ (0.4166 \times 10^6\ \phi + 82.83 \times 10^6\ \phi^3) = 0$

or $\ddot{\phi} + 7.15441\ \phi + 1422.47\ \phi^3 = 0$

The above can be solved by Duffings method by writing the equation as:

$$\ddot{\phi} + \alpha \phi + \beta \phi^3 = 0$$

and, further, if ϕ_o is roll amplitude (that is, maximum roll excursion from the level position), then the natural frequency can be shown to be

$$\omega^2 = \alpha + 3/4 \beta \phi_o^2$$

or

$$f_\phi = \frac{1}{2\pi} (\alpha + 3/4 \beta \phi_o^2)^{1/2} \text{ cps}$$

Substituting for α and β,

$$f_\phi = 0.4257 (1 + 149.118 \phi_o^2)^{1/2} \text{ cps}$$

APPENDIX B

ANALYSIS OF DAMPING

The heave, pitch, and roll motions of the craft are assumed to be uncoupled. In the roll case, because the forced roll oscillations are of relatively small amplitude, the nonlinearity can be ignored and the equation of motion written as:

$$A_\phi \ddot{\phi} + D_\phi \dot{\phi} + K_\phi \phi = 0$$

where: A_ϕ = roll inertia

D_ϕ = roll damping

K_ϕ = roll stiffness

Note that although this is a treatment of the case of the roll of the craft, the development of a theory for oscillations about the pitch axis is identical. Trying a solution of the form

$$\phi \propto e^{pt}$$

Then $A_\phi p^2 + D_\phi p + K_\phi = 0$

or $$p = -\frac{D_\phi}{2A_\phi} \pm \left(\frac{D_\phi^2}{4A_\phi^2} - \frac{K_\phi}{A_\phi} \right)^{1/2}$$

Now, writing $$\omega_o = \left\{ \frac{K_\phi}{A_\phi} - \frac{D_\phi^2}{4A_\phi^2} \right\}^{1/2}$$

this is the "damped natural frequency" of the roll mode. Because, in all practical cases, $\frac{D_\phi^2}{4A_\phi^2}$ is small compared with $\frac{K_\phi}{A_\phi}$, the damped natural frequency will only differ slightly from that of the undamped case.

If $\frac{D_\phi^2}{4A_\phi^2} = \frac{K_\phi}{A_\phi}$, no oscillatory solution exists, and this is known as the "critically damped case."

Denoting the critical damping by $D_{\phi crit}$ yields

$$D_{\phi crit} = 2(K_\phi A_\phi)^{1/2} = 2 \times 2\pi A_\phi f_\phi = 12.5664 A_\phi f_\phi$$

because $K_\phi^{1/2} = 2\pi f_\phi \left[A_\phi\right]^{1/2}$. For p it can be written that

$$p = -\frac{D_\phi}{2A_\phi} \pm i\omega_o$$

or, for convenience, $\alpha = \frac{D_\phi}{2A_\phi}$

$$p = -\alpha \pm i\omega_o$$

The solution for ϕ can thus be written

$$\phi = B_1 e^{-\alpha t + i\omega_o t} + B_2 e^{-\alpha t - i\omega_o t}$$

or, in an alternative form,

$$\phi = Ce^{-\alpha t} \sin(\omega_o t + \epsilon)$$

Thus it is evident that the term $Ce^{-\alpha t}$ will form the envelope of maximum or minimum values of the decaying oscillations following a disturbance of the system.

The analysis of records will be done as follows: Succeeding maximum excursions traced by the decaying oscillations will be denoted by δ_i and δ_{i+1} at times t_i and t_{i+1}

Then $$\delta_i = Ce^{-\alpha t_i}$$

and

$$\delta_{i+1} = Ce^{-\alpha t_{i+1}}$$

or, taking the natural logarithms and subtracting,

$$\text{Log}_e \delta_i - \text{Log}_e \delta_{i+1} = \alpha(t_{i+1} - t_i)$$

or

$$\alpha = \frac{1}{(t_{i+1} - t_i)} \text{Log}_e \frac{\delta_i}{\delta_{i+1}}$$

or

$$D = \frac{2A}{(t_{i+1} - t_i)} \text{Log}_e \frac{\delta_i}{\delta_{i+1}}$$

Finally,

$$\lambda = \frac{D}{D_{crit}} = \frac{2A}{D_{crit}(t_{i+1} - t_i)} \text{Log} \frac{\delta_i}{\delta_{i+1}}$$

DISTRIBUTION LIST

Chief, Bureau of Naval Weapons
Department of the Navy
Washington, D. C. 20360
ATTN: Code RAAD-3
Code RR-25

Chief of Naval Operations
Department of the Navy
Washington, D. C.
ATTN: OP-07T
OP-725

Chief of Naval Research
Department of the Navy
Washington, D. C. 20360
ATTN: Code 461
Code 438

Commanding Officer
ONR Branch Office
Navy #100, Box #39
Fleet Post Office
New York, New York
ATTN: CDR D. D. Farshing (7 copies)

Commanding Officer
ONR Branch Office
207 West 24th Street
New York, New York 10011

Director
Naval Research Laboratory
ATTN: Technical Information Division
Washington, D. C. 20390 (6 copies)

Chief, Bureau of Ships
Department of the Navy
Washington, D. C.
ATTN: Code 421 (2 copies)
Code 529 (2 copies)

Commanding Officer & Director
David Taylor Model Basin
Aerodynamics Laboratory
Washington, D. C.
ATTN: Mr. H. R. Chaplin

Commanding Officer & Director
David Taylor Model Basin
Hydrodynamics Laboratory
Carderock, Maryland
ATTN: Mr. A. Gersten

Commandant of the Marine Corps
Arlington Annex
Washington, D. C.
ATTN: Code AO4H (2 copies)

Marine Corps Development Center
Marine Corps Schools
Quantico, Virginia
ATTN: Air Section

Maritime Administration
441 G Street, N. W.
Washington, D. C.
ATTN: Mr. J. Higgins

Army Material Command
Director of Research & Development
Development Division
Mobility Branch
Subsystems Unit
Washington, D. C.
ATTN: Mr. K. Kasai

Commanding Officer
U. S. Army Transportation
Research Command
Fort Eustis, Virginia
ATTN: TCREC-TRC, Mr. W. Sickles

Defense Documentation Center
Cameron Station, Building 5
5010 Duke Street
Alexandria, Virginia (20 copies)

NASA
Langley Research Center
Langley AFB, Virginia
ATTN: Mr. A. W. Carter

Office, Director of Defense
Research and Engineering
Washington, D. C.
ATTN: Director of Aeronautics

University of Kansas
Department of Mechanics and
Aerospace Engineering
Lawrence, Kansas
ATTN: C. Cholias menos

Bell Aerosystems Company
P. O. Box #1
Buffalo 5, New York
ATTN: Mr. J. L. Wosser

General Dynamics Corporation
Convair Division
3165 Pacific Highway
San Diego, California
ATTN: Mr. W. D. Wood

General Dynamics Corporation
Electric Boat Division
Groton, Connecticut
ATTN: Mr. E. F. Davison

Library Institute of the Aeronautical
Science
2 East 64th Street
New York 21, New York

Vehicle Research Corporation
161 East California Boulevard
Pasadena, California
ATTN: Dr. S. Rethorst